Supporting Information

Cysteine-selective [^{188}Re]Re(V) radiolabelling of a Nanobody® for targeted radionuclide therapy using a "chelate-then-click" approach.

Diana R. Melis[1,2], Charlotte Segers[1], Jasmien Wellens[1], Michiel Van de Voorde[1], Olivier Blacque[3], Maarten Ooms[1], Gilles Gasser[2]* and Tomas Opsomer[1]*.

[1] Institute for Nuclear Medical Applications (NMA), Belgian Nuclear Research Centre (SCK CEN), 2400 Mol, Belgium.

[2] Chimie ParisTech, PSL University, CNRS, Institute of Chemistry for Life and Health Sciences, 75005 Paris, France.

[3] Department of Chemistry, University of Zurich, Winterthurerstrasse 190, 8057 Zurich, Switzerland.

*** Corresponding authors:**

Gilles Gasser: WWW : www.gassergroup.com; email : gilles.gasser@chimieparistech.psl.eu

Tomas Opsomer: email: tomas.opsomer@sckcen.be

Table of Contents

Experimental methods and materials

General details

All chemicals for synthesis were purchased from commercial sources and used without further purification. The bivalent HLE anti-c-Met V_HH was provided by Sanofi® (Ghent, Belgium). The c-Met V_HH is specific for human c-Met and displays no cross-reactivity with mouse c-Met. Compounds **1**, **2**, **3**, **5** and **6** were synthesised according to previously reported procedures.[1–3] Reactions were performed under standard atmospheric conditions unless otherwise stated. Thin layer chromatography (TLC) was performed using silica gel 60 F-254 (Merck) plates and column chromatography was done using Silica gel 60–200 µm (VWR). ^{1}H and ^{13}C{^{1}H} NMR spectra were measured on a Bruker Avance III HD 400 MHz spectrometer. The chemical shifts δ are reported in ppm (parts per million) relative to the respective solvent signals. Coupling constants *J* are given in Hertz (Hz). High-resolution ESI mass spectrometry (HR ESI-MS) spectra were recorded on an LTQ-Orbitrap XL (Thermo Scientific). The abbreviations, "app." and "ar." stand for "apparent" and "aromatic," respectively. Fourier-transform infrared spectroscopy (FT-IR) measurements were performed using an Agilent Cary 600 Series FT-IR Spectrometer with a PIKE GladiATR module. Instant thin layer chromatography (iTLC) was performed using glass microfiber chromatography paper strips impregnated with silica gel (iTLC-SG, Agilent Technologies, Belgium). The iTLC strips were analysed using an automated gamma counter after cutting the strips in two pieces (2480Wizard^2, Perkin Elmer, Belgium), or by using a TLC scanner (miniGITA, Elysia-Raytest®, Germany). Quantification of the V_HH concentration was determined using a NanoDrop® One UV-Vis spectrophotometer (Thermo Fischer Scientific).

HPLC methods

Analytical high-performance liquid chromatography (HPLC) and ESI-MS was carried out using a Waters preparative HPLC system equipped with a Waters 2487 dual wavelength UV/Vis detector and a Waters SQ Detector 2 mass spectrometer. Radio-HPLC (analytical and preparative) analyses were performed on a Waters Acquity Arc system

equipped with a Waters 2489 dual wavelength UV/Vis detector and a GABI Nova radio detector (Elysia-Raytest). The following HPLC methods were used on either of these two HPLC instruments:

Method A. Column: Waters XBridge® C18, 15 µm, 4.6 x 100 mm. Mobile phases: 0.1% (v/v) formic acid in milli-Q water (A) and 0.1% (v/v) formic acid in acetonitrile (B). Flow rate: 1 mL/min. Gradient: 0-2 min (5% B), 2-8 min (5-60% B), 8-9 min (60-100% B), 9-12 min (100% B), 12-13 min (100-5% B), 13-15 min (5% B).

Method B: Column: Waters XBridge® Peptide BEH C18, 5 µm, 4.6 x 150 mm. Mobile phases: 0.05% (v/v) TFA in milli-Q water (A) and 0.05% (v/v) TFA in acetonitrile (B). Flow rate: 1 mL/min. Gradient: 0-2 min (10% B), 2-5 min (10-70% B), 5-8 min (70-100% B), 8-12 min (100% B), 12-12.1 min (100-10% B), 12.1-15 min (10% B).

Method C: Column: Superdex® 75 10/300 GL. Mobile phase: PBS. Flow rate: 0.75 mL/min

Method D: Column: Waters BioResolve™ RP mAb Polyphenyl, 2.7 µm, 4.6 x 100 mm. Mobile phases: 0.1% (v/v) TFA in milli-Q water (A) and 0.1% (v/v) TFA in 1:1 acetonitrile:isopropanol (B). Flow rate: 1 mL/min. Gradient: 0-15 min (20-50% B), 15-18 min (50% B), 18-18.1 min (50-20% B), 18.1-20 min (20% B). Column temperature: 65 °C.

Synthesis

*Trt-N_2S_2-PEG_3-N_3 (**4**).* Trt-N_2S_2-COOH (compound **3** , 0.200 g, 0.271 mmol) was dissolved in 5.00 mL dry DCM under a N_2 atmosphere. EDC.HCl (0.055 g, 0.353 mmol) was then added, followed by HOBt (0.048 g, 0.353 mmol) and DIPEA (0.095 mL, 0.542 mmol) and the reaction mixture was stirred for 30 min at room temperature. Finally, NH_2-PEG_3-N_3 (0.081 mL, 0.407 mmol) was dissolved in 2.00 mL dry DCM and added to the reaction mixture, which was stirred at room temperature overnight. The reaction mixture was then diluted with DCM, washed with water (4 x 20.0 mL) and brine (1 x 20.0 mL), dried over $MgSO_4$ and filtered. The solvent was removed and the residue was purified via column chromatography with silica gel using a 9:1 mixture of ethyl acetate and methanol for afford compound **4** as a pale yellow oil (0.148 g, 58%). ^{1}H NMR (400 MHz, $CDCl_3$) δ: 2.31 (t, *J* = 6.49 Hz, 2H, H_g), 2.40 (t, *J* = 6.43 Hz, 2H, H_a), 2.50 (t, *J* = 6.50 Hz, 2H, H_f), 2.96 (s, 2H, H_e or H_h), 3.00 (s, 2H, H_e

or H_h), 3.04 (app. q, *J* = 6.29, 6.28 Hz, 2H, H_b), 3.34 – 3.38 (m, 4H, PEG), 3.45 – 3.69 (m, 12H, PEG), 6.95 (br t, *J* = 5.84 Hz, 1H, NH_c), 7.13 (br t, *J* = 5.82 Hz, 1H, NH_j), 7.18 – 7.28 (m, 18H, H_m & H_o), 7.36 – 7.39 (m, 12H, H_n). $^{13}C\{^1H\}$ NMR (101 MHz, $CDCl_3$) δ: 171.0 (C_d or C_j), 170.3 (C_d or C_j), 144.91 (C_l), 144.85 (C_l), 129.9 (C_m), 129.8 (C_m), 128.34 (C_n), 128.31 (C_n), 127.2 (C_o), 127.1 (C_o), 70.64 (PEG), 70.58 (PEG), 70.1 (PEG), 67.4 (C_k), 67.2 (C_k), 58.5 (C_e & C_h), 54.5 (C_f), 50.9 (PEG), 39.2 (PEG), 38.9 (PEG), 38.4 (C_b), 32.3 (C_a), 30.3 (C_g). **IR (ATR):** (ν_{max}/cm^{-1}) 3301, 3060, 2861, 2098 (N_3), 1660 (C=O). HRMS (ESI) *m/z*: $[M+H]^+$ calculated for $C_{54}H_{60}N_6O_5S_2$: 937.4139, found 937.4142.

*Perfluorophenyl (E)-4-oxo-4-phenylbut-2-enoate (**6**).* This compound is reported in literature[4], however, it was synthesised following a different procedure.[5] 3-Benzoylacrylic acid (0.500 g, 2.838 mmol), bis(pentafluorophenyl)carbonate (1.678 g, 4.257 mmol) and CsF (0.086 g, 0.568 mmol) were dissolved in anhydrous THF (10.0 mL) under N_2. The reaction mixture was left to stir at room temperature overnight. The solvent was removed and the residue redissolved in DCM and left to stand. A fluffy precipitate of the PFP by-product formed. The mixture was filtered into a separatory funnel and the filtrate was washed with saturated $NaHCO_3$ (2 x 100.0 mL), water (1 x 100.0 mL) and brine (2 x 100.0 mL). The organic layer was dried over $MgSO_4$, filtered and concentrated. Upon the addition and removal of pentane, pale yellow crystals formed to yield compound **6** (0.500 g, 52%). The characterisation data was found to be in accordance with that reported in literature.[4]

*DBCO-PEG$_4$-CA (**7**).* Compound **6** (0.072 g, 0.209 mmol) was dissolved in anhydrous DCM (2.0 mL) in a round bottom flask. In a separate flask, compound **5** (0.142 g, 0.271 mmol) was dissolved in anhydrous DCM (2.0 mL), followed by the addition of DIPEA (0.015 mL, 0.418 mmol). The latter mixture was added dropwise to the first and the reaction mixture was left to stir at room temperature overnight. The reaction mixture was then diluted with DCM, washed with water (2 x 20.0 mL) and brine (1 x 20.0 mL), dried over Na_2SO_4 and filtered. The solvent was removed and the residue was purified via column chromatography with silica gel using a 95:5 mixture of DCM and methanol to afford compound **7** as a yellow oil (0.115 g, 81%). ^1H NMR (400 MHz, $CDCl_3$) δ: 1.92-1.99 (m, 1H, H_k), 2.30-2.32 (m, 2H, PEG), 2.47-2.54 (m, 1H, H_k), 3.27-3.32 (m, 2H, H_j), 3.47-3.69 (m, 19H, H_m and PEG), 5.13 (d, *J*

= 13.9 Hz, 1H, H_m), 6.63 (br t, *J* = 5.8 Hz, 1H, NH), 7.03 (d, *J* = 15.1 Hz, 1H, H_f), 7.24-7.39 (m, 7H, DBCO CH ar.), 7.48-7.52 (m, 2H, H_b), 7.58-7.62 (m, 1H, H_a), 7.65 (br d, *J* = 7.2 Hz, 1H, DBCO CH ar.), 7.95 (d, *J* = 15.1 Hz, 1H, H_g), 7.93-8.04 (m, 2H, H_c). $^{13}C\{^1H\}$ NMR (101 MHz, $CDCl_3$) δ: 189.9 (C=O), 172.0 (C=O), 171.1 (C=O), 164.2 (C=O), 151.1 (4° C), 148.1 (4° C), 137.0 (C_d), 135.8 (C_f), 133.6 (C_a), 132.8 (C_g), 132.1 (DBCO CH ar.), 129.1 (DBCO CH ar.), 128.83 (C_b), 128.79 (C_c), 128.6 (DBCO CH ar.), 128.3 (DBCO CH ar.), 128.2 (DBCO CH ar.), 127.8 (DBCO CH ar.), 127.2 (DBCO CH ar.), 125.5 (DBCO CH ar.), 123.0 (4° C), 122.5 (4° C), 114.7 (4° C), 107.8 (4° C), 70.5 (PEG), 70.3 (PEG), 70.25 (PEG), 70.20 (PEG), 69.6 (PEG), 67.1 (PEG), 55.5 (C_m), 53.4 (4° C), 39.8 (PEG), 36.8 (PEG), 35.2 (C_j), 34.7 (C_k). **IR (ATR):** (ν_{max}/cm^{-1}) 3284, 2865, 1646 (C=O). HRMS (ESI) *m/z*: $[M+Na]^+$ calculated for $C_{39}H_{43}N_3O_8$: 704.2942, found 704.2970.

*^{nat}ReO(N_2S_2-CH_2COOEt) (**Re-2**).* Trt-N_2S_2-COOEt (compound **2**, 0.228 g, 0.298 mmol) was dissolved in trifluoroacetic acid (4.0 mL) in an ice bath for 10 min with stirring, resulting in a bright yellow solution. Et_3SiH was added dropwise until the disappearance of the bright yellow colour. The volatiles were removed with a stream of N_2 and then by rotary evaporation. The residue was then redissolved in methanol (6.0 mL), followed by addition of a 1.0 M solution of NaOAc in methanol (6.0 mL). $(Ph_3P)_2ReOCl_3$ (0.372 g, 0.447 mmol)) was added and the mixture was refluxed at 75 °C overnight. After cooling to room temperature, the dark purple suspension was diluted with ethyl acetate (20.0 mL) and then filtered. The filtrate was concentrated and the residue was loaded onto silica and purified by column chromatography (100% DCM to 90:10 DCM:EtOAc), yielding **Re-2** as purple crystals (0.088 g, 62%). Note: Transesterification of the ethyl ester to the methyl ester readily occurs in methanol, leading to a mixture of the two products). ^1H NMR (400 MHz, CD_3OD) δ: 1.32 (t, *J* = 7.2 Hz, 3H, H_j), 1.71-1.80 (m, 1H, H_e), 2.97 (app. dt, *J* = 3.7, 13.8 Hz, 1H, H_f), 3.10-3.16 (m, 2H, H_a & H_b), 3.46 (app. tdd, *J* = 1.5, 3.7, 13.7, 1H, H_f) 3.74-3.81 (m, 1H, H_e), 3.81 (s, methyl ester Hs from transesterification in MeOH), 4.04-4.08 (m, 1H, H_a), 4.24-4.32 (m, 1H, H_i), 4.47-4.73 (m, 4H, H_b, H_d & H_g), 5.16 (m, 1H, H_d). $^{13}C\{^1H\}$ NMR (101 MHz, CD_3OD) δ: 168.7 (C=O), 168.2 (C=O), 68.8 (C_d), 67.0, 66.7 (C_e), 63.0 (C_i), 62.6, 62.4 (C_g), 60.7 (C_b), 53.0 (methyl ester C from transesterification in

MeOH), 47.8 (C_a), 40.4 (C_f), 14.4 (C_j). **IR (ATR):** (ν_{max}/cm^{-1}) 1736 (C=O), 1662 (C=O), 953 (Re=O). HRMS (ESI) *m/z*: $[M+H]^+$ calculated for $C_{39}H_{43}N_3O_8$: 481.0260, found 481.0258.

*^{nat}ReO(N_2S_2-CH_2COOH) (**Re-3**).* Compound **Re-2** (0.085 g, 0.177 mmol) was dissolved in THF (2.0 mL) and water (0.5 mL). LiOH (0.010 g, 0.354 mmol) was then added and the reaction mixture was left to stir at room temperature for 2 h. After this time, the THF was removed using a rotary evaporator and 1.0 M HCl was added until a pH of 1.0 was reached. H_2O (5.0 mL) was then added and the compound extracted with ethyl acetate (3 x 20.0 mL). The organic layer was dried over $MgSO_4$, filtered and the solvent removed, yielding **Re-3** as a purple crystalline solid (0.054 g, 68%). ^{1}H NMR (400 MHz, CD_3OD) δ: 1.71 (app. tdd, *J* = 1.3, 4.5, 13.1 Hz, 1H, H_e), 2.93-2.98 (m, 1H, H_f), 3.04-3.18 (m, 2H, H_a & H_b), 3.42-3.50 (m, 1H, H_f), 3.85 (app. dd, *J* = 3.0, 12.6 Hz, 1H, H_e), 4.03-4.07 (m, 1H, H_a), 4.50-4.69 (m, 3H, H_b, H_d & H_g), 4.67 (d, *J* = 17.3 Hz, 1H, H_g), 5.15 (d, *J* = 17.3 Hz, 1H, H_d). ^{13}C{^{1}H} NMR (101 MHz, CD_3OD) δ: 191.1 (C_h), 169.6 (C_c), 68.9 (C_d), 66.4 (C_e), 62.7 (C_g), 60.7 (C_b), 47.5 (C_a), 40.3 (C_f). **IR (ATR):** (ν_{max}/cm^{-1}) 1710 (C=O), 1564, 970 (Re=O). HRMS (ESI) *m/z*: $[M-H]^-$ calculated for $C_8H_{13}N_2O_4ReS_2$: 450.9802, found 450.9790.

*^{nat}ReO(N_2S_2-PEG_3-N_3) (**Re-4**).* Compound **Re-3** (0.11 g, 0.244 mmol) was dissolved in dry DMF (7.0 mL) under a N_2 atmosphere. EDC.HCl (0.061 g, 0.317 mmol) was then added, followed by HOBt (0.043 g, 0.317 mmol) and DIPEA (0.127 mL, 0.732 mmol) and the reaction mixture was stirred for 30 min at room temperature. Finally, NH_2-PEG_3-N_3 (0.082 mL, 0.414 mmol) was dissolved in dry DMF (3.0 mL) and added to the reaction mixture, which was stirred at room temperature overnight. After this time, the DMF was removed by co-evaporation with toluene using a rotary evaporator. The residue was redissolved in DCM and purified by prep-TLC (DCM/MeOH 95:5) to yield **Re-4** as a purple crystalline solid (0.048 g, 30%). ^{1}H NMR (400 MHz, $CDCl_3$) δ: 1.54-1.61 (m, 1H, H_e), 2.89 (app. dd, *J* = 4.4, 13.8 Hz, 1H, H_f), 3.13-3.29 (m, 2H, H_a & H_b), 3.39-3.45 (m, 6H, PEG), 3.48-3.52 (m, 2H, H_f), 3.60-3.75 (m, 34H, PEG), 3.95 (app. dd, *J* = 3.4, 12.3 Hz, 1H, H_e), 4.09-4.13 (m, 1H, H_a), 4.24 (d, *J* = 16.0 Hz, 1H, H_g), 4.60-4.66 (m, 2H, H_d & H_g), 4.75 (d, *J* = 17.4 Hz, 1H, H_d), 4.96 (d, *J* = 17.4 Hz, 1H, H_d). ^{13}C{^{1}H} NMR (101 MHz, $CDCl_3$) δ: 188.3 (C=O), 165.4 (C=O), 72.6 (PEG), 70.8 (PEG), 70.7 (PEG), 70.5 (PEG), 70.2 (PEG), 70.0 (PEG), 69.3 (PEG), 68.6 (C_d), 64.4 (C_e),

63.2 (C_g), 61.9 (PEG), 60.1 (C_b), 51.0, 50.8 (PEG), 48.7 (C_a), 39.6 (C_f). **IR (ATR):** (ν_{max}/cm^{-1}) 2918, 2868, 2098 (N_3), 1659 (C=O), 964 (Re=O). HRMS (ESI) *m/z*: $[M+H]^+$ calculated for $C_{16}H_{29}N_6O_6ReS_2$: 654.1292, found 654.1254. (Note: Integration of ^1H spectra of PEG-containing compounds generally results in an overestimation of the number of protons. This is often the result of the presence of tightly-bound H_2O and/or hydroxylic solvents.)

X-ray crystallography

Diffraction quality crystals of **Re-2** were obtained by slow evaporation from methanol in an NMR tube, while crystals of **Re-3** were grown from the slow evaporation of methanol layered with pentane. Single crystal X-ray diffraction data were collected at 160(1) K on a Rigaku OD Synergy-Hypix diffractometer using the copper X-ray radiation (λ = 1.54184 Å) from a dual wavelength X-ray source and an Oxford Instruments Cryojet XL cooler. The selected suitable single crystal was mounted using polybutene oil on a flexible loop fixed on a goniometer head and immediately transferred to the diffractometer. Pre-experiment, data collection, data reduction and analytical absorption correction[6] were performed with the program suite *CrysAlisPro*.[7] Using *Olex2*,[8] the structure was solved with the SHELXT[9] small molecule structure solution program and refined with the SHELXL2018/3 program package[10] by full-matrix least-squares minimization on F2. *PLATON*[11] was used to check the result of the X-ray analysis. In the crystal structure of **Re-2**, the ethyl group was disordered over two sets of positions with site-occupancy factors of 0.490(12) and 0.510(12). CCDC entries 2384422 for **Re-2** and 2384423 for **Re-3** contain the supplementary crystallographic data for this paper. These data are provided free of charge www.ccdc.cam.ac.uk/structures.

V_HH bioconjugation

The dimeric V_HH (V_HH-S-S-V_HH) was reduced into its monomeric form (V_HH-SH) prior to use. This was done by stirring the V_HH dimer (0.30 µmol) in a solution of 10 mM dithiothreitol (DTT), 20 mM HEPES and 150 mM NaCl

(total volume: 1.4 mL) at room temperature for 1 h. Complete conversion to the monomeric form was observed using SEC-HPLC (280 nm, HPLC method C). The solution was then purified using a PD-10 desalting column (GE Healthcare Bio-Science AB, Uppsala, Sweden) where the V_HH-SH was eluted with a solution of 20 mM HEPES and 150 mM NaCl (1.9 mL). The V_HH-SH was eluted directly into a LoBind Eppendorf containing a three-molar excess of DBCO-PEG_4-CA (**7**) (0.99 µmol) in 150 µL of milli-Q grade water with 5% DMSO. The solution was stirred at 37°C for 1.5 h and thereafter purified using a PD-10 desalting column, where the DBCO-PEG_4-V_HH was eluted with ~1.8 mL milli-Q grade water. The final V_HH solution was then lyophilised and reconstituted in a smaller volume of HEPES-buffered saline (pH 7.4). The purified product was analysed using SEC-HPLC (HPLC method C): 16.97 min, 97.2% purity. ESI-MS *m/z* (decon.) calculated for DBCO-PEG_4-V_HH: 27269.8, found: 27268.0. The protein concentration of the DBCO-PEG_4-V_HH construct was determined using spectrophotometry at 280 nm (NanoDrop® One, Thermo Fisher Scientific), with ε = 41000 $L.mol^{-1}.cm^{-1}$ and M = 26588 $g.mol^{-1}$.

In addition, following the method above, *N*-ethylmaleimide (NEM) was reacted with the V_HH-SH monomer to form V_HH-NEM. SEC-HPLC (HPLC method C): 16.65 min, 96.0% purity. ESI-MS *m/z* (decon.) calculated for V_HH-NEM: 26715.14, found: 26714.50.

$^{188}W/^{188}Re$ generator

An in-house $^{188}W/^{188}Re$ generator was prepared for the daily production of $[^{188}Re]ReO_4^-$ for our radiolabelling studies. The amount of activity that could be eluted off the generator was 200-350 MBq in less than 1.0 mL. Detailed descriptions on the generator fabrication and quality control of its eluate can be found at the website of the SECURE project (https://enen.eu/index.php/portfolio/secure-project/). This information was submitted in the form of a report which was created within the project SECURE (Strengthening the European Chain of sUpply for next generation medical RadionuclidEs) funded by the European Union under grant agreement No. 101061230.

^{188}Re-radiolabelling and SPAAC click reaction

The radiolabelling of the N_2S_2-PEG_3-N_3 chelator (**4**) was done over two steps. Optimisations were performed by changing different variables such as the amount of $SnCl_2$, the amount of chelator, the reaction volume, the temperature, the reaction time and the effect of having a N_2 atmosphere. The best condition ensured the greatest Radiochemical conversion (RCC) from [^{188}Re]ReO_4^- to [^{188}Re]ReO(N_2S_2-PEG_3-N_3). The optimised conditions were as follows: The citrate buffer and ascorbic acid solution were purged with N_2 before use. In the first step, to a 1.5 mL Eppendorf tube was added $SnCl_2.2H_2O$ (10 µL of a 22 mM solution in 0.1 M HCl), citrate buffer pH 5.0 (90 µL, 1.0 M), ascorbic acid (20 µL of a 0.68 M solution in citrate buffer) and [^{188}Re]ReO_4^- (150-170 MBq) in saline. The total reaction volume was 500 µL. N_2 was put into the headspace of the tube and the solution was heated at 90 °C for 30 min to yield [^{188}Re]Re(V)-citrate. RCC was determined by a two-strip iTLC method described previously[12], which also determines the amount of colloidal rhenium present in solution (one strip developed in saline and the other in acetone). In the second step, in a 1.5 mL microcentrifuge tube (Eppendorf), TFA (50 µL) was added to the N_2S_2-PEG_3-N_3 chelator (**4**) (700 nmol) and shaken for ~5-10 min to remove the trityl protecting groups. Triethylsilane (40 µL) was thereafter added and the solution was shaken for a further 5 min. The bright yellow colour disappeared immediately upon the addition of the triethylsilane. The volatiles were removed under a stream of N_2 and the residue was redissolved in EtOH (100 µL). To this tube was added 120-140 MBq of the [^{188}Re]Re(V)-citrate solution and enough citrate buffer (1.0 M, pH 5) to bring the volume up to 750 µL. Again, N_2 was put into the headspace of the tube and the labelling mixture was reacted for 15 min at 90 °C to yield [^{188}Re]ReO(N_2S_2-PEG_3-N_3). This labelling mixture was divided into 3 equal fractions which were consecutively purified using HPLC method B, collecting the peak of interest at ~7.5 min. The purified fractions were collected into one Protein LoBind centrifuge tube (Falcon™) containing a solution of sodium ascorbate (20 µL, 1.0 M) and thereafter dried using a Smart Evaporator (BioChromato, Inc., Japan). After evaporating until dry, the [^{188}Re]ReO(N_2S_2-PEG_3-N_3) was redissolved in a sodium citrate solution of pH 8 (25 µL, 0.3 M, 0.02% Tween® 80). To this, the DBCO-PEG_4-V_HH in HEPES buffer (enough for 5 MBq/nmol) was added and the reaction was allowed

to proceed for 30 min and monitored by iTLC (ACN/H_2O, 3:1). After 30 min, the mixture was diluted in saline (300 µL) and purified with a preconditioned PD MiniTrap™G-25 desalting cartridge (Cytiva), whereby the final [^{188}Re]Re-V_HH construct was eluted in saline (600 µL).

In vitro stability

The stability of [^{188}Re]Re-V_HH was evaluated by incubating the radioconjugate in saline or human serum (Merck) for 48 h. In general, ~4-5 MBq of the radioconjugate was incubated at 37 °C after a 3-fold dilution in saline or a 5-fold dilution in serum. In addition, the effect of ascorbate and pH on the stability of the conjugate in saline was tested by adding 30 µL of a 0.63 M solution of ascorbate at pH 5.5 or pH 7.0 to achieve the same respective pH in the final solutions. The final concentration of ascorbate was 32 mM in each solution. Aliquots were removed at various timepoints and analysed by iTLC (ACN/H_2O, 3:1) and radio-HPLC (HPLC method D). Saline samples were analysed by iTLC and HPLC, while serum samples were only analysed by iTLC. The data were expressed as a percentage of activity associated with the V_HH at a given time point.

Cell lines

Human glioblastoma (U87MG) and pancreatic cancer (BxPC3) cell lines were obtained from ATCC. U87MG cells were cultured in Eagle's Minimum Essential Medium (EMEM; ATCC-30-2003), while BxPC3 cells were maintained in RPMI-1640 (Gibco A1049101), both supplemented with 10% foetal bovine serum (Gibco 10270106), 100 units/mL penicillin, and 100 µg/mL streptomycin (Gibco 15140122). Cultures were kept in a humidified incubator at 37 °C with 5% CO_2. To ensure cell line integrity, regular checks for *Mycoplasma* contamination were performed using the VenorGeM® Classic *Mycoplasma* Detection Kit for Conventional PCR (Minerva Biolabs 11-1050), following the manufacturer's guidelines.

In vitro cell-binding assays

The c-Met-expressing U87MG and BxPC3 cell lines were chosen to study total cell binding of [^{188}Re]Re-V_HH. Both cell lines were tested in suspension as a consequence of the lower molar activity reached in the radiolabelling. Each cell suspension was diluted with HEPES-buffered medium to obtain a final concentration of 2 x 10^6 cells/mL. From each cell suspension, 6 x 0.5 mL was transferred into 6 x 1.5 mL Protein LoBind microcentrifuge tubes. Each tube was then incubated with 0.5 mL of 1 nM [^{188}Re]Re-V_HH in medium at 37 °C for 2 h on a rocking platform within the incubator to maintain a single cell suspension. In parallel, receptor blocking was performed by addition of an excess of non-chelator associated V_HH-NEM (1 nmol) to 3 of the 6 tubes per cell line. At the end of incubation, all tubes were centrifuged at 100 rcf for 7 min and the supernatant was collected (wash fraction). The pellet was washed with a further 0.5 mL PBS and the supernatant again pooled with the wash fraction. Each pellet was thereafter resuspended in 1.5 mL PBS and collected separately (bound fraction). The amount of [^{188}Re]Re-V_HH associated with the cells (bound fraction) was assessed using an automatic gamma counter (2480Wizard^2, Perkin Elmer, Belgium) and counts were decay corrected to the start of counting.

Preclinical studies

Animals

All animal experiments were performed in compliance with the Ethical Committee Animal Studies of Medanex Clinic (EC MxCl 2023-215), the Belgian laboratory animal legislation and the European Communities Council Directive of September 2010 (2010/63/EU). Male NMRI nude Foxn1$^{nu/nu}$ mice were purchased from Janvier (Bio Services, Uden, The Netherlands) and housed in individually-ventilated cages under standard laboratory conditions (22 °C, 12 h light/dark cycle) at the animal facility of SCK CEN. All animals had access to food and water ad libitum.

Tumour inoculation

BxPC3 tumour models were generated by anesthetizing male NMRI nude mice (8 weeks old) with 2.5% isoflurane in O_2 at a flow rate of 0.2 L.min^{-1} and subcutaneously injecting on the right shoulder 3 x 10^6 BxPC3 cells, resuspended in PBS with 30% Cultrex.[13] Tumours were left to develop for a minimum of 2 weeks before experiments were performed.

Ex vivo biodistribution

The pharmacokinetic behaviour of [^{188}Re]Re-V_HH was evaluated by biodistribution studies in BxPC3 tumour-bearing xenograft mice. All mice were anesthetised with isoflurane (2.5% in O_2, 1 L.min^{-1}) and injected with 1.11 nmol (1.44 – 1.84 MBq) of [^{188}Re]Re-V_HH via a tail vein. The mice were sacrificed by an overdose of pentobarbital (200 µL of a 60 mg/mL solution) at 4 h, 12 h, 24 h or 48 h post injection (p.i.) (n = 4 animals per time point). Blood was collected by cardiac puncture. Blood and the organs of interest were collected in tared tubes, weighed and their uptake of radioactivity was determined using an automated gamma counter (2480Wizard^2, Perkin Elmer, Zaventem, Belgium). Collected counts were converted to MBq based on a calibration factor. All radioactivity measurements were decay corrected to the time of injection, and the injected activity per gram of tissue (% IA/g) was calculated based on measured organ weights. For the calculation of the total activity in the blood, bone and muscle, their respective masses were assumed to be 7%, 12% and 40%, respectively, of the total mouse body mass according to literature values.[14,15] The results are presented as standardised uptake values (SUV), determined using SUV = (MBq_{tissue}/g_{tissue})/($MBq_{injected}/g_{mouse}$).

Characterisation of synthesised compounds

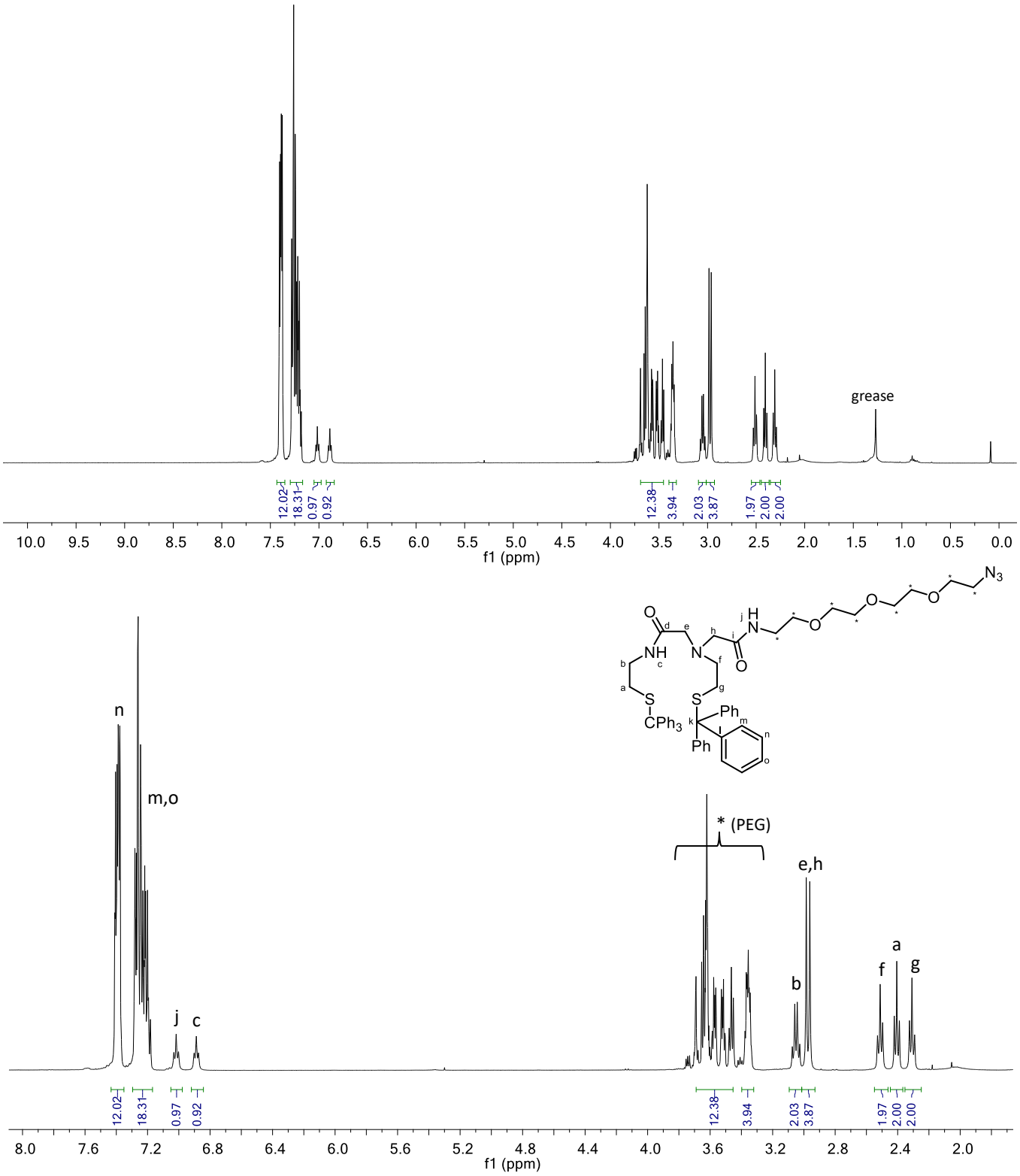

Figure S1. ^{1}H NMR spectrum (full and expanded) of compound **4** in $CDCl_3$.

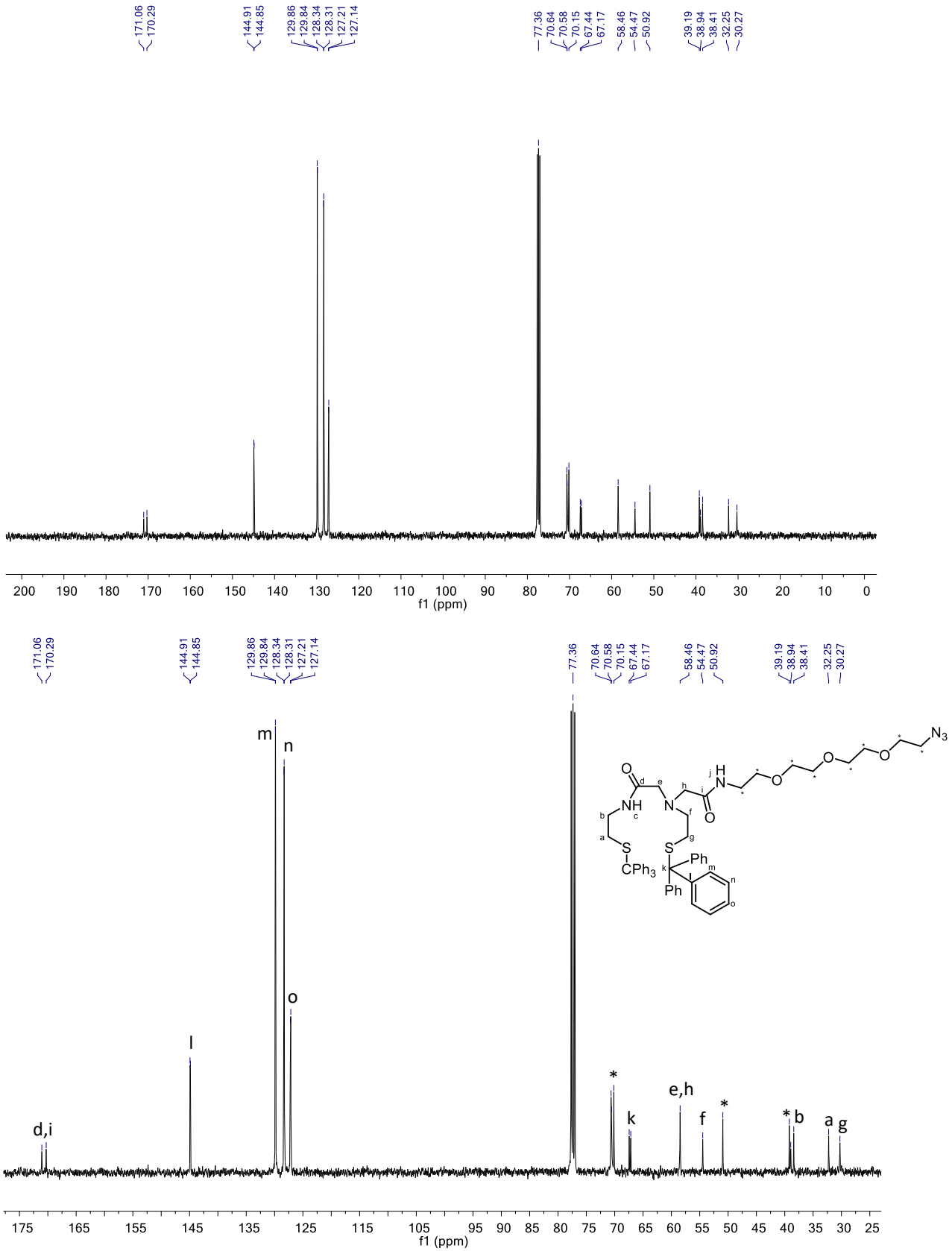

Figure S2. $^{13}C\{^{1}H\}$ NMR spectrum (full and expanded) of compound **4** in $CDCl_3$.

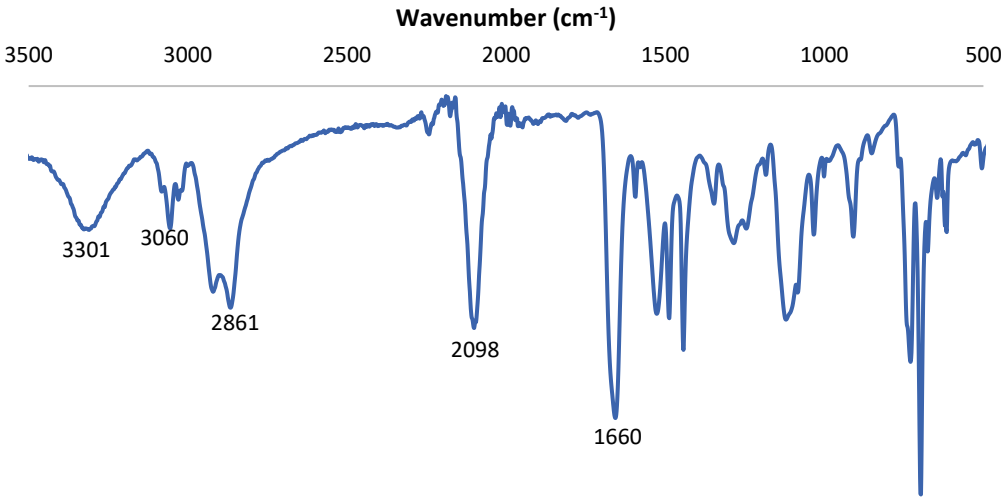

Figure S3: FT-IR spectrum of compound **4**.

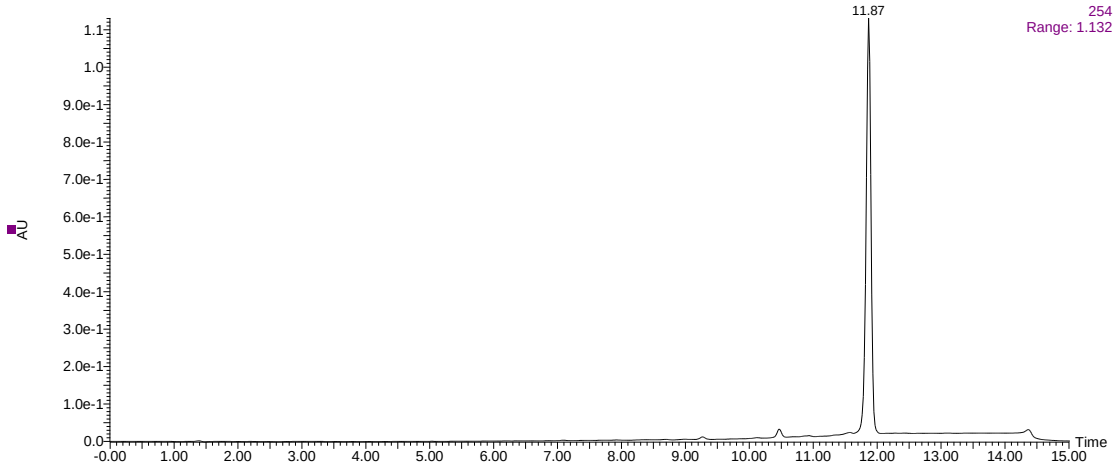

Figure S4: HPLC chromatogram of compound **4** at 254 nm using HPLC method A.

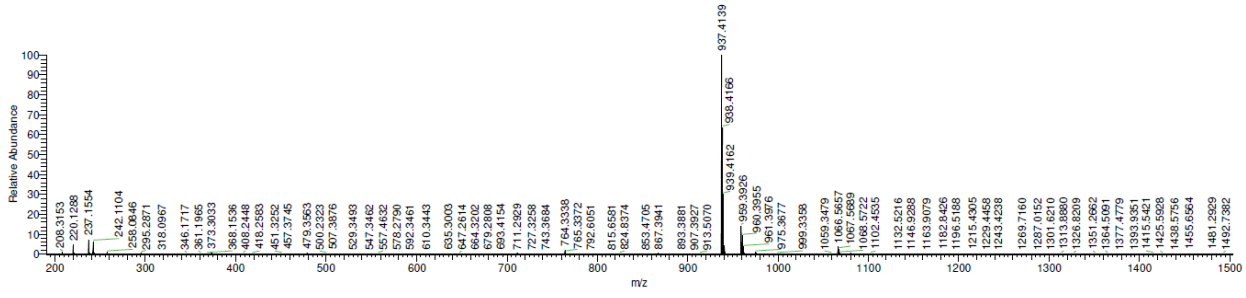

Figure S5: HR ESI-MS spectrum of compound **4**.

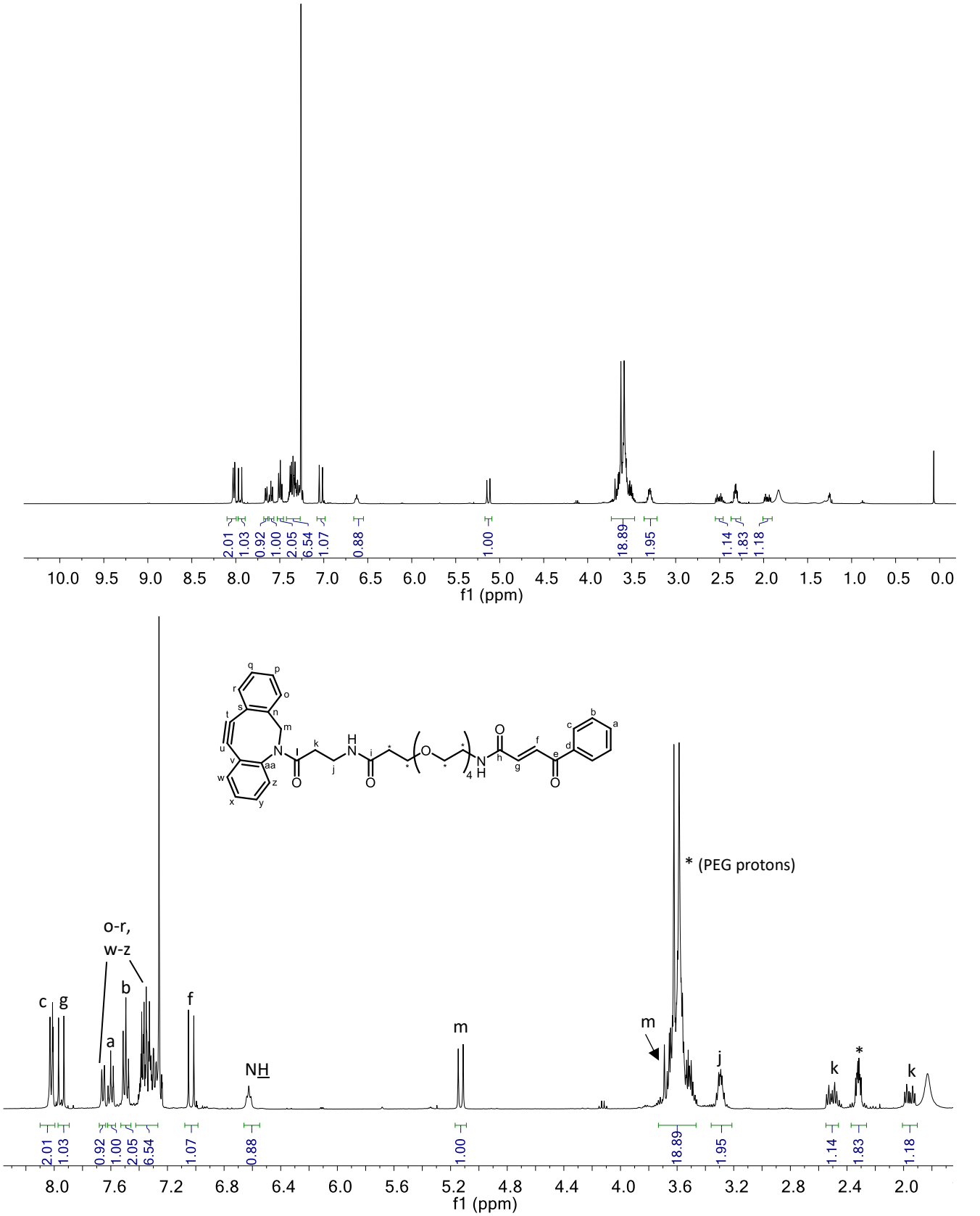

Figure S6. ^{1}H NMR spectrum (full and expanded) of compound **7** in $CDCl_3$.

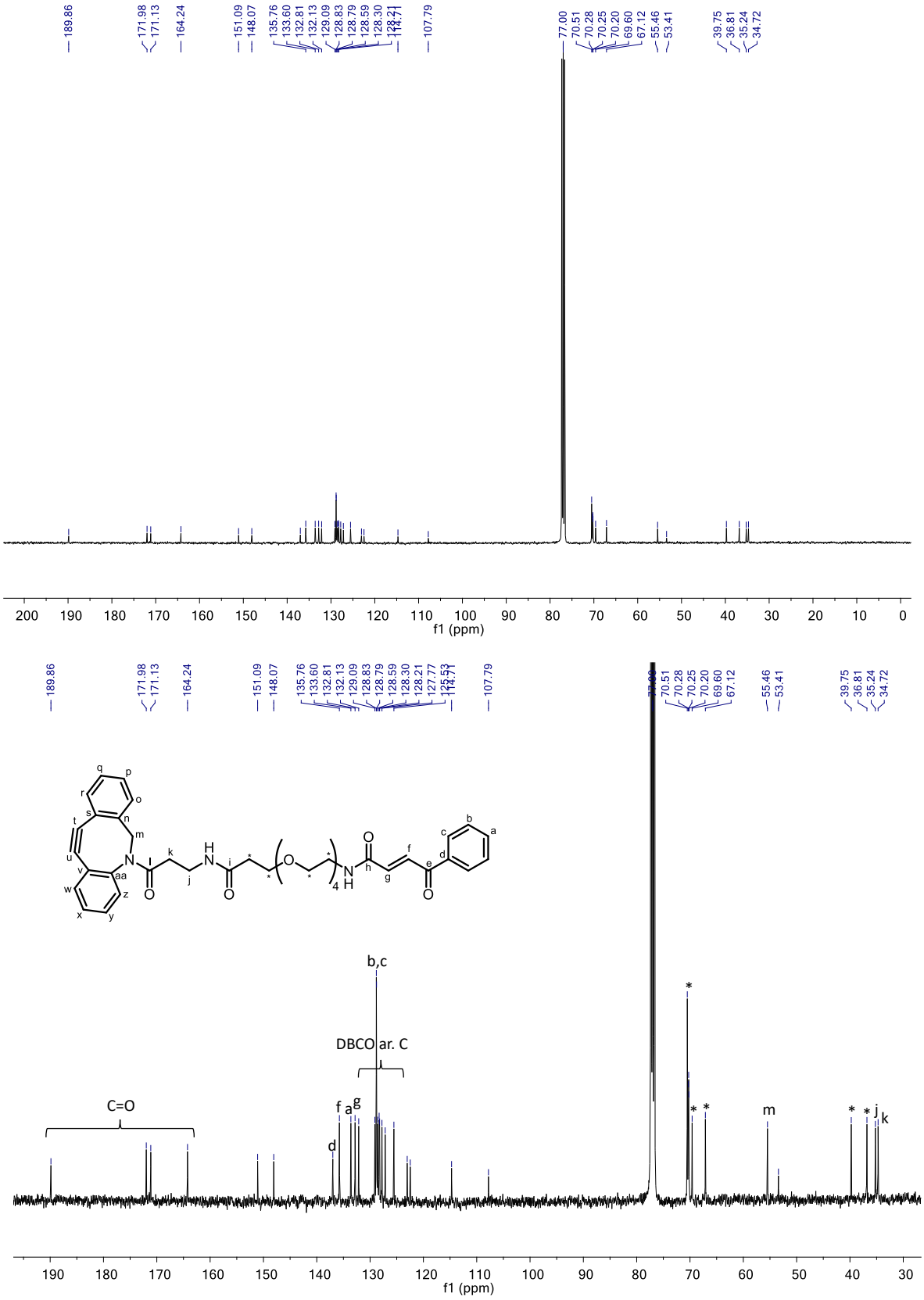

Figure S7. $^{13}C\{^{1}H\}$ NMR spectrum (full and expanded) of compound **7** in $CDCl_3$.

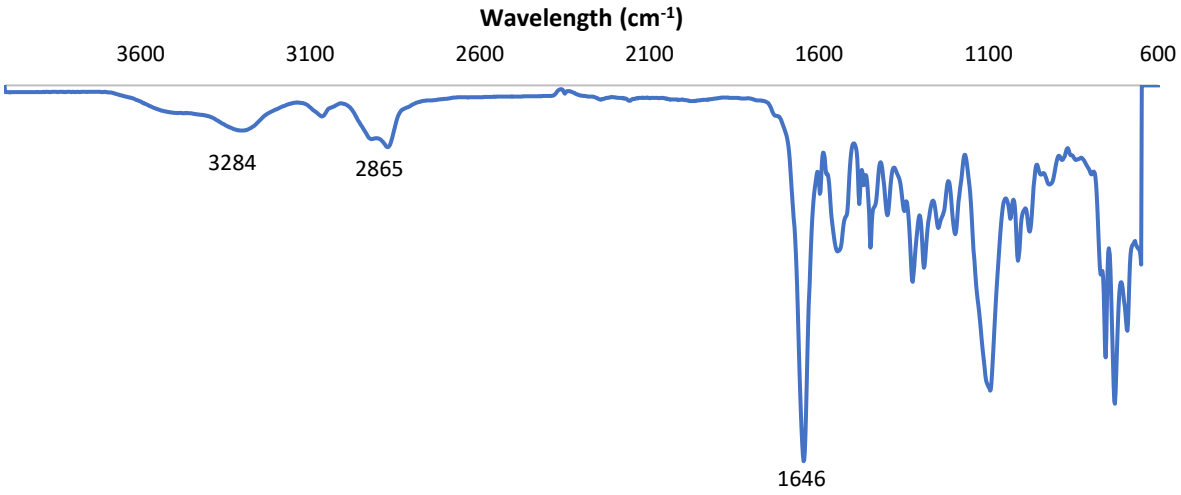

Figure S8: FT-IR spectrum of compound **7**.

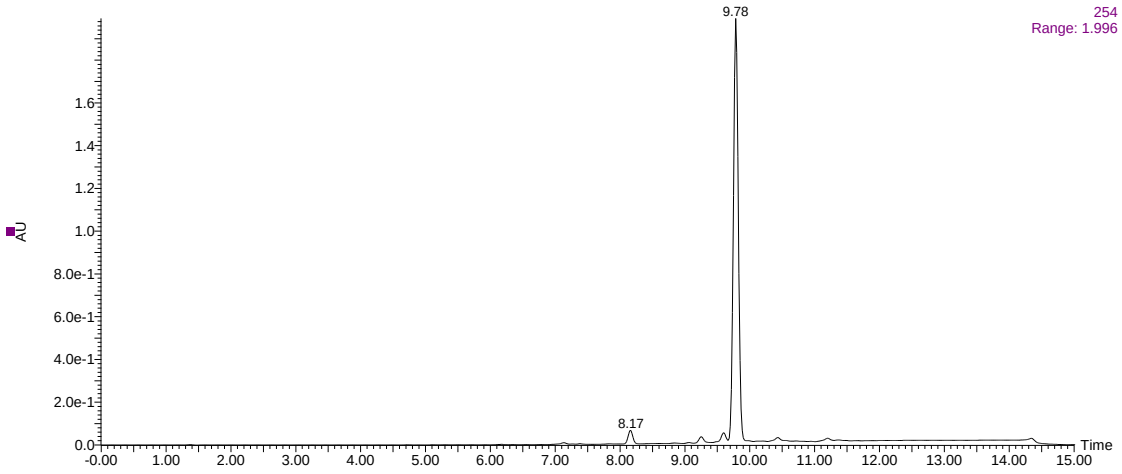

Figure S9: HPLC chromatogram of compound **7** at 254 nm using HPLC method A.

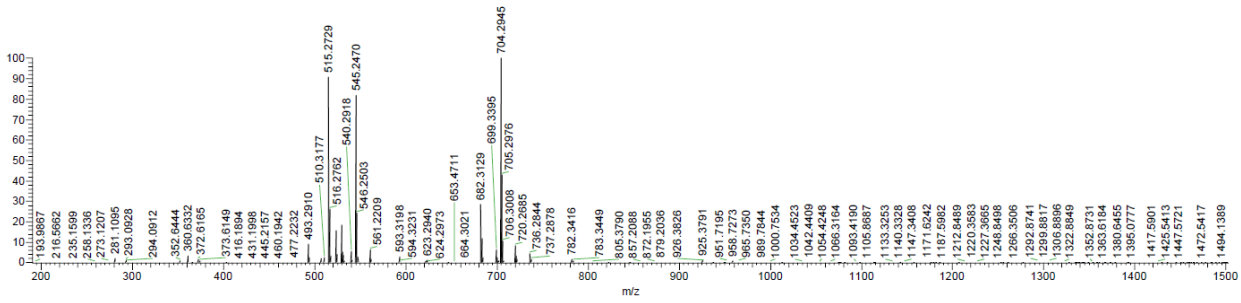

Figure S10: ESI-MS spectrum of compound **7**.

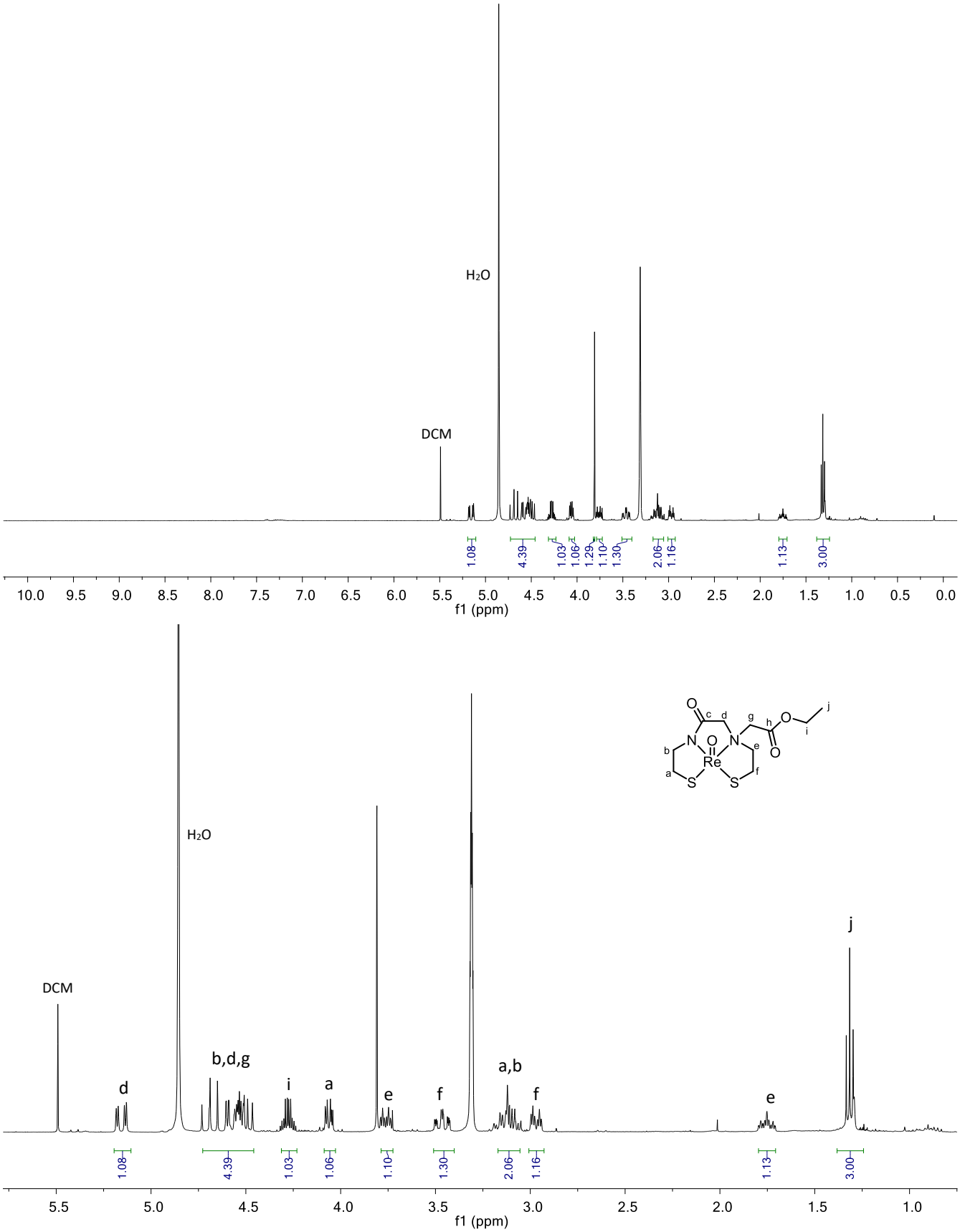

Figure S11. ^{1}H NMR spectrum (full and expanded) of complex **Re-2** in CD_3OD.

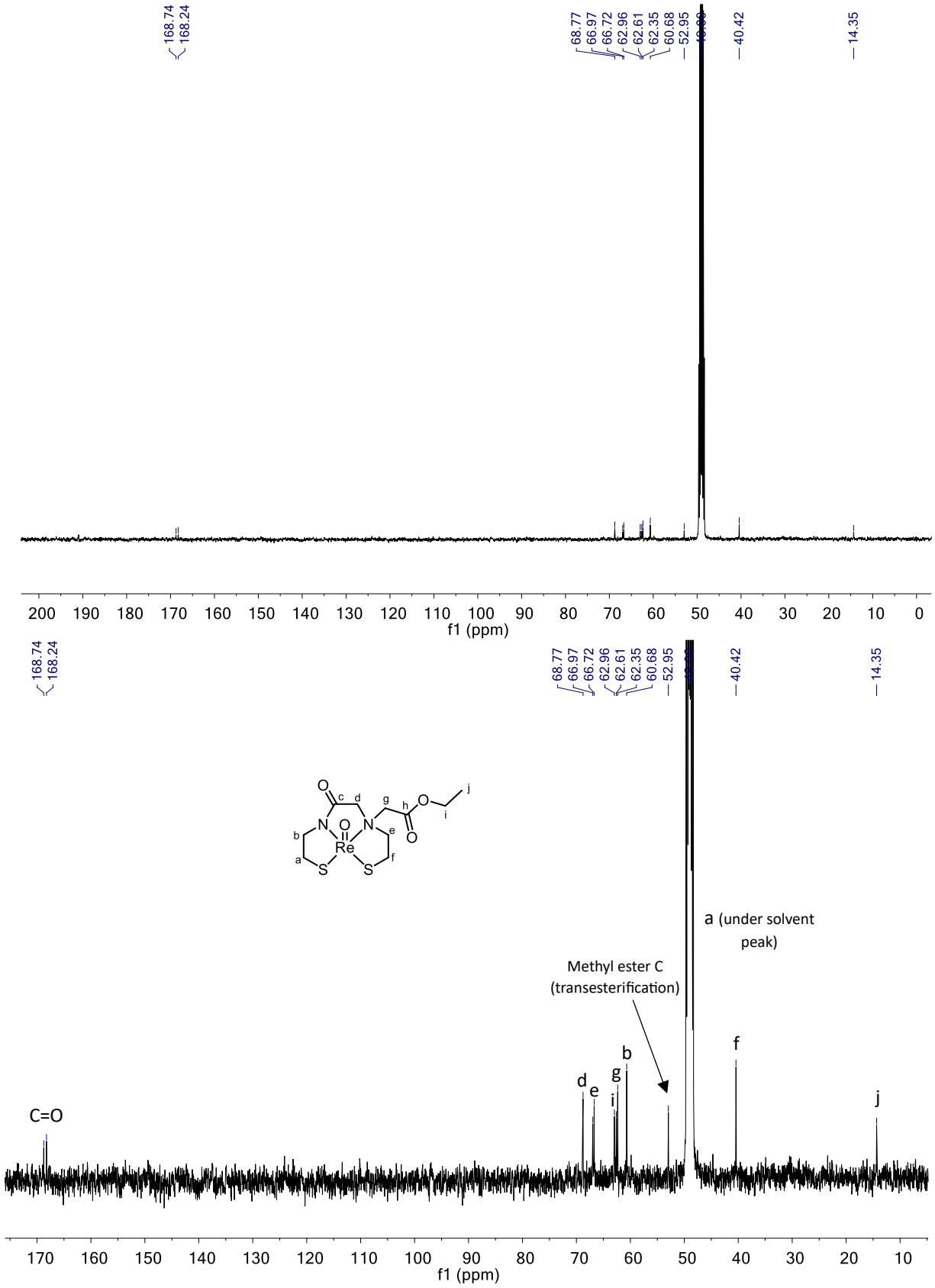

Figure S12. $^{13}C\{^{1}H\}$ NMR spectrum (full and expanded) of complex **Re-2** in CD_3OD.

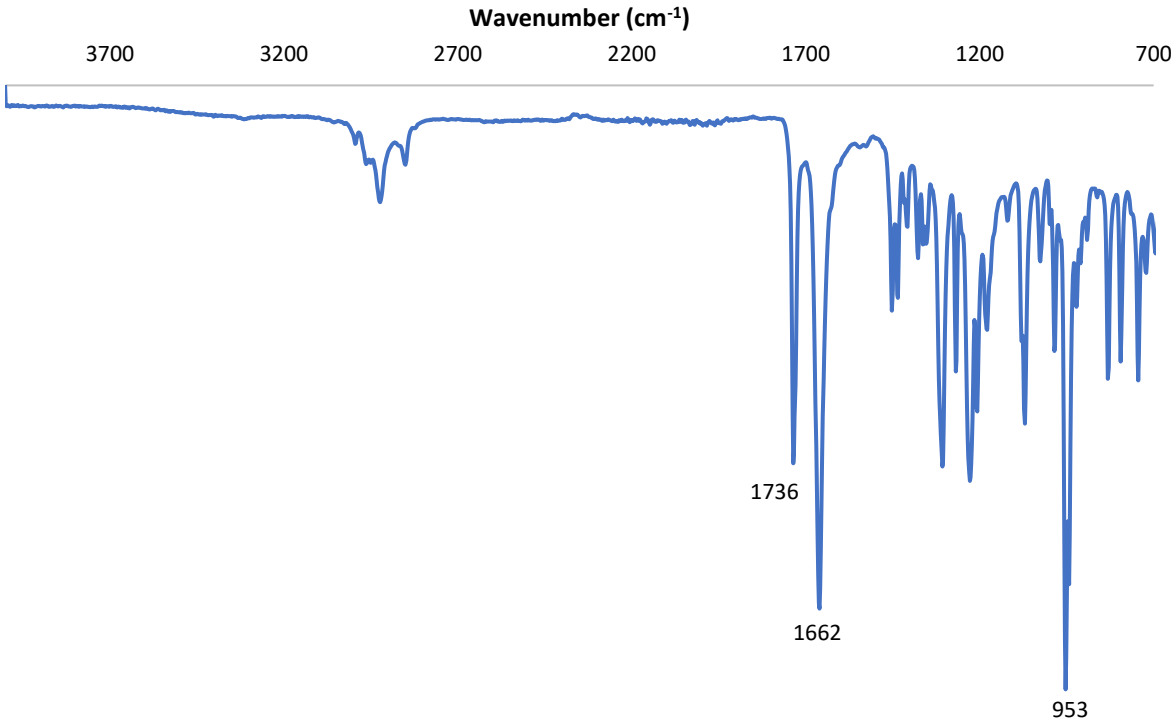

Figure S13: FT-IR spectrum of complex **Re-2**.

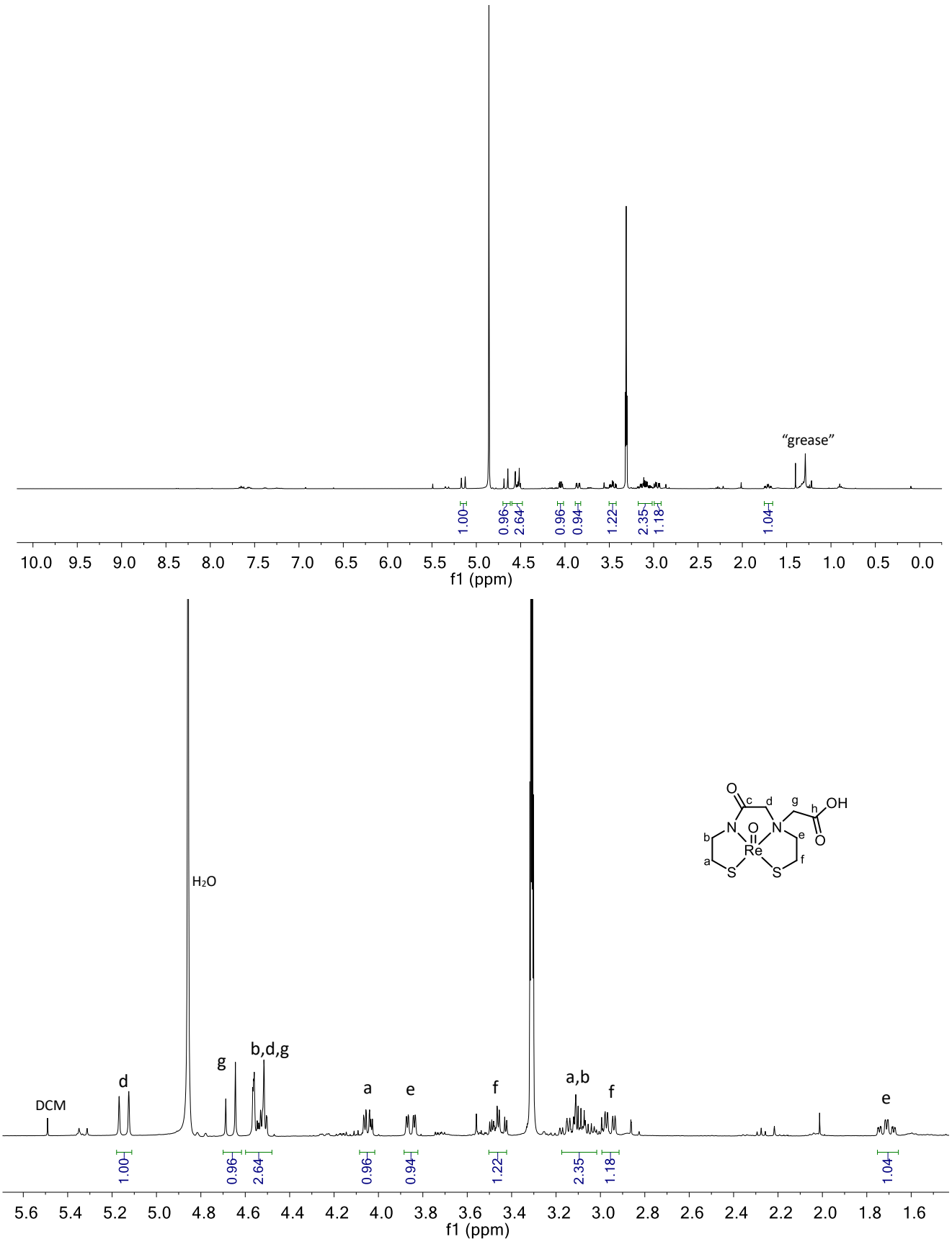

Figure S14. ^{1}H NMR spectrum (full and expanded) of complex **Re-3** in CD_3OD.

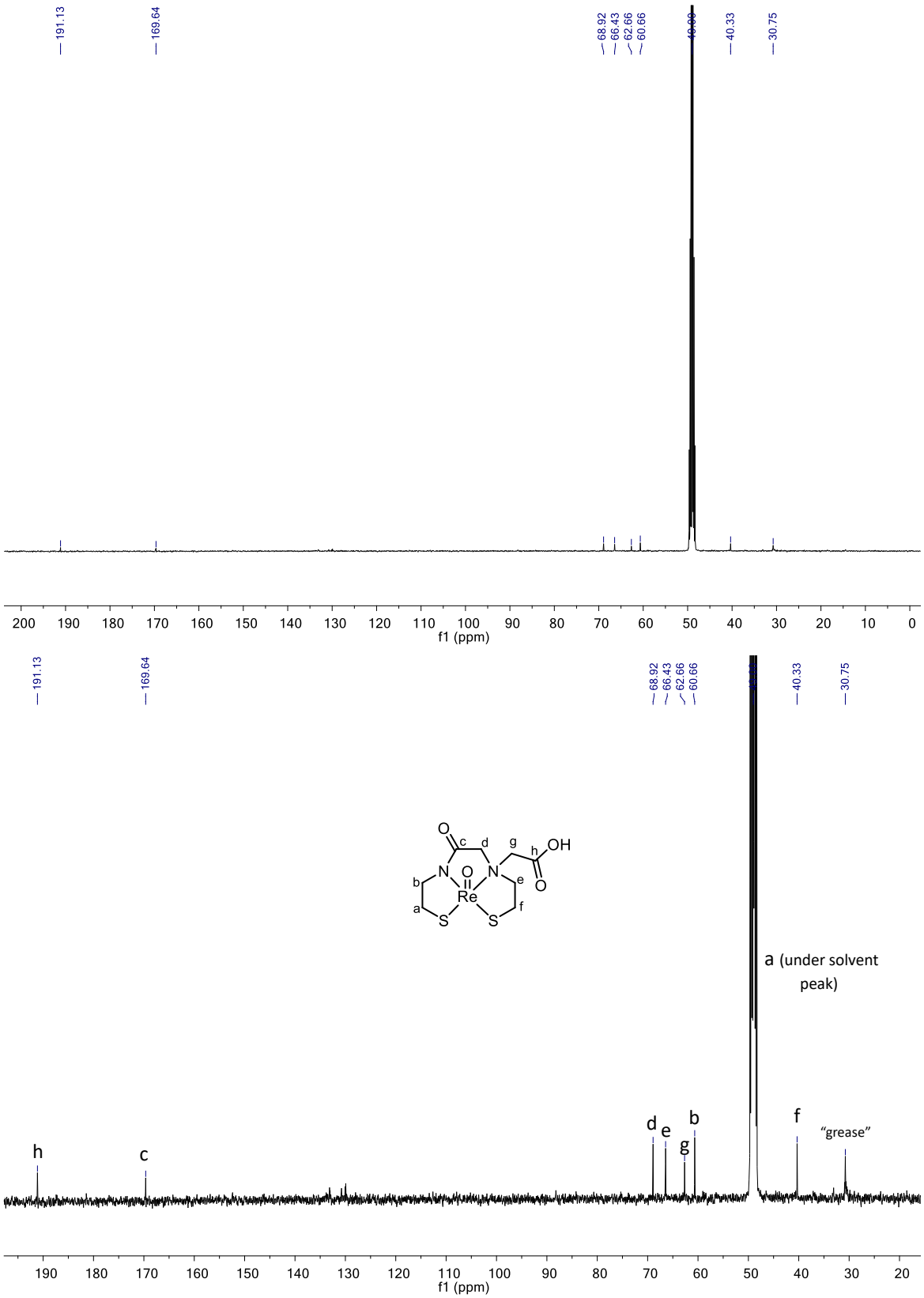

Figure S15. $^{13}C\{^{1}H\}$ NMR spectrum (full and expanded) of complex **Re-3** in CD_3OD.

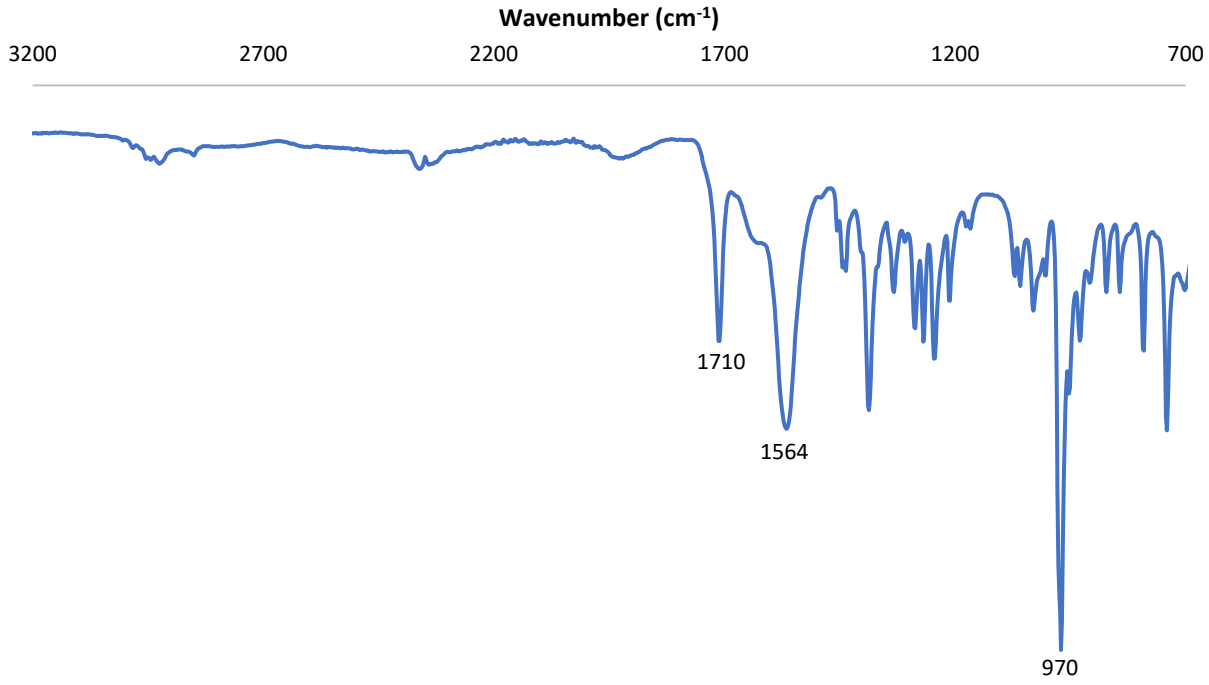

Figure S16. FT-IR spectrum of complex **Re-3**.

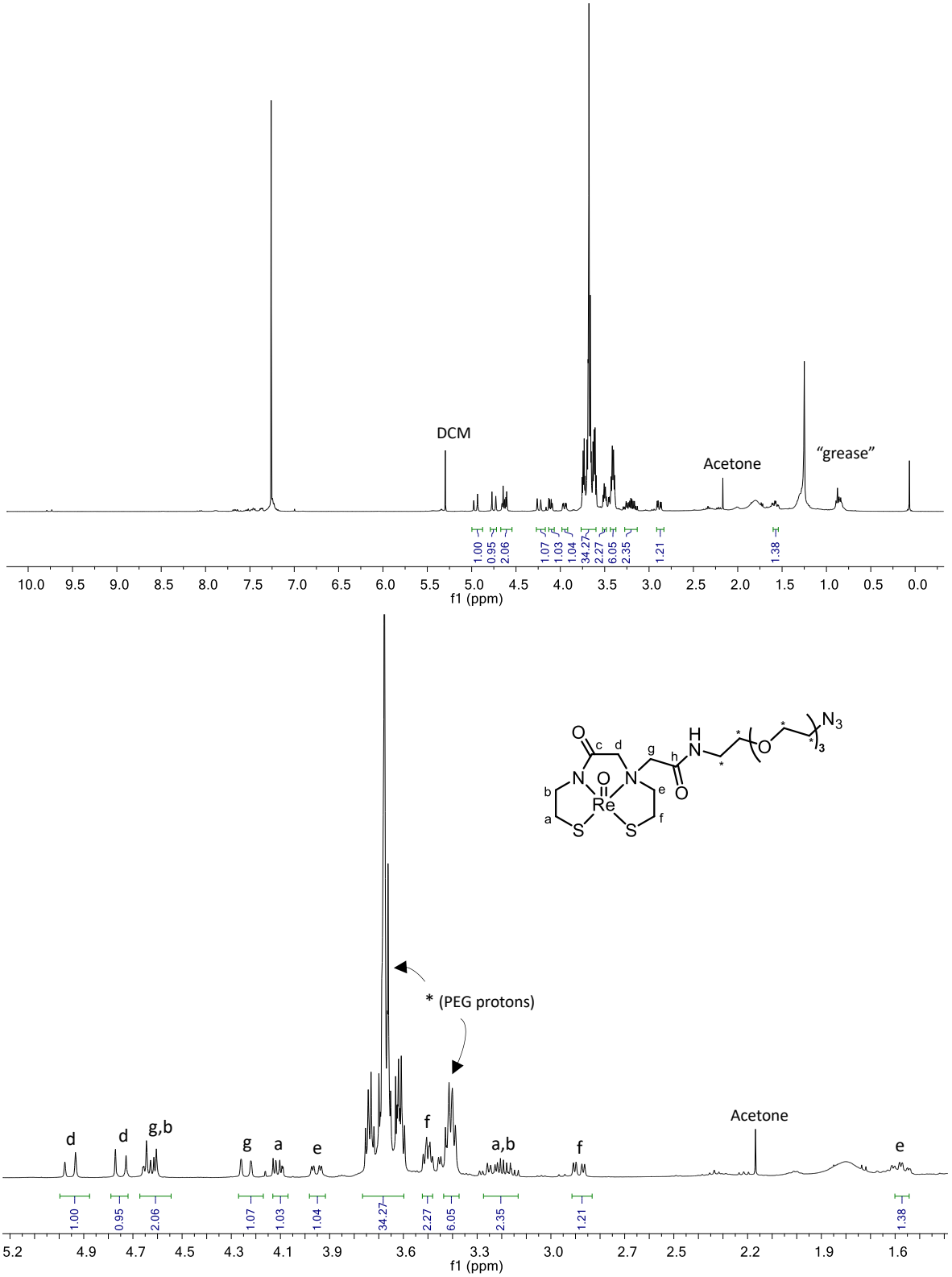

Figure S17. ^{1}H NMR spectrum (full and expanded) of complex **Re-4** in $CDCl_3$.

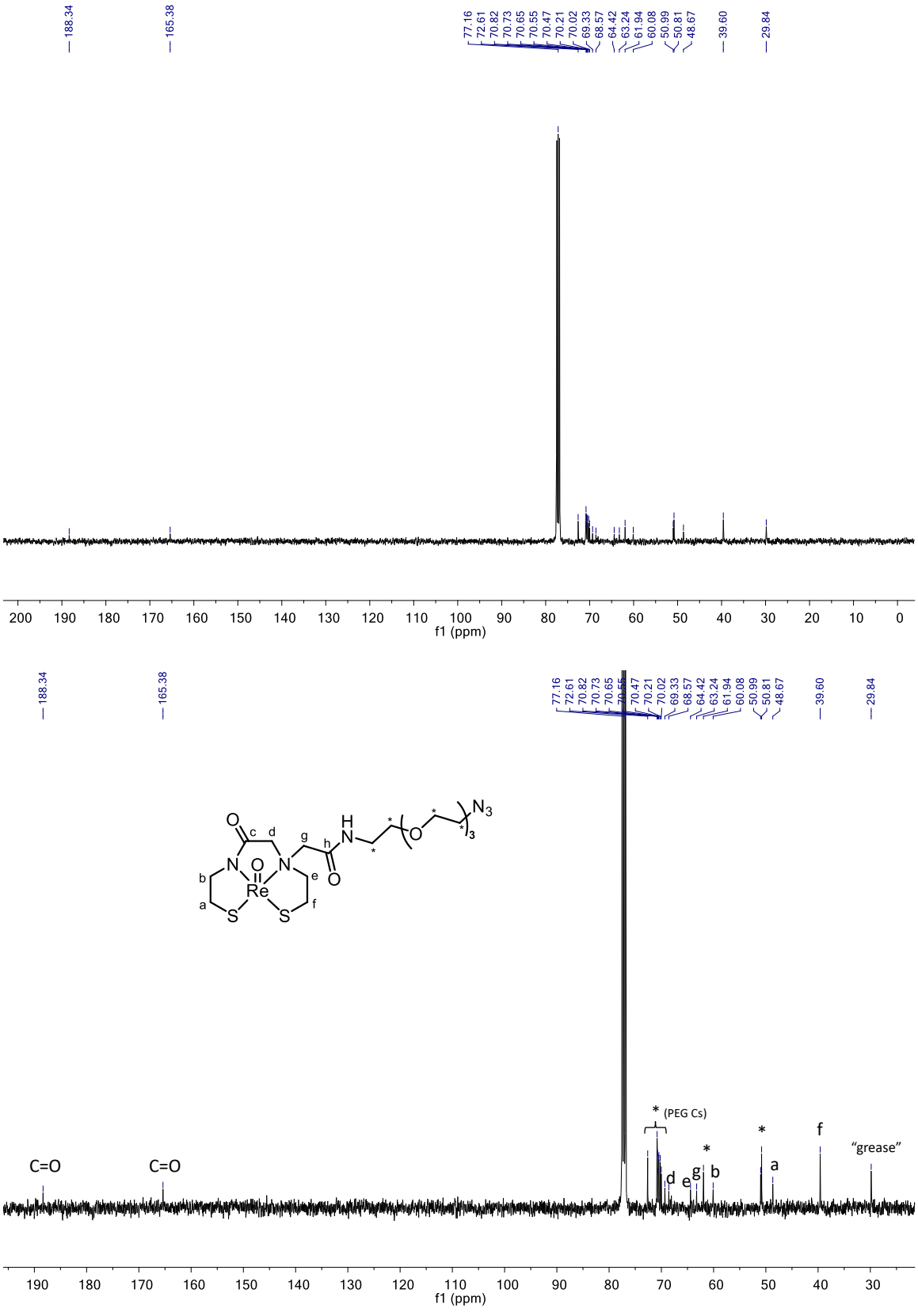

Figure S18. $^{13}C\{^{1}H\}$ NMR spectrum (full and expanded) of complex **Re-4** in $CDCl_3$.

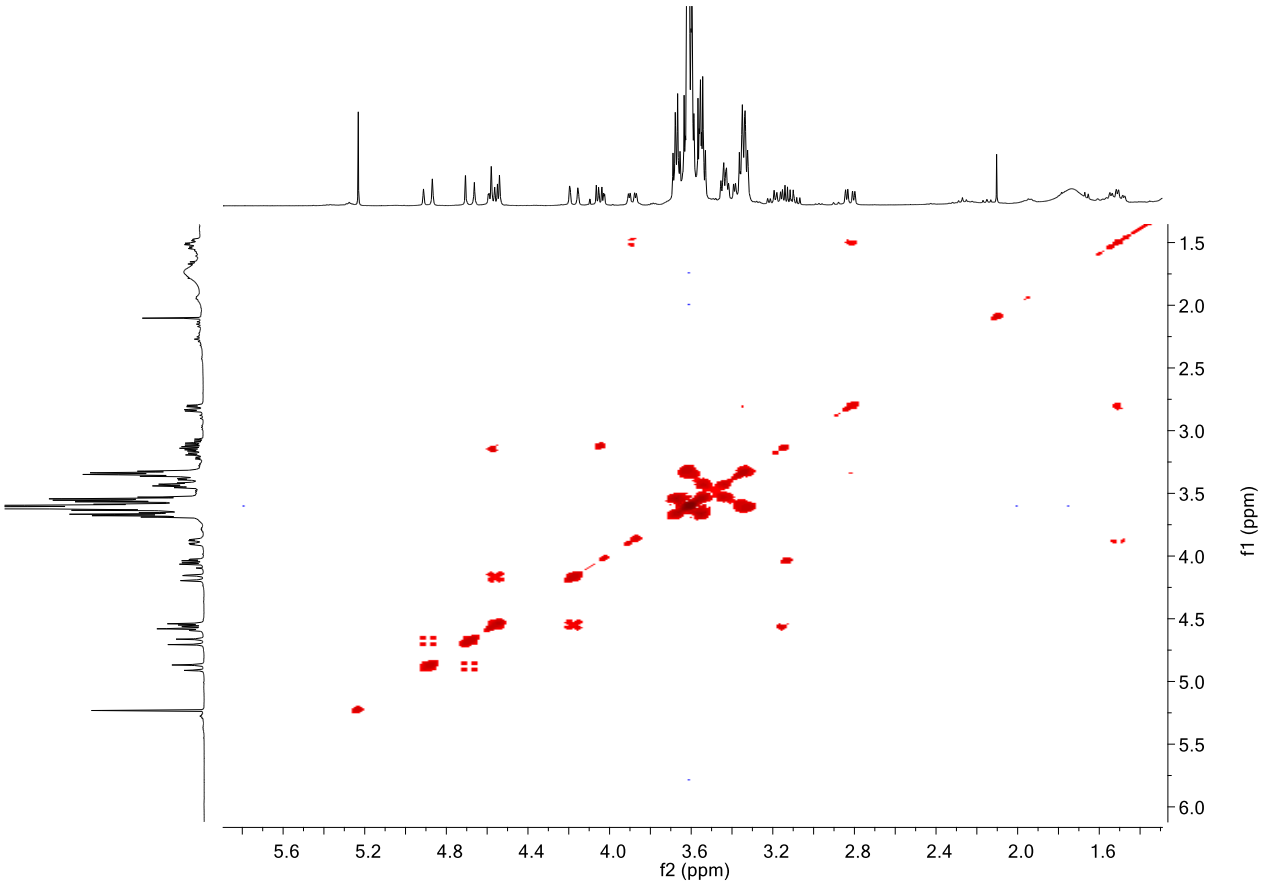

Figure S19. ^{1}H-^{1}H COSY spectrum of complex **Re-4** in $CDCl_3$.

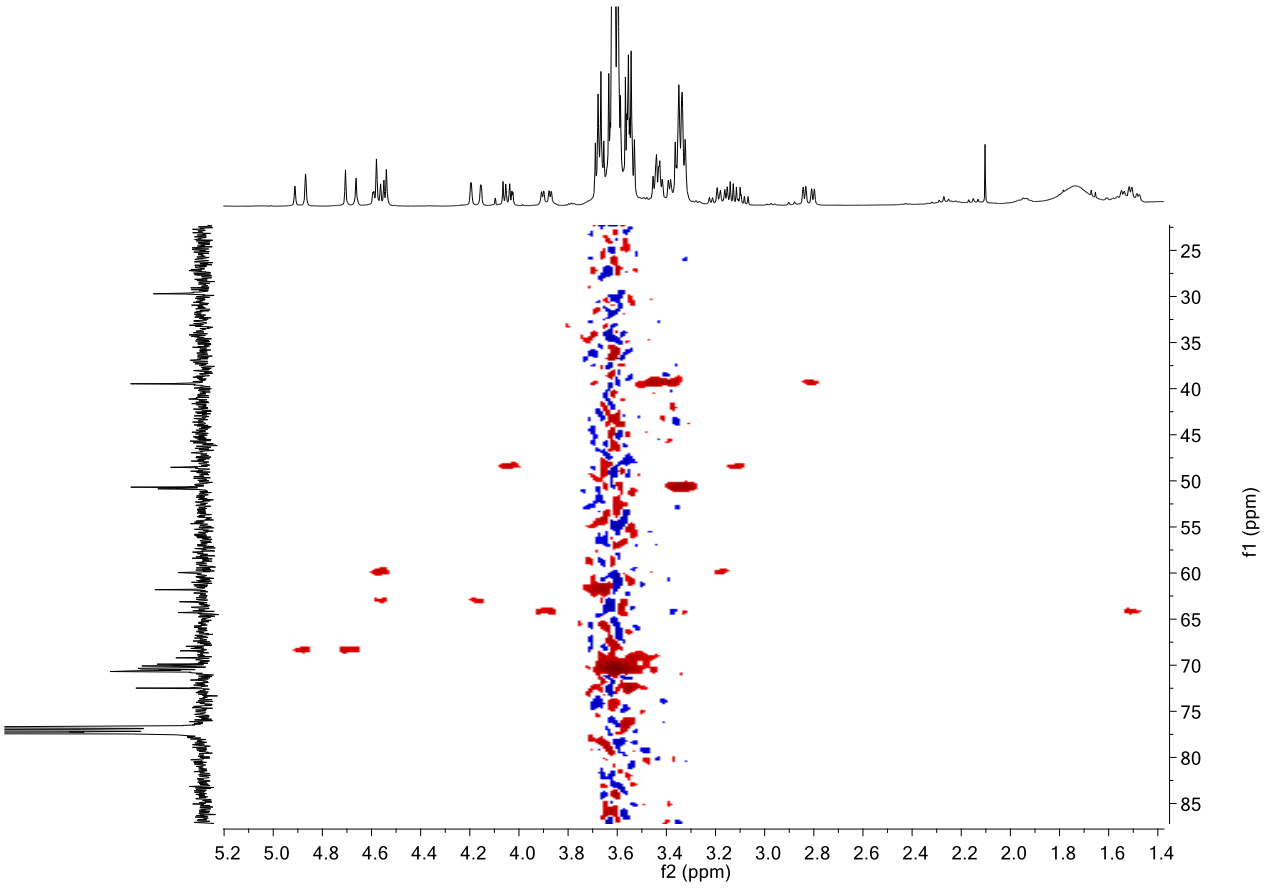

Figure S20. ^{1}H-^{13}C HSQC spectrum of complex **Re-4** in $CDCl_3$.

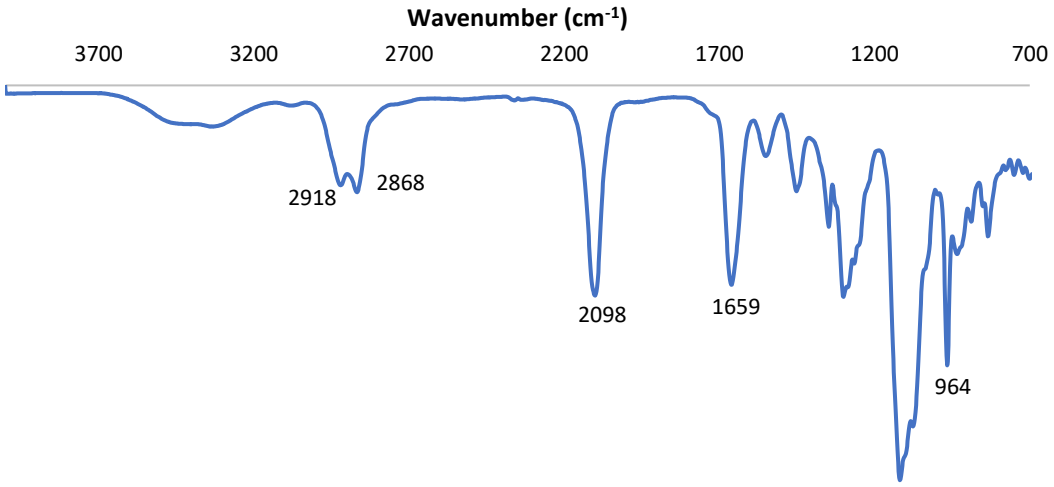

Figure S21. FT-IR spectrum of complex **Re-4**.

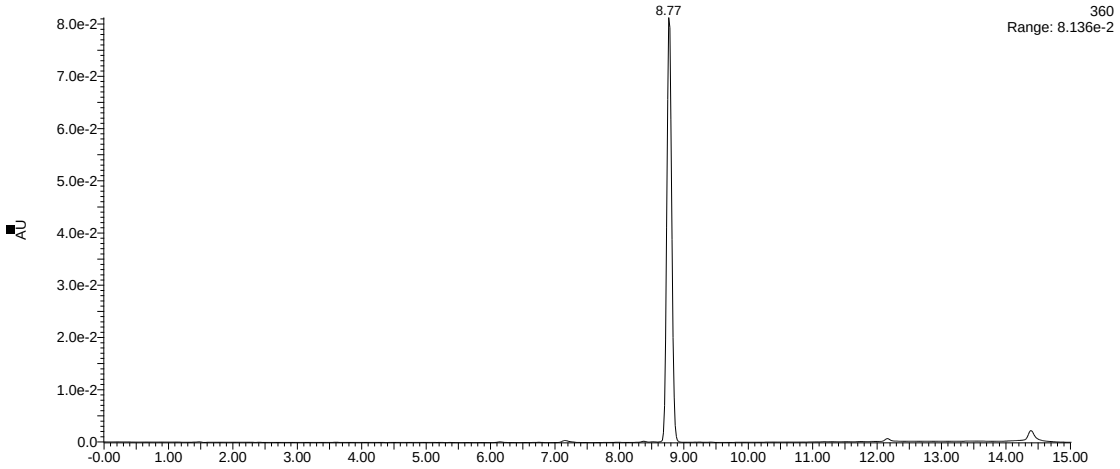

Figure S22. HPLC chromatogram of complex **Re-4** at 360 nm using HPLC method A.

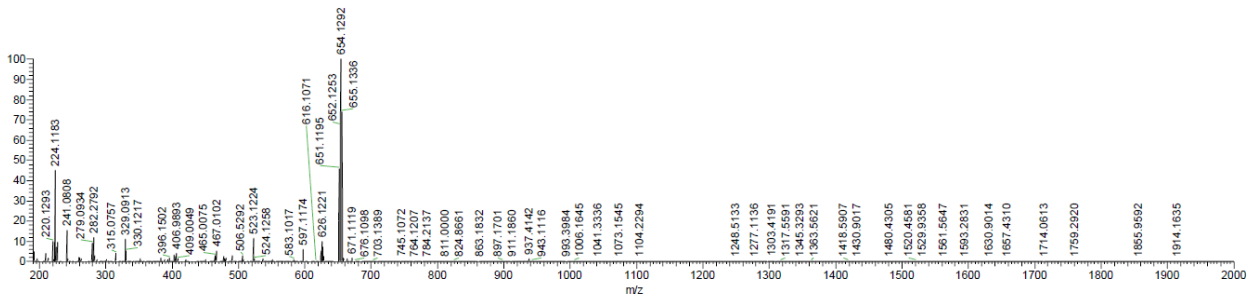

Figure S23. HR ESI-MS spectrum of complex **Re-4**.

X-ray crystallography

Table S1. Crystal data and structure refinement parameters for **Re-2** and **Re-3**.

	Re-2	**Re-3**
Empirical formula	$C_{10}H_{17}N_2O_4ReS_2$	$C_8H_{13}N_2O_4ReS_2$
Formula weight	479.57	451.52
Temperature/K	160(1)	160(1)
Crystal system	monoclinic	orthorhombic
Space group	$P2_1/c$	Fdd2
a/Å	7.79663(15)	27.8226(4)
b/Å	10.5671(2)	20.2490(3)
c/Å	18.0745(3)	8.86174(14)
α/°	90	90
β/°	101.4253(18)	90
γ/°	90	90
Volume/Å^3	1459.62(5)	4992.52(13)
Z	4	16
ρ_{calc}g/cm^3	2.182	2.403
μ/mm^{-1}	19.077	22.251
F(000)	920.0	3424.0
Crystal size/mm^3	0.11 × 0.1 × 0.07	0.2 × 0.14 × 0.07
Radiation	Cu Kα (λ = 1.54184)	Cu Kα (λ = 1.54184)
2Θ range for data collection/°	9.746 to 136.458	10.808 to 136.476
Index ranges	-9 ≤ h ≤ 9, -11 ≤ k ≤ 12, -21 ≤ l ≤ 21	-33 ≤ h ≤ 32, -24 ≤ k ≤ 24, -10 ≤ l ≤ 10
Reflections collected	14212	12564
Independent reflections	2676 [R_{int} = 0.0284, R_{sigma} = 0.0195]	2223 [R_{int} = 0.0352, R_{sigma} = 0.0202]
Data/restraints/parameters	2676/63/194	2223/1/156
Goodness-of-fit on F^2	1.276	1.043
Final R indexes [I>=2σ (I)]	R_1 = 0.0266, wR_2 = 0.0578	R_1 = 0.0298, wR_2 = 0.0752
Final R indexes [all data]	R_1 = 0.0271, wR_2 = 0.0581	R_1 = 0.0298, wR_2 = 0.0753
Largest diff. peak/hole / e Å^{-3}	0.85/-1.12	1.03/-1.13

V_HH Bioconjugation

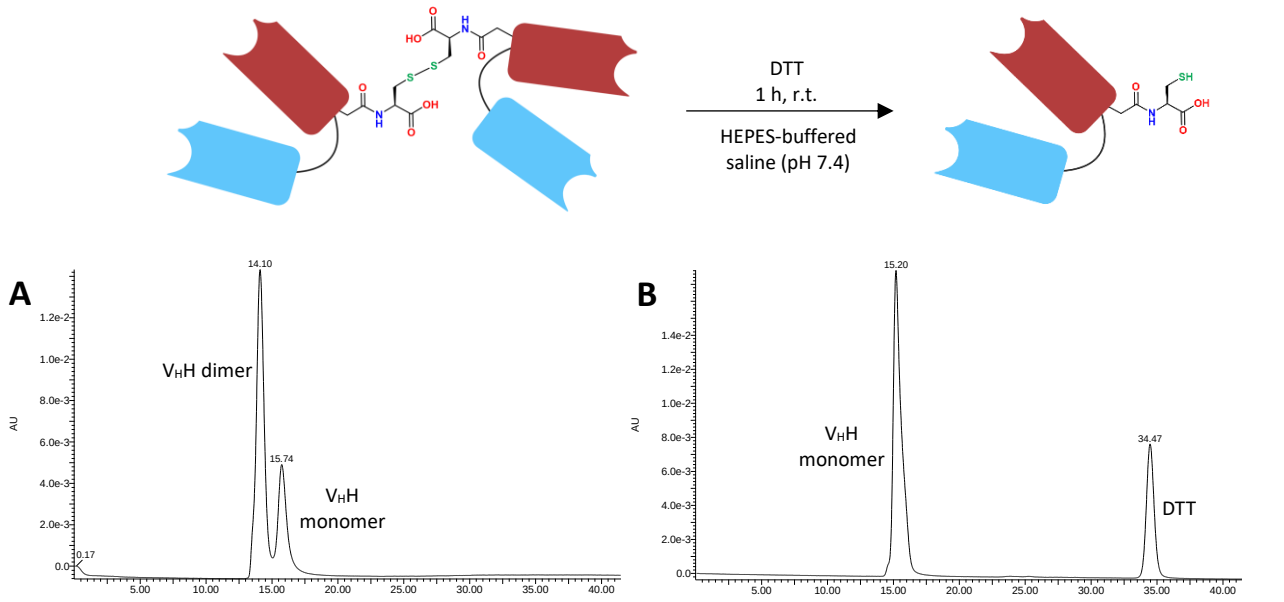

Figure S24. SEC-HPLC chromatograms (280 nm) of (**A**) the dimeric form of the V_HH and (**B**) the monomeric form of the V_HH after reduction with DTT. (HPLC method C)

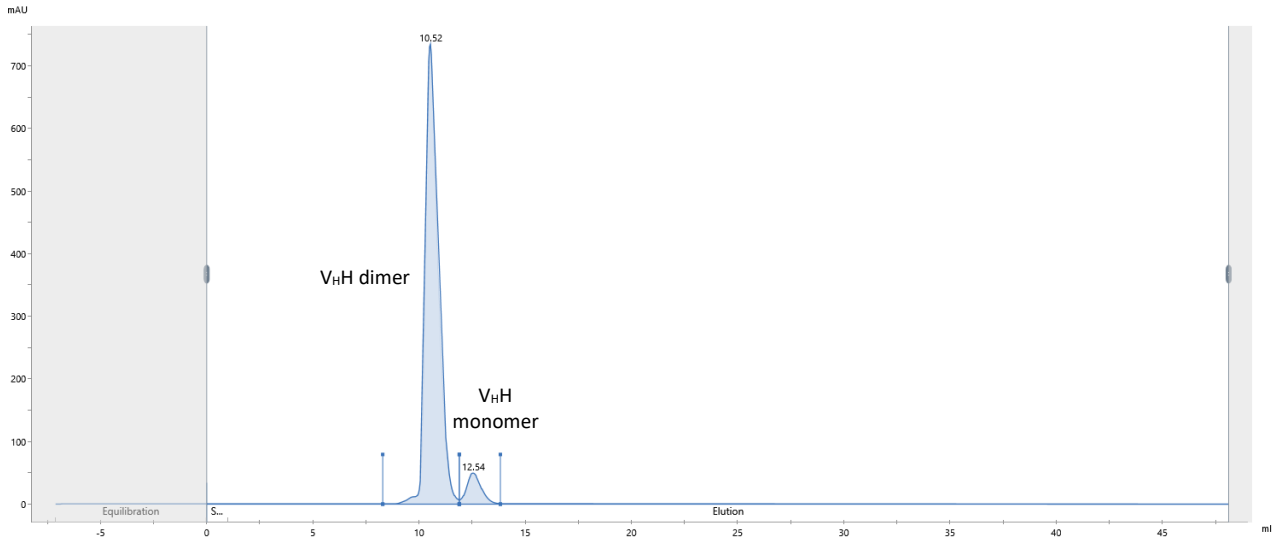

Figure S25. SEC-HPLC chromatogram of the dimeric form of the V_HH using HPLC method C on an ÄKTA pure™ chromatography system.

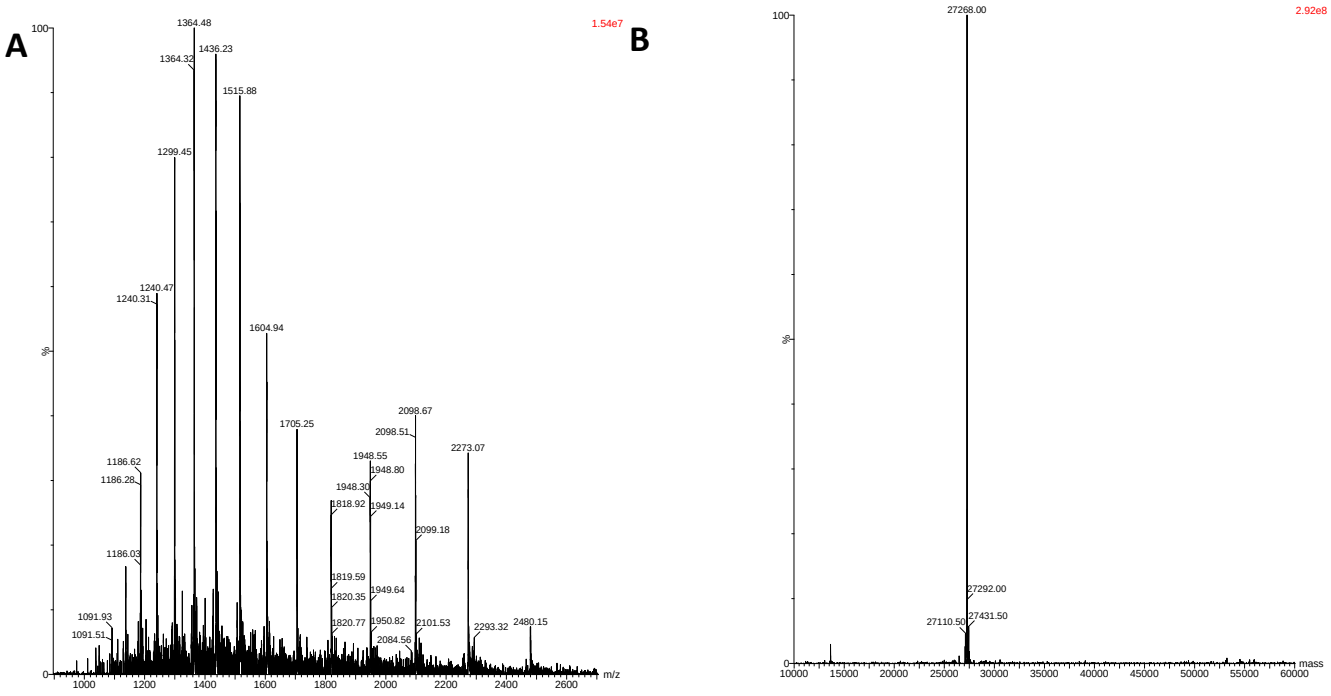

Figure S26. LC-MS analysis of DBCO-PEG$_4$-V$_H$H. (**A**) Continuous ion series and (**B**) deconvoluted mass spectrum obtained using the MaxEnt algorithm. Solvent: 1:1 milli-Q water and acetonitrile (with 0.1% formic acid). Flow rate: 1 mL/min.

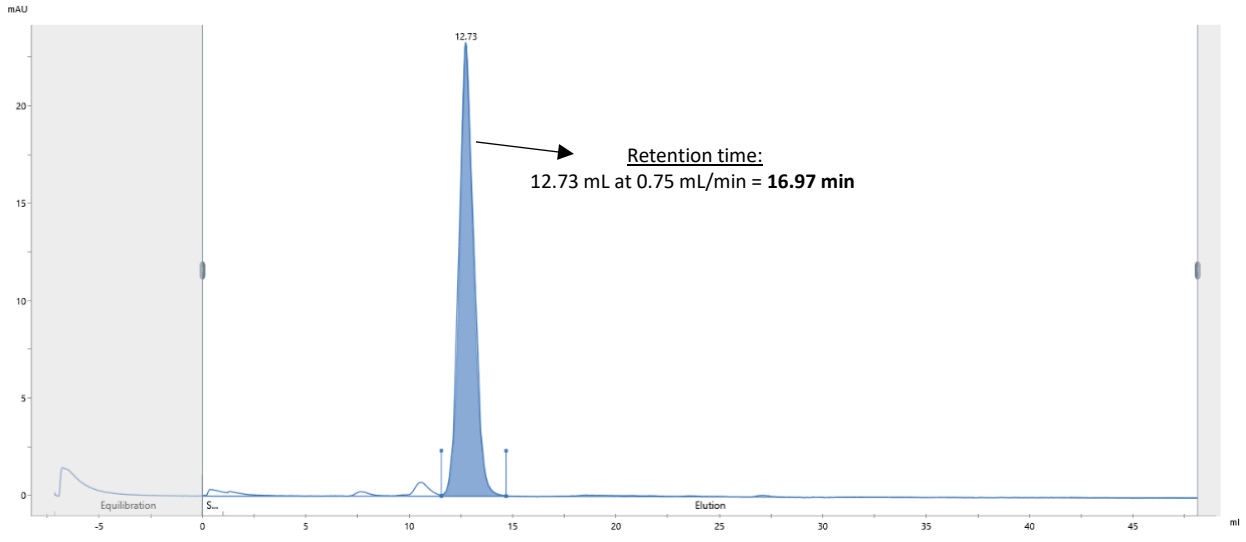

Figure S27. SEC-HPLC chromatogram of DBCO-PEG$_4$-V$_H$H showing its purity using HPLC method C on an ÄKTA pure™ chromatography system. The purity of the conjugate (highlighted) is 97.2%.

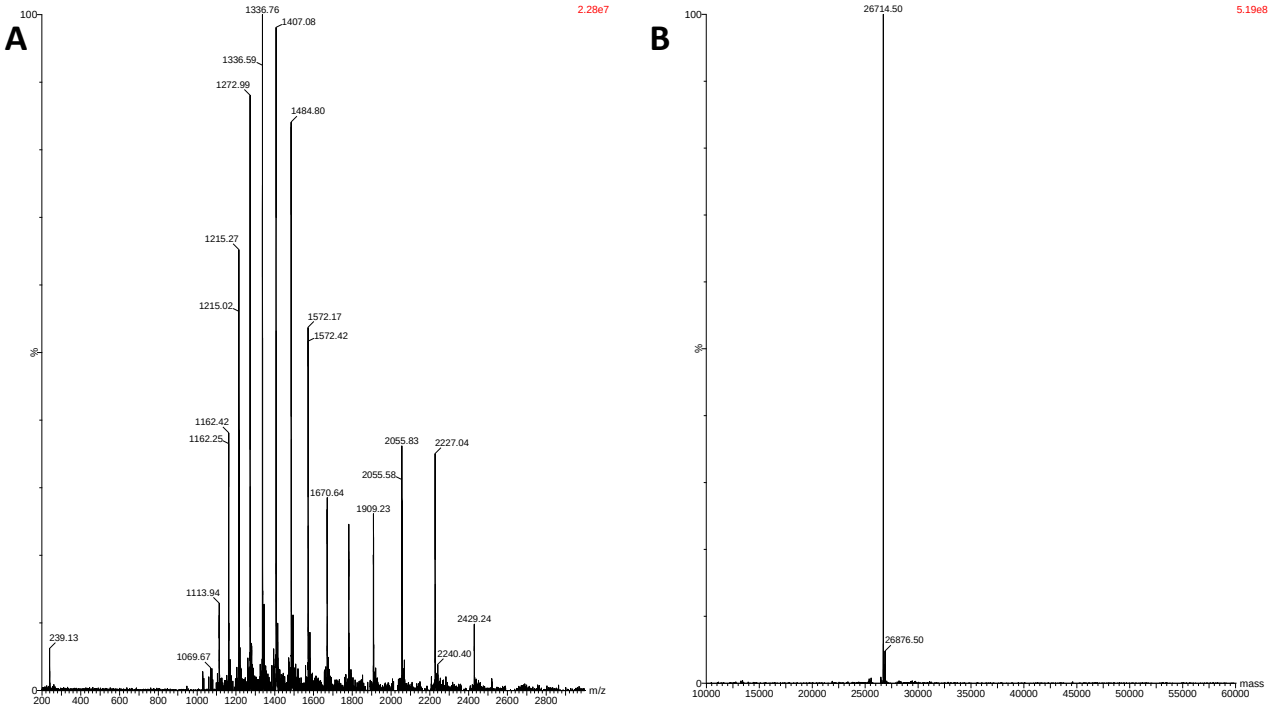

Figure S28. LC-MS analysis of NEM-V_HH. (**A**) Continuous ion series and (**B**) deconvoluted mass spectrum obtained using the MaxEnt algorithm. Solvent: 1:1 milli-Q water and acetonitrile (with 0.1% formic acid). Flow rate: 1 mL/min.

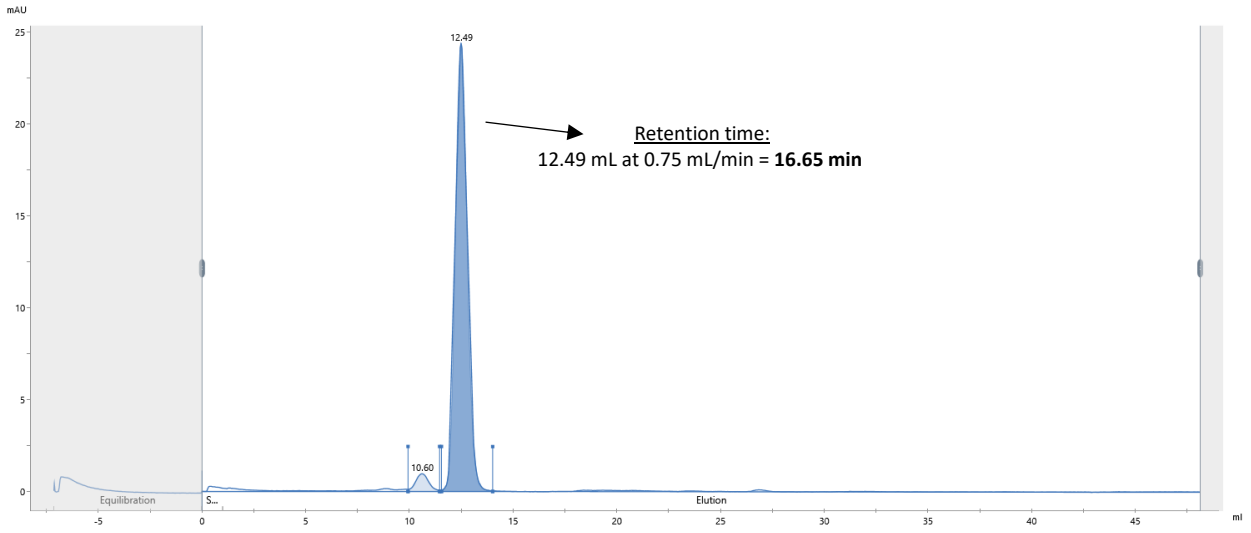

Figure S29. SEC-HPLC chromatogram of NEM-V_HH showing its purity using HPLC method C on an ÄKTA pure™ chromatography system. The purity of the conjugate (highlighted) is 96.0%

[^{188}Re]ReO(N_2S_2-PEG_3-N_3) radiolabelling

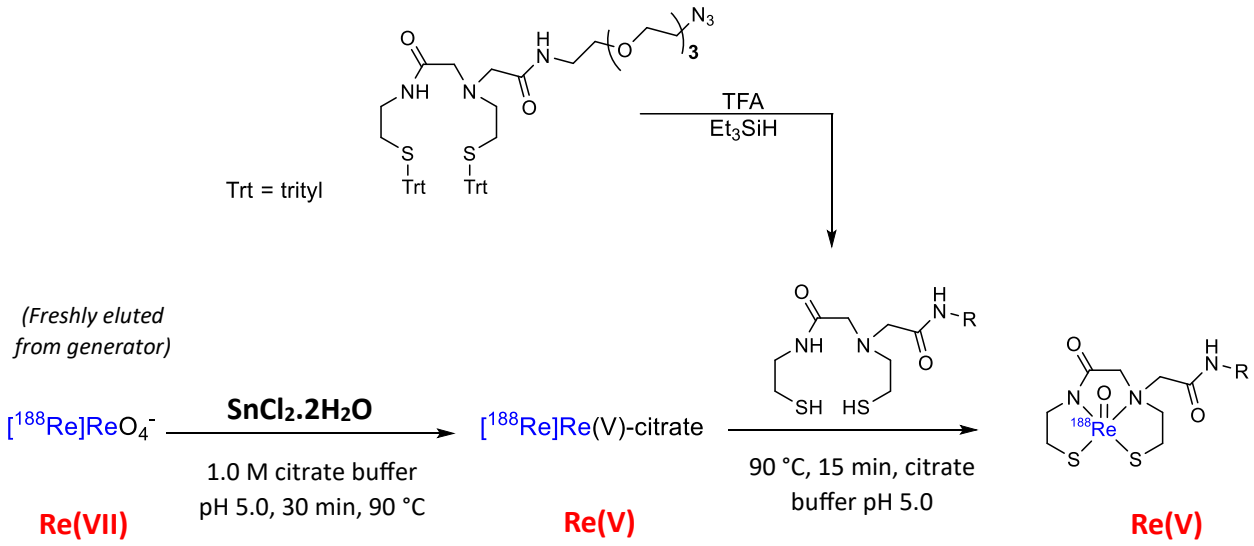

Scheme S1. Two-step procedure for the labelling of [^{188}Re]ReO(N_2S_2-PEG_3-N_3).

Two-strip iTLC method for [^{188}Re]Re(V)-citrate

To determine the radiochemical conversion (RCC) of [^{188}Re]ReO_4^- to [^{188}Re]Re(V)-citrate and assess for the presence of hydrophobic and hydrophilic impurities, a two-strip TLC method was employed. Briefly, 2-3 µL of the [^{188}Re]Re(V)-citrate product mixture was pipetted onto the base of two iTLC-SG chromatography strips (Agilent Technologies, Belgium) about 1.5 cm from the bottom. One strip was developed in acetone in which [^{188}Re]Re(V)-citrate and [^{188}Re]$(ReO_2)_n$ (reduced hydrolysed ^{188}Re) stay on the baseline and [^{188}Re]ReO_4^- moves with the solvent front (Strip **A**, Figure S32). The other strip was developed in saline, in which [^{188}Re]Re(V)-citrate and [^{188}Re]ReO_4^- move with the solvent front while [^{188}Re]$(ReO_2)_n$ remains on the baseline (Strip **B**, Figure S32). The RCC of [^{188}Re]Re(V)-citrate was determined using the equation below:

$$\text{RCC (\%)} = \underbrace{\frac{A_{bottom} \times 100}{A_{total}}}_{\text{TLC system } \mathbf{B}} - \underbrace{\frac{A_{bottom} \times 100}{A_{total}}}_{\text{TLC system } \mathbf{A}}$$

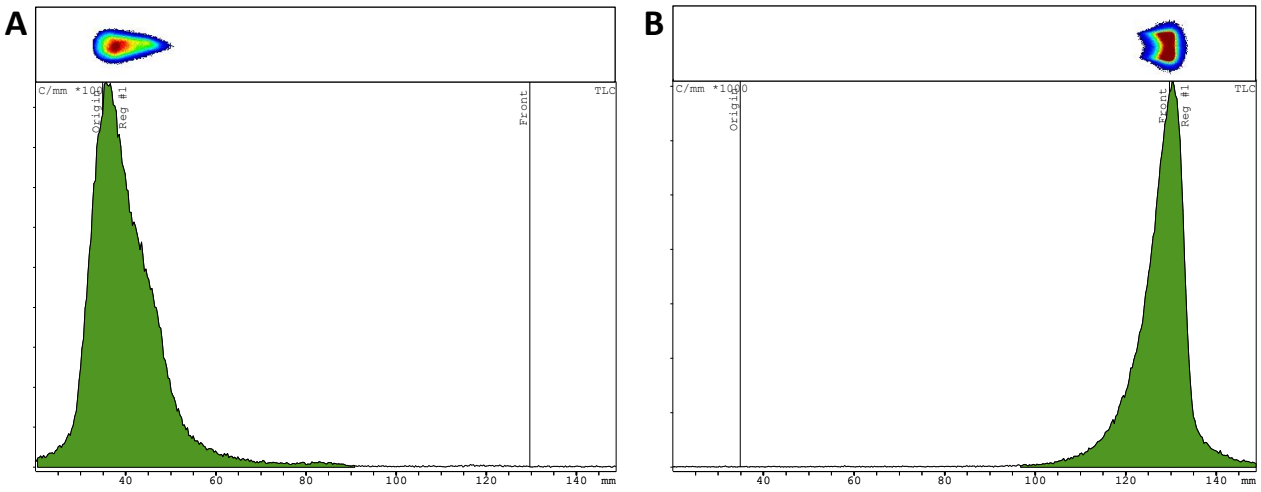

Figure S30. iTLC chromatograms of the [^{188}Re]Re(V)-citrate product mixture run in (**A**) acetone and (**B**) saline and scanned using a TLC scanner (miniGITA, Elysia Raytest, Germany) and a CR-35 Bio Test-Imager (Dürr-ndt, Germany).

$SnCl_2$ reduction of compound Re-4

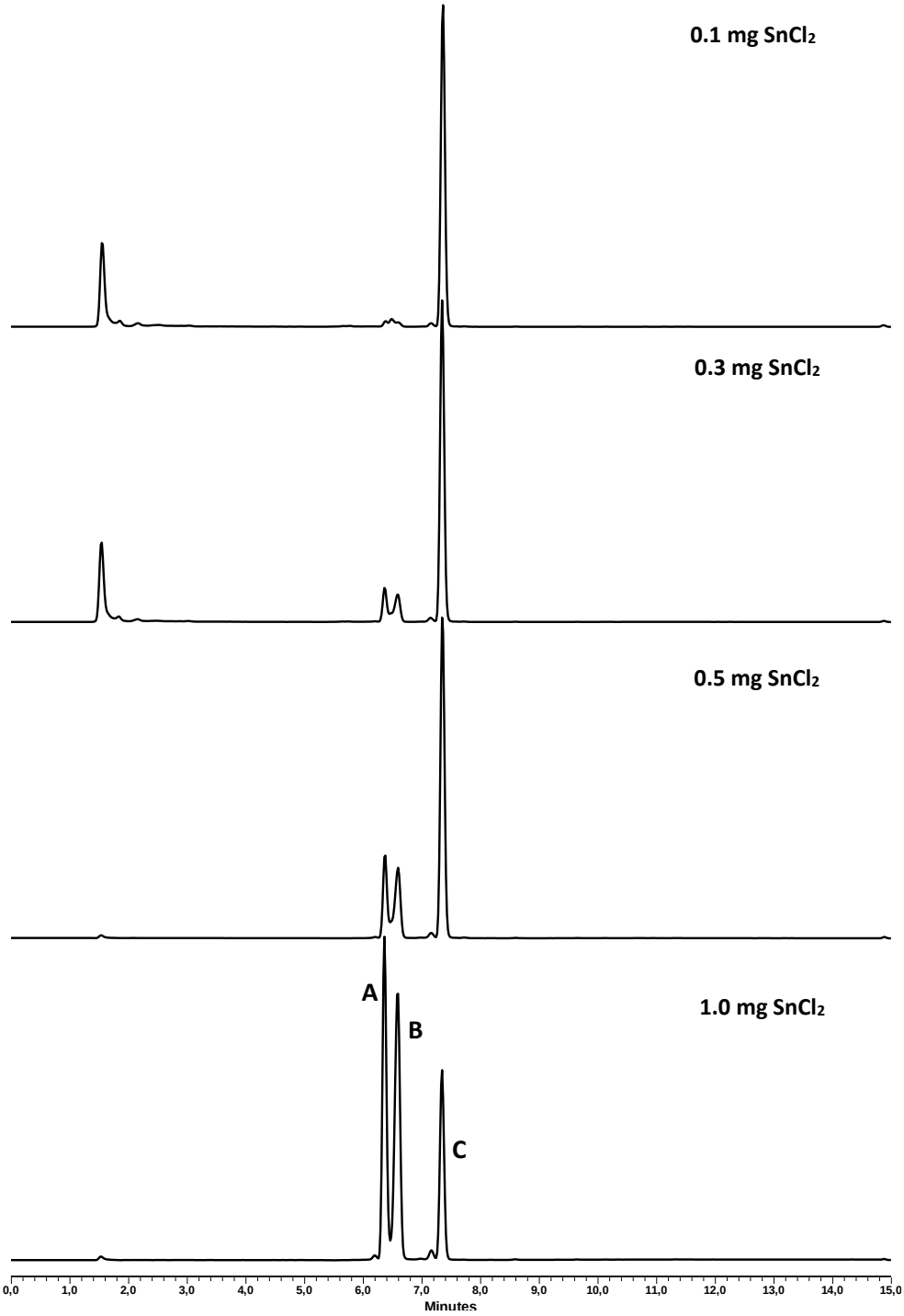

Figure S31. HPLC chromatograms recorded at 358 nm (HPLC method A) of the intentional reduction of compound **Re-4** (1.0 mg) with increasing amounts of $SnCl_2$ (0.1 mg – 1.0 mg) in ethanol at room temperature. The ESI-MS spectrum of each of the products (A, B and C) can be found in Figure S32.

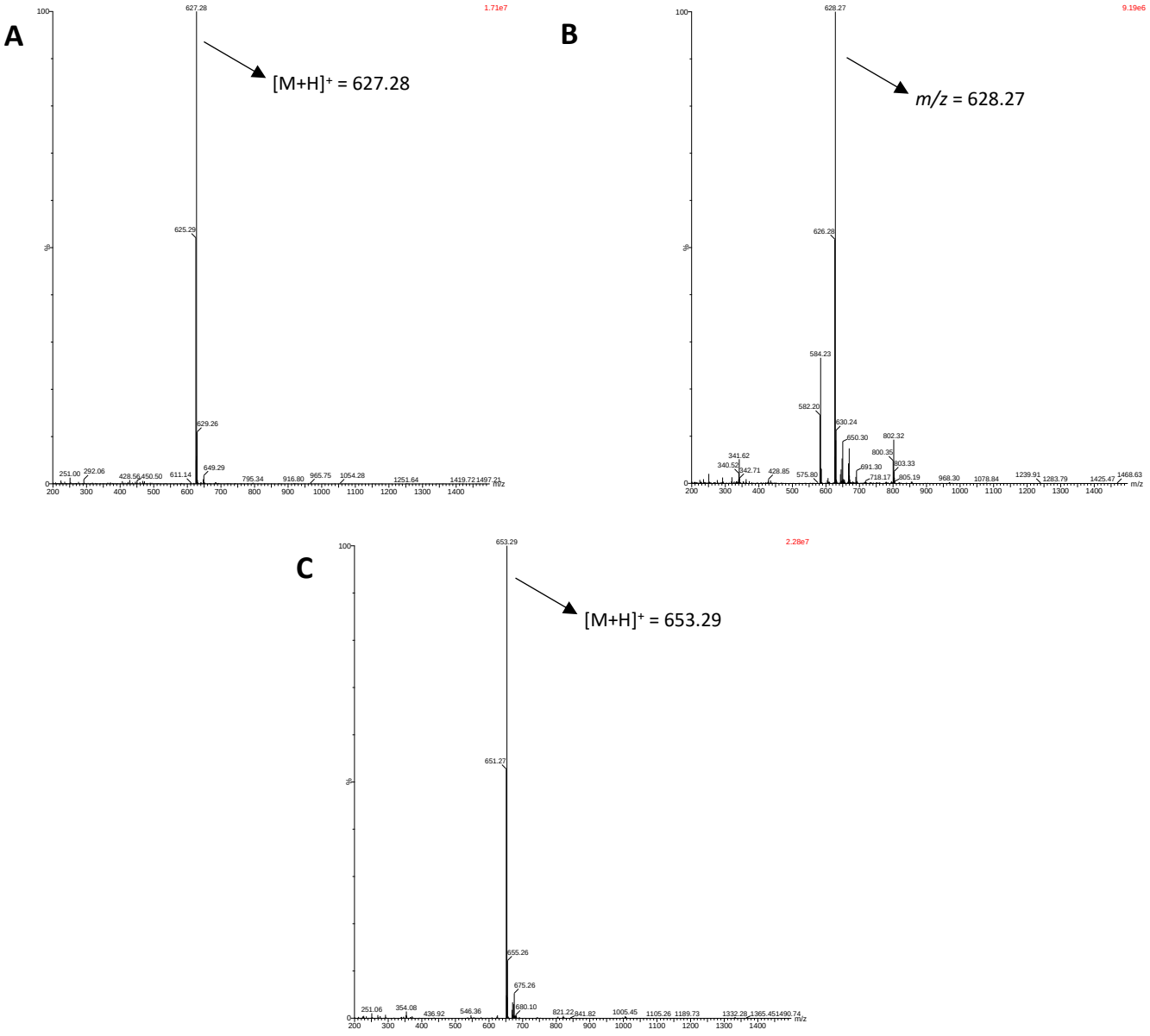

Figure S32. ESI-MS spectra of the three products of the reduction (A, B and C) in Figure S31 (HPLC method A). (**A**) **Re-4** with the N_3 reduced to NH_2, (**B**) unknown reduction product of **Re-4** and (**C**) **Re-4** with the N_3 unreduced.

HPLC analysis of the radiolabelling byproducts

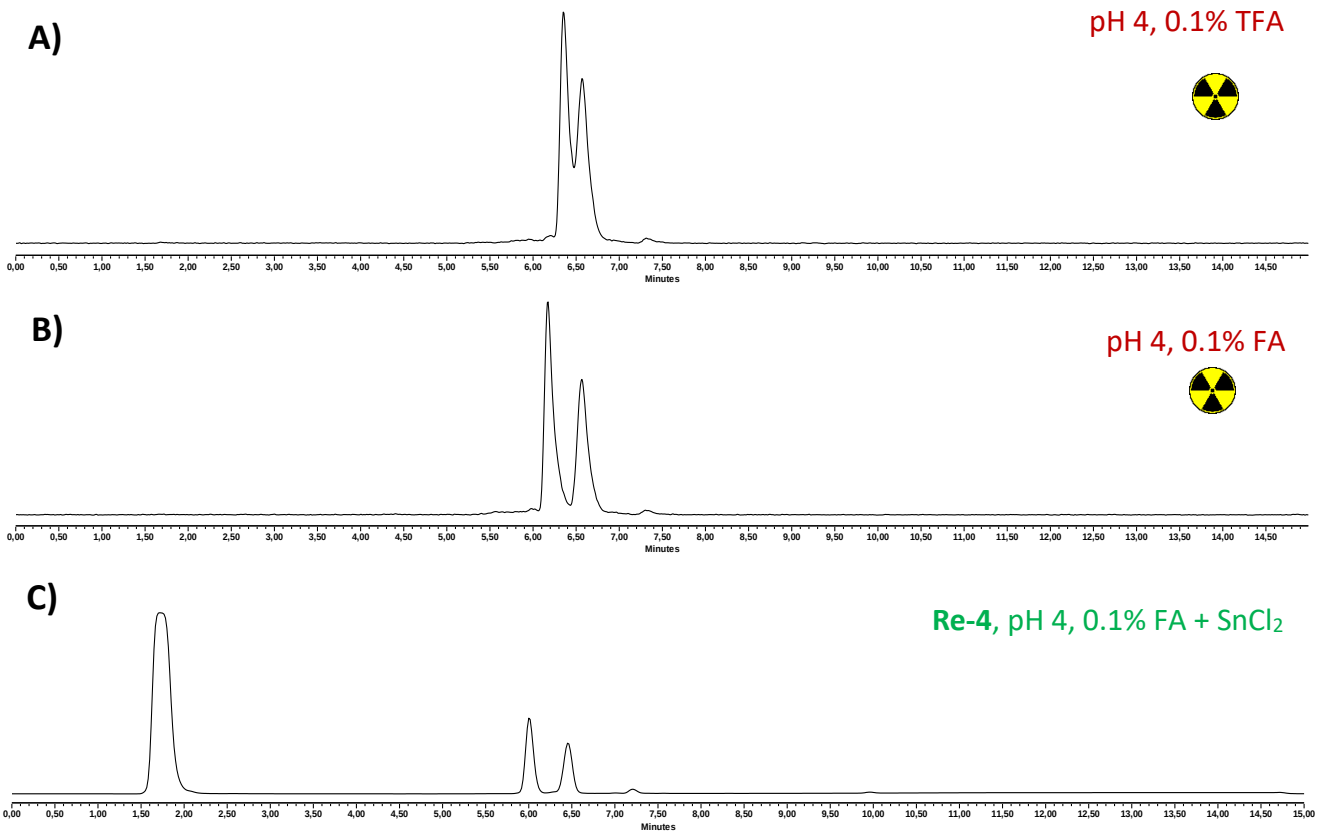

Figure S33. Testing the radiolabelling at pH 4 with an excess of $SnCl_2$ (HPLC method B). **(A)** Radio-HPLC chromatogram of the radiolabelling products with 0.1% TFA in the mobile phase, **(B)** Radio-HPLC chromatogram of the radiolabelling products with 0.1% formic acid (FA) instead of TFA in the mobile phase, **(C)** UV HPLC chromatogram (254 nm) of the "cold" **Re-4** complex reduced with $SnCl_2$ under the radiolabelling conditions used (0.1% FA in the mobile phase).

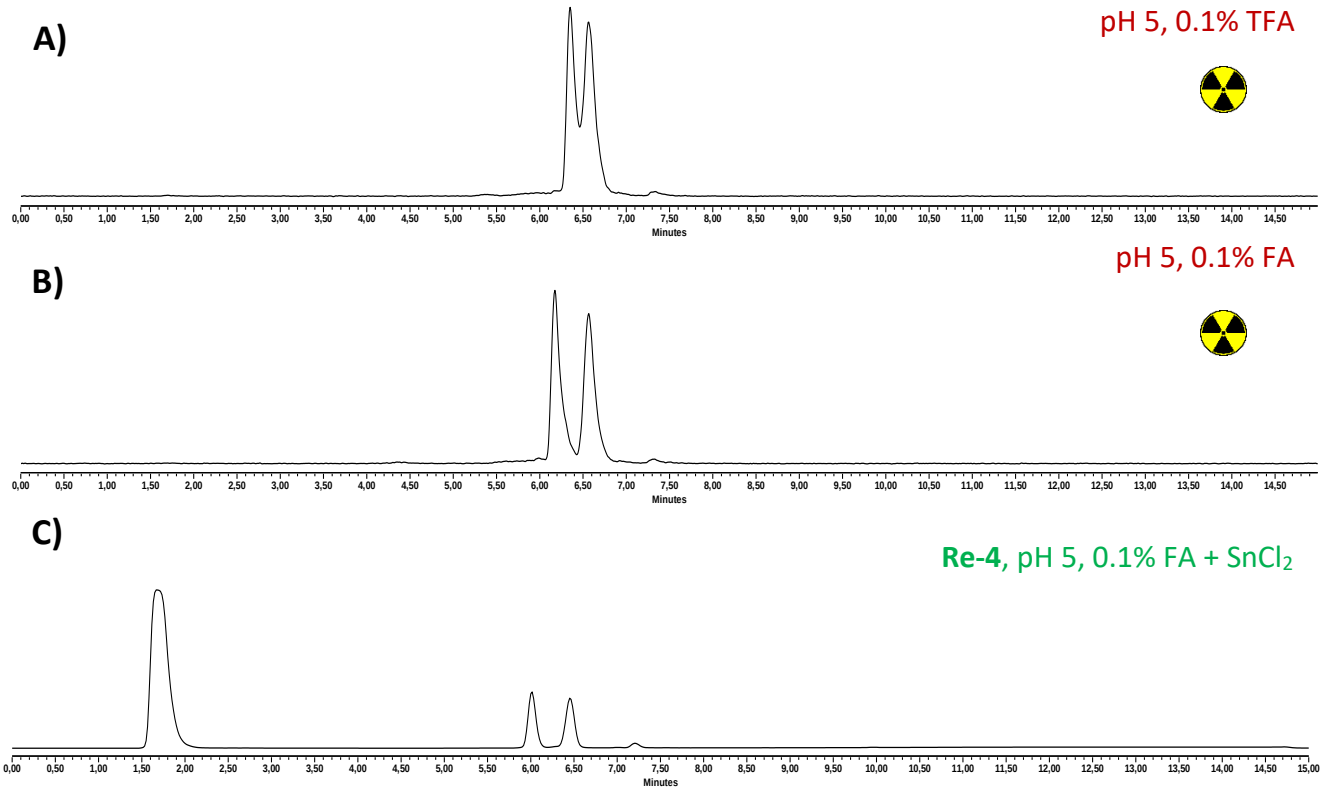

Figure S34. Testing the radiolabelling at pH 5 with an excess of $SnCl_2$ (HPLC method B). **(A)** Radio-HPLC chromatogram of the radiolabelling products with 0.1% TFA in the mobile phase, **(B)** Radio-HPLC chromatogram of the radiolabelling products with 0.1% formic acid (FA) instead of TFA in the mobile phase, **(C)** UV HPLC chromatogram (254 nm) of the "cold" **Re-4** complex reduced with $SnCl_2$ under the radiolabelling conditions used (0.1% FA in the mobile phase).

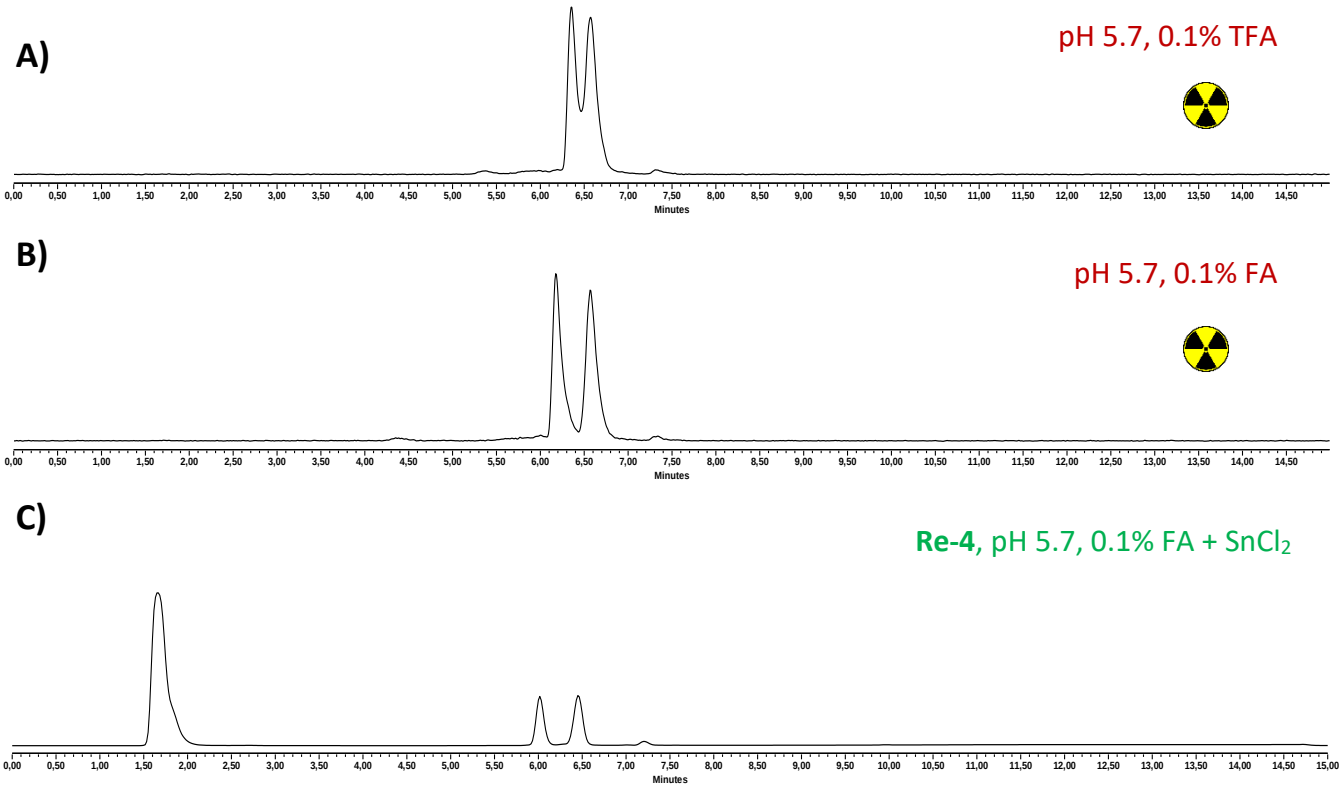

Figure S35. Testing the radiolabelling at pH 5.7 with an excess of $SnCl_2$ (HPLC method B). **(A)** Radio-HPLC chromatogram of the radiolabelling products with 0.1% TFA in the mobile phase, **(B)** Radio-HPLC chromatogram of the radiolabelling products with 0.1% formic acid (FA) instead of TFA in the mobile phase, **(C)** UV HPLC chromatogram (254 nm) of the "cold" **Re-4** complex reduced with $SnCl_2$ under the radiolabelling conditions used (0.1% FA in the mobile phase).

Separation of deprotected chelator 4 and complex Re-4

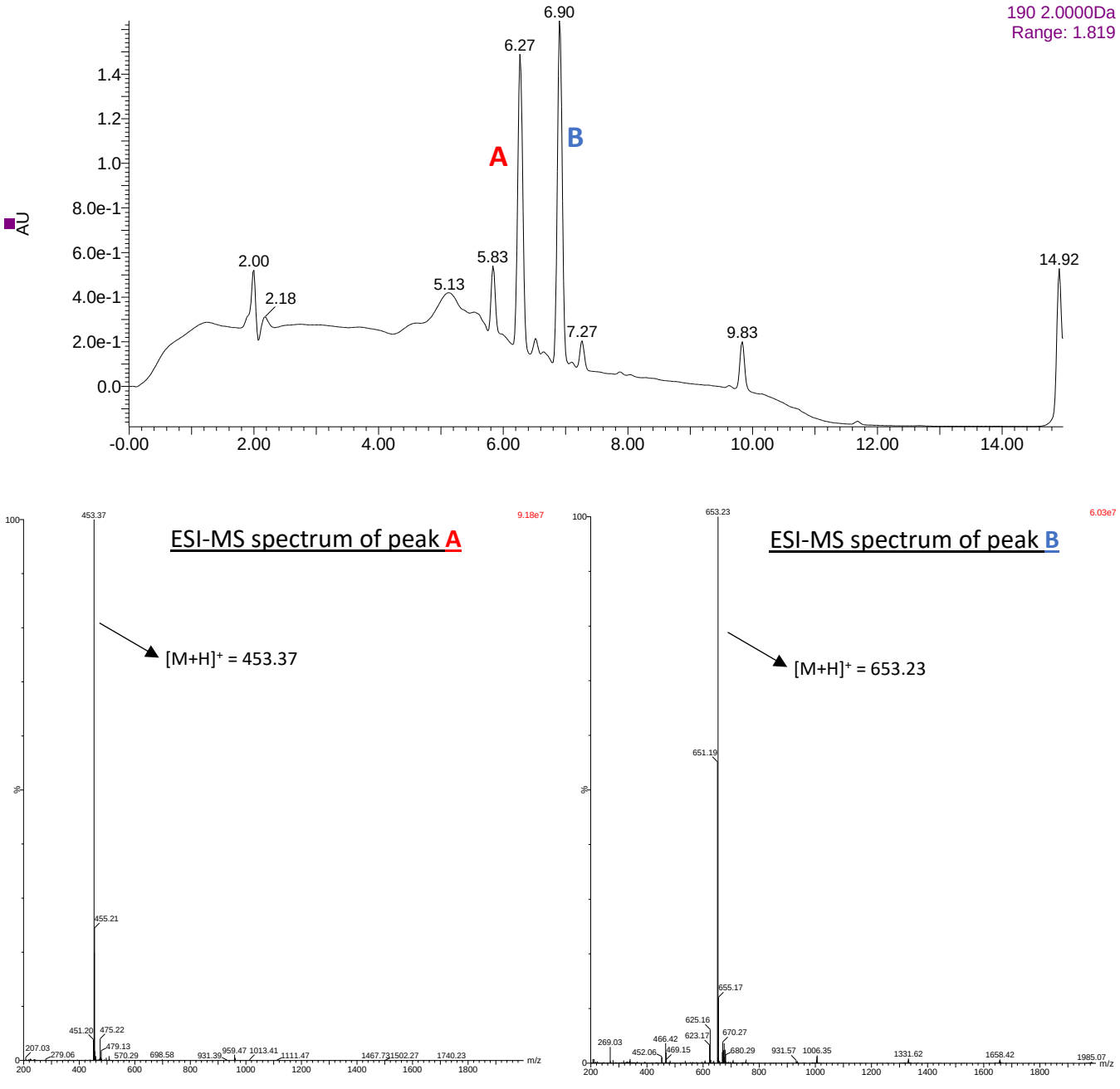

Figure S36. HPLC chromatogram recorded at 190 nm (HPLC method A) and ESI-MS spectra indicating the difference in retention time between the deprotected chelator (**A**) and the ^{nat}Re(V) complex, **Re-4** (**B**).

SPAAC click reaction iTLCs

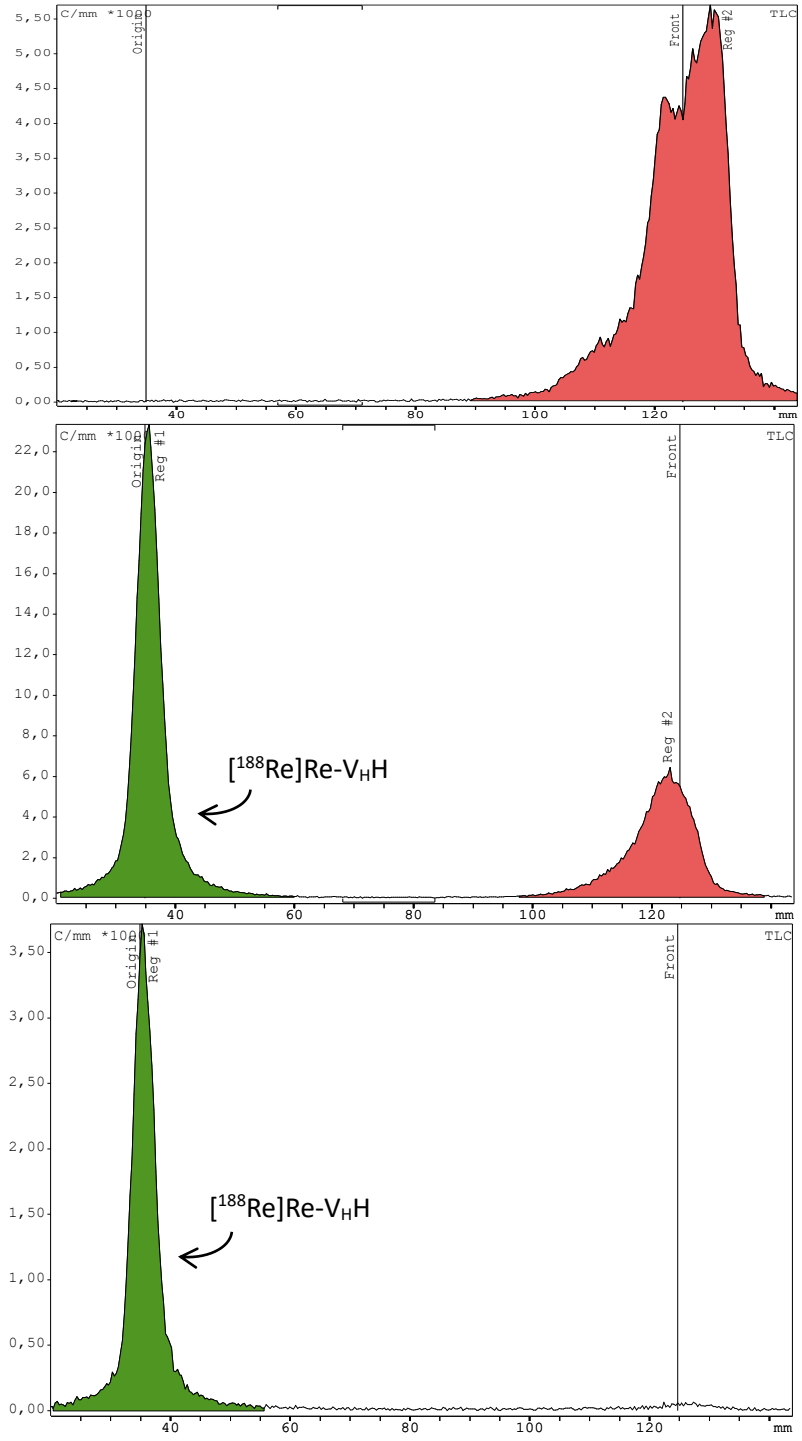

Figure S37. iTLC chromatograms run in ACN:H_2O (3:1) and scanned using a TLC scanner (miniGITA, Elysia Raytest). Any activity associated with the V_HH remains at the baseline of the iTLC strip while any "unclicked" activity moves with the solvent front **(A)** [^{188}Re]ReO(N_2S_2-PEG_3-N_3); **(B)** SPAAC click reaction after 30 min and **(C)** [^{188}Re]Re-V_HH after PD MiniTrap™ purification.

In vitro stability

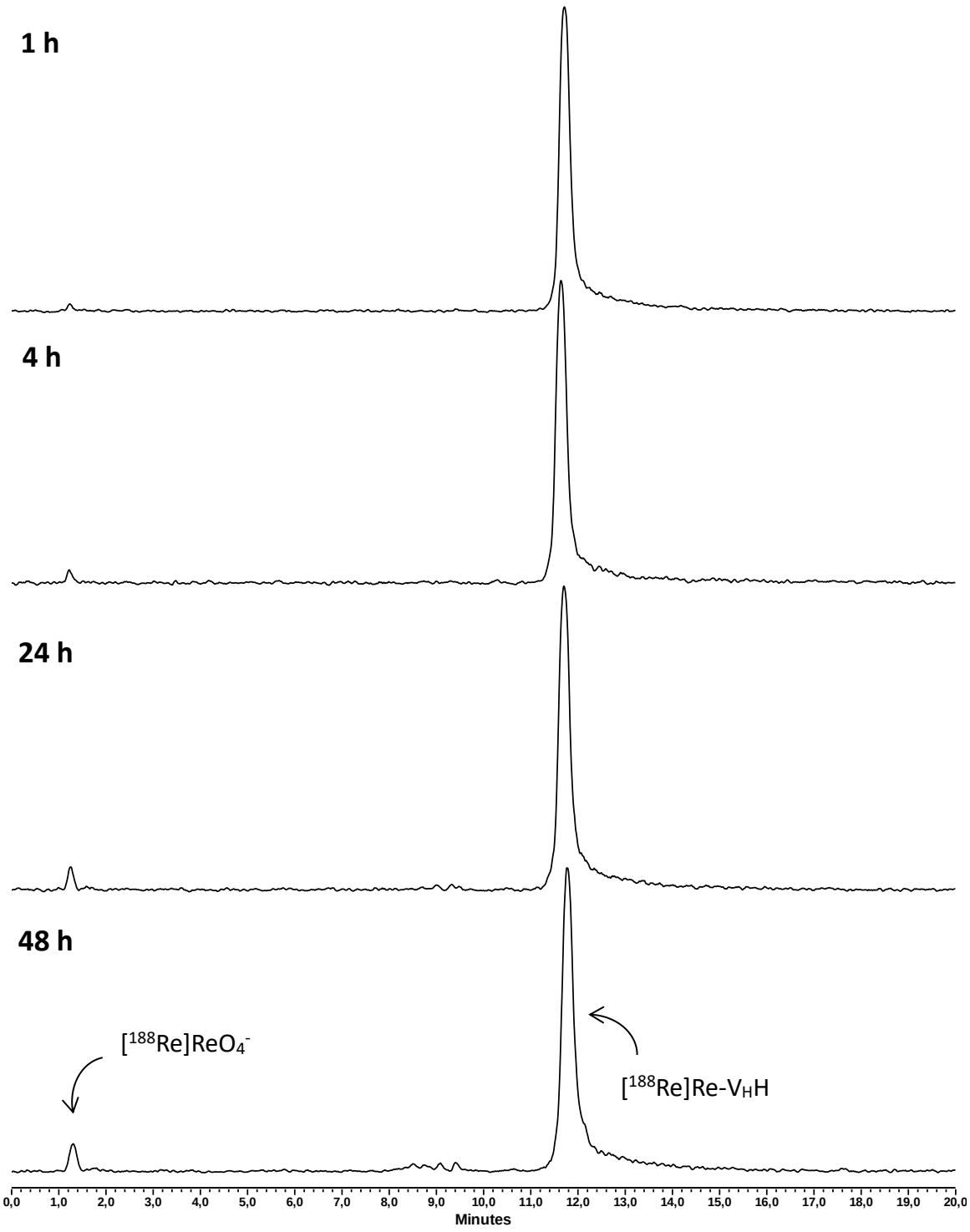

Figure S38. Radio-HPLC chromatograms showing the stability of [^{188}Re]Re-V_HH in saline with ascorbate at pH 5.5 over time (1 h, 4 h, 24 h and 48 h after PD MiniTrap™ purification.) (HPLC method D)

Ex vivo biodistribution

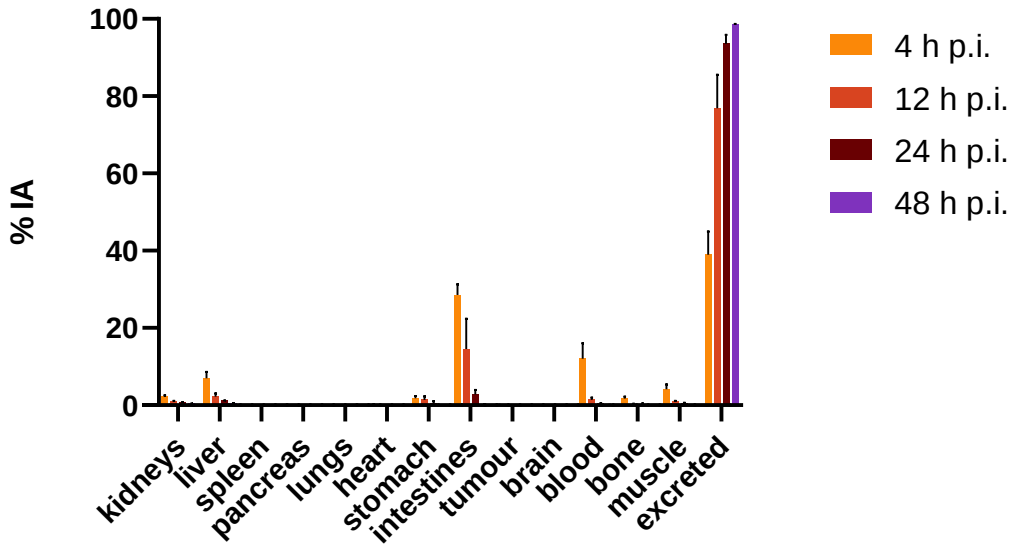

Figure S39. *Ex vivo* biodistribution over 48 hours expressed as a percentage of injected activity (% IA) of [^{188}Re]Re-V_HH in BxPC3 xenografted tumour mice (p.i. = post injection).

Table S2. *Ex vivo* biodistribution data over 48 hours expressed as a percentage of injected activity (% IA*) of [^{188}Re]Re-V_HH in BxPC3 xenografted tumour mice. Values represent mean ± standard deviation (n=4).

	% IA			
	4 h	**12 h**	**24 h**	**48 h**
kidneys	2.20 ± 0.36	1.01 ± 0.09	0.710 ± 0.089	0.419 ± 0.065
liver	7.00 ± 1.66	2.23 ± 0.81	1.096 ± 0.128	0.456 ± 0.095
spleen	0.11 ± 0.02	0.02 ± 0.01	0.006 ± 0.002	0.002 ± 0.000
pancreas	0.10 ± 0.02	0.02 ± 0.01	0.005 ± 0.001	0.002 ± 0.000
lungs	0.03 ± 0.05	0.08 ± 0.01	0.027 ± 0.010	0.010 ± 0.003
heart	0.23 ± 0.09	0.03 ± 0.01	0.015 ± 0.008	0.003 ± 0.001
intestines	28.55 ± 2.72	14.56 ± 7.80	2.790 ± 1.141	0.235 ± 0.061
tumour	0.09 ± 0.05	0.02 ± 0.01	0.009 ± 0.002	0.003 ± 0.001
brain	0.03 ± 0.01	0.01 ± 0.01	0.002 ± 0.000	0.001 ± 0.000
blood	12.05 ± 3.98	1.41 ± 0.52	0.434 ± 0.145	0.095 ± 0.025
bone	1.74 ± 0.46	0.32 ± 0.08	0.267 ± 0.186	0.040 ± 0.015
muscle	4.16 ± 1.19	0.96 ± 0.16	0.429 ± 0.200	0.112 ± 0.011
excreted	38.92 ± 6.06	76.86 ± 8.65	93.526 ± 2.325	98.473 ± 0.222

* % IA calculated as (cpm in organ/total cpm) x 100.

Table S3. *Ex vivo* biodistribution data over 48 hours expressed as a percentage of injected activity per gram (% IA/g*) of [^{188}Re]Re-V_HH in BxPC3 xenografted tumour mice. Values represent mean ± standard deviation (n=4).

	% IA/g			
	4 h	**12 h**	**24 h**	**48 h**
kidneys	3.37 ± 0.56	1.44 ± 0.16	1.046 ± 0.117	0.638 ± 0.115
liver	3.06 ± 0.81	0.85 ± 0.25	0.499 ± 0.088	0.209 ± 0.053
spleen	0.77 ± 0.26	0.14 ± 0.04	0.060 ± 0.026	0.014 ± 0.003
pancreas	0.43 ± 0.10	0.07 ± 0.01	0.024 ± 0.006	0.008 ± 0.002
lungs	1.56 ± 0.29	0.27 ± 0.04	0.095 ± 0.026	0.031 ± 0.009
heart	1.29 ± 0.51	0.18 ± 0.05	0.071 ± 0.031	0.017 ± 0.005
tumour	1.81 ± 0.68	0.40 ± 0.09	0.191 ± 0.068	0.050 ± 0.013
brain	0.10 ± 0.04	0.02 ± 0.00	0.005 ± 0.001	0.002 ± 0.000
blood	4.41 ± 1.39	0.52 ± 0.18	0.155 ± 0.058	0.034 ± 0.010
bone	0.63 ± 0.16	0.12 ± 0.03	0.094 ± 0.064	0.015 ± 0.006
muscle	1.52 ± 0.41	0.35 ± 0.06	0.155 ± 0.080	0.040 ± 0.005

* % IA/g calculated as % IA/weight of organ

Table S4. *Ex vivo* biodistribution data over 48 hours expressed as standardised uptake values (SUV*) of [^{188}Re]Re-V_HH in BxPC3 xenografted tumour mice. Values represent mean ± standard deviation (n=4).

	SUV			
	4 h	**12 h**	**24 h**	**48 h**
kidneys	1.32 ± 0.24	0.56 ± 0.04	0.420 ± 0.038	0.255 ± 0.038
liver	1.20 ± 0.34	0.33 ± 0.10	0.200 ± 0.029	0.083 ± 0.018
spleen	0.30 ± 0.11	0.06 ± 0.02	0.024 ± 0.010	0.006 ± 0.001
pancreas	0.62 ± 0.04	0.03 ± 0.01	0.010 ± 0.002	0.003 ± 0.001
lungs	0.61 ± 0.12	0.11 ± 0.02	0.038 ± 0.008	0.012 ± 0.003
heart	0.51 ± 0.20	0.07 ± 0.02	0.028 ± 0.011	0.007 ± 0.002
tumour	0.71 ± 0.27	0.16 ± 0.04	0.082 ± 0.022	0.020 ± 0.005
brain	0.04 ± 0.02	0.02 ± 0.01	0.002 ± 0.000	0.001 ± 0.000
blood	1.72 ± 0.57	0.20 ± 0.07	0.062 ± 0.021	0.014 ± 0.004
bone	0.25 ± 0.07	0.05 ± 0.01	0.038 ± 0.027	0.006 ± 0.002
muscle	0.59 ± 0.17	0.14 ± 0.02	0.061 ± 0.029	0.016 ± 0.002

* SUV calculated as [activity in organ (cpm)/weight of organ (g)]/[total activity recovered (cpm) /body weight (g)].

Table S5. Tumour-to-blood SUV ratios of [^{188}Re]Re-V_HH in BxPC3 xenografted tumour mice at different time points post-injection (p.i.).

Time post-injection (p.i.) (h)	Tumour-to-blood
4	0.41 ± 0.07
12	0.82 ± 0.20
24	1.31 ± 0.51
48	1.56 ± 0.49

Attempted use of IEDDA chemistry in the cysteine-selective [^{188}Re]Re(V) radiolabelling of a Nanobody®

In an effort to try to improve the yield of the click reaction between the ^{188}Re-labelled N_2S_2 chelator and V_HH conjugate, the inverse electron demand Diels-Alder (IEDDA) variants of the chelator (**9**) and bioconjugation handle (**12**) were synthesised (Scheme S2). The IEDDA reaction, involving a tetrazine and a strained alkene, like trans-cyclooctene (TCO), is a highly valuable conjugation method in radiopharmaceutical development due to its fast kinetics, high chemoselectivity and reduced lipophilicity of its reagents compared to those used for SPAAC.[16–21] Given these advantages, particularly its fast reaction kinetics, it was anticipated that the IEDDA reaction would enhance the overall yield of the final click reaction, and thus the molar activity.

RESULTS AND DISCUSSION

Synthesis

The trityl-protected N_2S_2-PEG_4-MeTz chelator (**9**) was synthesised via the amide coupling of H_2N-PEG_4-MeTz (**8**), previously synthesised in literature[22], to the N_2S_2-COOH chelator (**3**) (Scheme S2A). The TCO-functionalised carbonylacrylic (CA) compound for cysteine V_HH modification was synthesised following a modified literature[4] procedure to produce TCO-PEG_3-CA (**12**) (Scheme S2C). Finally, the "cold" ^{nat}ReO(N_2S_2-PEG_4-MeTz) complex (**Re-9**) was synthesised in one step after deprotection of the trityl protecting groups and reaction with $(Ph_3P)_2ReOCl_3$ (Scheme S2B). Detailed spectra and characterisation data are provided on page S43.

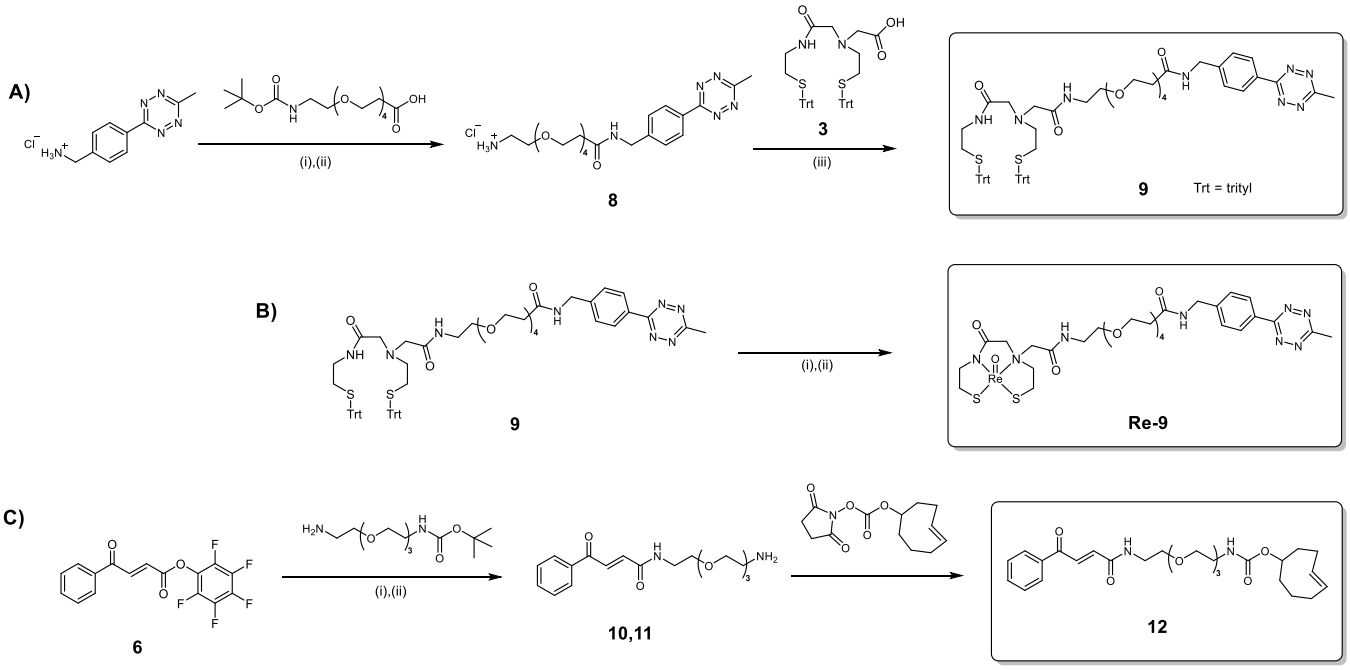

Scheme S2. (A) Synthesis of the N_2S_2-PEG_4-MeTz chelator, **9**. Reagents and conditions: (i) Boc-NH-PEG_4-COOH, EDC, HOBt, DMF, r.t., 20 h *(75%)*; (ii) DCM, HCl (4.0 M in dioxane), r.t., 2 h *(96%)*; (iii) EDC, HOBt, DCM, r.t., 20 h *(60%)*. **(B)** Synthesis of the ^{nat}ReO(N_2S_2-PEG_4-MeTz) complex, **Re-9**. Reagents and conditions: (i) TFA, Et_3SiH, 0°C, 20 min. (ii) $(PPh_3)_2ReOCl_3$, NaOAc, MeOH, 75°C, 18 h *(46%)*. **(C)** Synthesis of the TCO-PEG_3-CA ligand, **12**. Reagents and conditions: (i) Boc-NH-PEG_3-NH_2, DIPEA, DCM, r.t., 1 h *(87%)*; (ii) TFA, DCM, r.t., 1 h *(96%)*; (iii) DCM, DIPEA, r.t., 24 h *(35%)*.

Cysteine-selective V_HH bioconjugation

In a similar fashion to the bioconjugation performed with DBCO-PEG_4-CA (**7**), the bivalent HLE anti-c-Met V_HH was conjugated to the TCO-PEG_3-CA ligand (**12**) via its terminal cysteine residue. After 1.5 h, this yielded the desired TCO-V_HH construct after a final PD-10 purification. ESI-MS analysis of the conjugate showed a single mass corresponding to the expected mass of the desired V_HH-TCO construct after deconvolution (Figure S57). The purity of the final conjugate was determined to be 89.0% via SEC-HPLC (Figure S58).

[^{188}Re]Re(V)-radiolabelling of N_2S_2-PEG_4-MeTz (9)

Similar to the radiolabelling of N_2S_2-PEG_3-N_3 (**4**), the labelling of N_2S_2-PEG_4-MeTz (**9**) was also performed in two steps (Scheme S3). This involved producing a [^{188}Re]Re(V)-citrate precursor by reducing [^{188}Re]ReO_4^- with $SnCl_2$ in citrate buffer, and then adding an aliquot of this to the freshly-deprotected chelator, **9**, in an attempt to afford the final labelled compound, [^{188}Re]ReO(N_2S_2-PEG_4-MeTz).

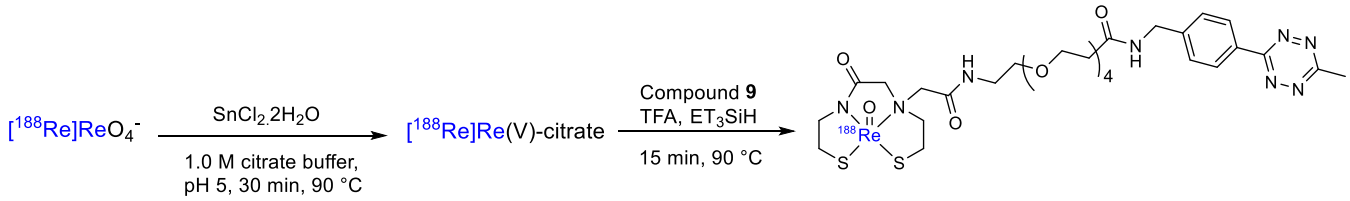

Scheme S3. Two-step procedure for the labelling of [^{188}Re]ReO(N_2S_2-PEG_4-MeTz).

An initial observation upon TFA deprotection of the trityls on chelator **9** was the presence of multiple peaks in the corresponding HPLC chromatogram (Figure S56B). This was accompanied, on occasion, with the loss of the bright pink colour associated with the presence of the tetrazine in solution, indicating that the TFA likely affected the structure of the tetrazine. TFA was also used to deprotect the trityls of chelator **9** in the synthesis of the ^{nat}Re-N_2S_2-PEG_4-Tz (**Re-9**) complex and this likely contributed to the low yield of 46%. On a nanoscale, however, this could present a problem for the radiolabelling of the chelator. In spite of this potential issue, it was decided to attempt the radiolabelling anyway to see whether we could still achieve the desired ^{188}Re-labelled product.

The optimised conditions used for labelling N_2S_2-PEG_3-N_3 (**4**) were also applied to this labelling procedure. While the radiolabelling proceeded with minimal [^{188}Re]ReO_4^- or [^{188}Re]Re(V)-citrate remaining after 30 min, upon HPLC analysis, the major product of the labelling did not co-elute with the ^{nat}Re(V) analogue, **Re-9** (Figure S37). Since tetrazines are susceptible to reducing conditions, this peak could potentially be the result of the $SnCl_2$ reducing agent in the labelling mixture reducing the tetrazine on the chelator to a non-reactive dihydrotetrazine.[23,24] When an excess of $SnCl_2$ was added to the ^{nat}Re(V) analogue, **Re-9**, to intentionally reduce the tetrazine, the HPLC UV-

trace of the resulting product aligned with the radio-HPLC trace of the major peak of the labelling mixture (Figure S37). Additionally, LC-MS analysis of the $SnCl_2$-reduced **Re-9** complex showed the mass of the reduced species is 2 Da higher than that of **Re-9** (Figure S55), supporting the theory that a dihydrotetrazine is formed. Unfortunately, we could not lower the amount of $SnCl_2$ used in our reaction since we were already using the lowest amount possible to reduce the $[^{188}Re]ReO_4^-$, as determined by our optimisations for radiolabelling chelator **4**. Attempts were made to radiolabel without the addition of ascorbic acid, a known mild reducing agent used to keep radioactive formulations stable. This, however, resulted in very low yields in the first step when synthesising $[^{188}Re]$Re(V)-citrate. Additionally, we also tried to perform this radiolabelling ensuring an inert atmosphere in the first step but performing the second step in the presence of air in the hopes of oxidising any excess Sn(II) in solution before it can reduce the tetrazine. This was unsuccessful as the $[^{188}Re]$Re(V) core did not stay reduced in the presence of air, rapidly oxidising to $[^{188}Re]ReO_4^-$ instead.

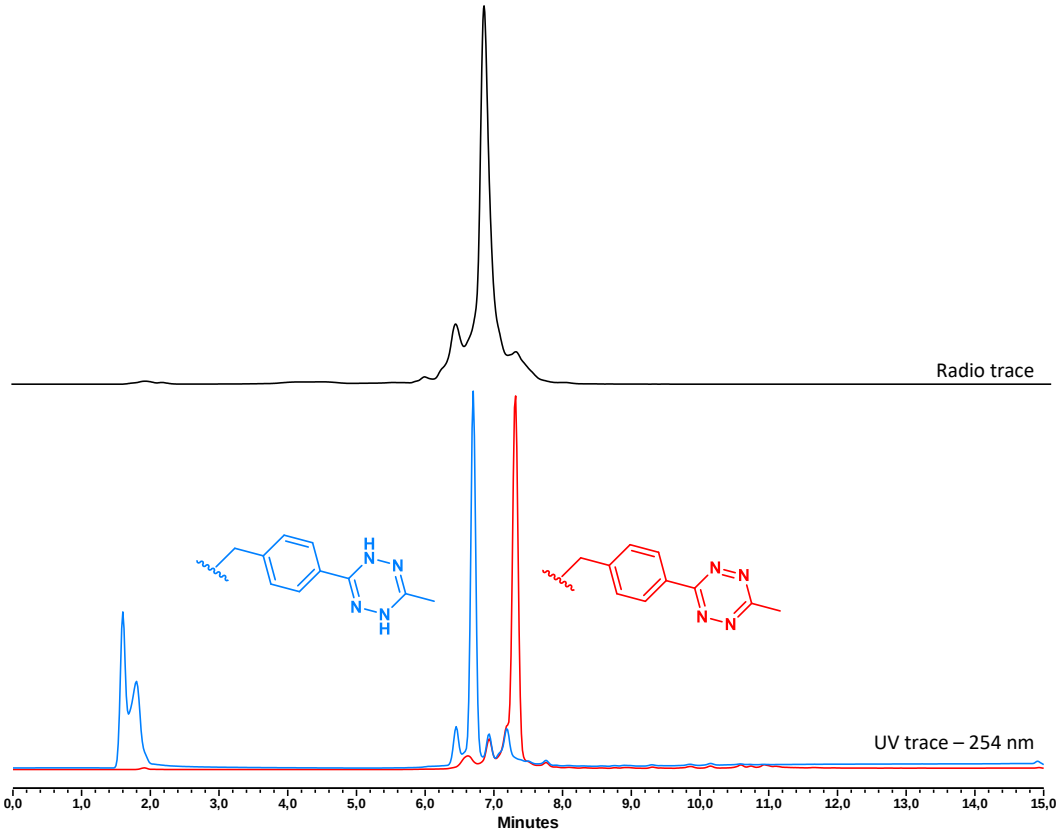

Figure S40. Radio-HPLC chromatogram of the crude labelling mixture (black) compared to the UV chromatograms of the ^{nat}Re(V) complexes, **Re-9** (red) and **Re-9** reduced with $SnCl_2$ (blue).

In spite of the result observed in Figure 1, we decided to try to purify the main product of the labelling and attempt to perform the IEDDA click reaction with the TCO-V_HH. Prep-HPLC purification of the peak at 6.8 min (Figure S37) was performed and the resulting radio-HPLC chromatogram showed that the retention time of the purified species remained unchanged, aligning with the peak of **Re-9** treated with $SnCl_2$ (Figure S59). This was then reacted with the TCO-V_HH conjugate for 30 min at an apparent molar activity 5 MBq/nmol. Unfortunately, as expected, the yield remained low with only ~5% of the total activity attached to the V_HH after 30 min. This provided the final confirmation that the tetrazine had been inactivated during labelling, thereby preventing the IEDDA reaction from occurring.

Unlike the reduction of an azide to an amine which is irreversible, a dihydrotetrazine can be oxidised to a tetrazine in a number of ways. This often includes the exposure to air (oxygen)[25], the use of chemical oxidants[26,27], or through electro- or photochemical oxidation.[24,28,29] However, it is likely that none of these oxidation methods are compatible with a compound containing the [^{188}Re]Re(V) core, as reduced ^{188}Re readily oxidised to perrhenate in just the presence of air. Because of this persistent issue with the tetrazine reduction, this chelator system could not be used further for radiolabelling a V_HH with ^{188}Re.

MATERIALS AND METHODS

Synthesis

*Trt-N_2S_2-PEG_4-MeTz (**9**).* MeTz-PEG_4-NH_2 compound **8** (0.128 g, 0.174 mmol), EDC.HCl (0.035 g, 0.227 mmol) and HOBt (0.031 g, 0.227 mmol) were dissolved in 6.00 mL dry DCM under a nitrogen atmosphere. To this, DIPEA (0.090 mL, 0.521 mmol) was added and the reaction mixture was stirred for 30 min at room temperature. Finally, compound **3** (0.110 g, 0.227 mmol) was dissolved in 2.00 mL dry DCM and added to the reaction mixture, which was stirred at room temperature overnight. The reaction mixture was then diluted with

DCM, washed with water (3 x 20.0 mL) and brine (1 x 20.0 mL), dried over $MgSO_4$ and filtered. The solvent was removed and the residue was purified via column chromatography with silica gel using a 9:1 mixture of ethyl acetate and methanol for afford compound **9** as a bright pink oil (0.123 g, 60.3%). ^{1}H NMR (400 MHz, $CDCl_3$) δ: 2.28 (t, *J* = 6.55 Hz, 2H, H_f), 2.37 (t, *J* = 6.50 Hz, 2H, H_a), 2.48 (t, *J* = 6.58 Hz, 2H, H_e), 2.54 (t, *J* = 5.75 Hz, 2H, PEG), 2.93 (s, 2H, H_d or H_g), 2.96 (s, 2H, H_d or H_g), 3.02 (app. q, *J* = 6.36 Hz, 2H, H_b), 3.07 (s, 3H, PEG), 3.29-3.33 (m, 2H, PEG), 3.40-3.63 (m, 15H, PEG), 3.76 (t, *J* = 5.75 Hz, 2H, PEG), 4.54 (app. d, *J* = 5.98 Hz, 2H, H_j), 6.98 (br t, *J* = 5.29 Hz, 1H, NH), 7.04 (br t, *J* = 5.62 Hz, 1H, NH), 7.15-7.28 (m, 18H, H_t & H_v), 7.32-7.42 (m, 12H, H_u), 7.49 (d, *J* = 8.54 Hz, 2H, H_l), 8.52 (d, *J* = 8.42 Hz, 2H, H_m). ^{13}C{^{1}H} NMR (101 MHz, $CDCl_3$) δ: 21.3 (C_q), 30.0 (C_f), 32.1 (C_a), 37.1 (PEG), 38.2 (C_b), 39.0 (PEG), 43.1 (C_i), 54.1 (C_e), 58.1 (C_d or C_g), 58.2 (C_d or C_g), 66.9 (C_r), 67.2 (C_r), 69.7 (PEG), 70.2 (PEG), 70.4 (PEG), 70.5(PEG), 70.58 (PEG), 70.61 (PEG), 126.9 (C_v), 127.0 (C_v), 128.0 (C_u), 128.1 (C_u), 128.2 (C_m), 128.3 (C_l), 129.6 (C_t), 129.7 (C_t), 130.8 (4° C), 144.0 (4° C), 144.7 (C_s), 144.8 (C_s), 164.0 (4° C), 167.3 (4° C), 170.1 (C=O), 170.2 (C=O), 171.9 (C=O). LC-MS (ESI) *m/z*: $[M+H]^+$ calculated for $C_{67}H_{74}N_8O_7S_2$: 1167.52, found 1167.74.

*Boc-NH-PEG$_3$-CA (**10**).* This compound was synthesised following a modified procedure.[4] Compound **6** (0.207 g, 0.604 mmol) was dissolved in dry DCM (2.00 mL) under N_2. To this stirring solution, a solution of Boc-NH-PEG_3-NH_2 (0.212 g, 0.425 mmol) and DIPEA (0.210 mL, 1.20 mmol) in dry DCM (2.00 m) was added. The reaction mixture was stirred for 1 h at room temperature, after which the solvent was removed and the product purified via column chromatography with silica gel (DCM/2% MeOH). This yielded compound **10** as a pale-yellow oil (0.238 g, 87.4%). ^{1}H NMR (400 MHz, CD_3OD) δ: 1.42 (m, 9H, H_k), 3.21 (t, *J* = 5.58 Hz, 2H, PEG), 3.48-3.53 (m, 4H, PEG), 3.59-3.67 (m, 10H, PEG), 7.05 (d, *J* = 15.31 Hz, 1H, H_f), 7.54-7.57 (m, 2H, H_b), 7.65-7.68 (m, 1H, H_a), 7.88 (d, *J* = 15.32 Hz, 1H, H_g), 8.02-8.05 (m, 2H, H_c). ^{13}C{^{1}H} NMR (101 MHz, CD_3OD) δ: 28.8 (C_k), 40.9 (PEG), 41.3 (PEG), 70.3 (PEG), 71.1 (PEG), 71.2 (PEG), 71.3 (PEG), 71.6 (PEG), 80.1 (C_j), 129.9 (C_c), 130.0 (C_b), 134.1 (C_g), 134.9 (C_a), 136.6 (C_f), 138.3 (C_d), 158.4 (C=O), 166.7 (C=O), 191.5 (C=O).

*H_2N-PEG$_3$-CA (**11**).* This compound was synthesised following a modified procedure.[4] Compound **10** (0.238 g, 0.528 mmol) was dissolved in DCM (3.00 mL) and TFA (0.75 mL) was added. This solution was stirred for

1 h at room temperature, after which the solvent was removed and the product purified via flash column chromatography (DCM to DCM/10% MeOH). This yielded compound **11** as a yellow oil (0.178 g, 96.3%). ^{1}H NMR (400 MHz, CD_3OD) δ: 3.13-3.15 (m, 2H, PEG), 3.51-3.54 (m, 2H, PEG), 3.62-3.72 (m, 12H, PEG), 7.04 (d, *J* = 15.26 Hz, 1H, H_f), 7.54-7.58 (m, 2H, H_b), 7.65-7.70 (m, 1H, H_a), 7.90 (d, *J* = 15.27 Hz, 1H, H_g), 8.03-8.06 (m, 2H, H_c). $^{13}C\{^{1}H\}$ NMR (101 MHz, CD_3OD) δ: 40.6 (PEG), 40.7 (PEG), 67.9 (PEG), 70.3 (PEG), 71.2 (PEG), 71.5 (PEG), 129.8 (C_c), 130.1 (C_b), 134.1 (C_g), 135.0 (C_a), 136.5 (C_f), 138.3 (C_d), 166.8 (C=O), 179.1 (C=O).

*TCO-PEG$_3$-CA (**12**).* This compound was synthesised following a modified procedure.[4] TCO-NHS ester (0.0245 g, 0.0917 mmol) was dissolved in dry DCM (0.5 mL) under N_2. To this, a solution of compound **11** (0.073 g, 0.208 mmol) and DIPEA (0.040 mL, 0.240 mmol) in dry DCM was added dropwise while stirring. The reaction mixture was stirred for 24 h at room temperature while protected from light. The solvent was then removed and the product purified via column chromatography with silica gel (EtOAc to EtOAc/2% MeOH). This yielded compound **12** as a pale-yellow oil (0.016 g, 34.7%). ^{1}H NMR (400 MHz, CD_3OD) δ: 1.52-2.39 (m, 10H, H_k, H_l, H_o, H_p & H_q), 3.27-3.29 (m, 2H, PEG), 3.51-3.55 (m, 4H, PEG), 3.61-3.67 (m, 10H, PEG), 4.79-4.83 (m, 1H, H_j), 5.49-5.70 (m, 2H, H_m & H_n), 7.06 (d, *J* = 15.33 Hz, 1H, H_f), 7.54-7.58 (m, 2H, H_b), 7.64-7.69 (m, 1H, H_a), 7.88 (d, *J* = 15.31 Hz, 1H, H_g), 8.02-8.05 (m, 2H, H_c). $^{13}C\{^{1}H\}$ NMR (101 MHz, CD_3OD) δ: 29.0 (TCO C), 30.9 (TCO C), 33.7 (TCO C), 35.3 (TCO C), 40.9 (PEG), 41.7 (PEG), 42.0 (TCO C), 70.3 (PEG), 71.0 (PEG), 71.2 (PEG), 71.3 (PEG), 71.4 (PEG), 71.6 (C_j), 129.9 (C_c), 130.0 (C_b), 132.6 (C_n), 134.1 (C_g), 134.9 (C_a), 136.4 (C_m), 136.6 (C_f), 138.3 (C_d), 158.7 (C=O), 166.7 (C=O), 191.5 (C=O). LC-MS (ESI) *m/z*: $[M+H]^+$ calculated for $C_{27}H_{38}N_2O_7$: 503.28, found 503.39.

*^{nat}Re-N$_2$S$_2$-PEG$_4$-Tz (**Re-9**).* Compound **9** (0.033 g, 0.028 mmol) was dissolved in DCM (1.0 mL) and the flask placed into an ice bath. To this, TFA (2.0 mL) was added and the solution was stirred for 10 min. Et_3SiH was then added dropwise until the disappearance of the yellow colour in the solution. The volatiles were removed with a stream of N_2 and then by rotary evaporation and the residue redissolved in methanol (3.0 mL), followed by a 1.0 M solution of NaOAc in methanol (2.0 mL). $(Ph_3P)_2ReOCl_3$ (0.035 g, 0.042 mmol)) was added and the mixture was refluxed at 75 °C for 3 h and then stirred at room temperature overnight. The dark pink solution was diluted with

ethyl acetate (10.0 mL) and then filtered through Celite®. The filtrate was concentrated and the residue was loaded onto silica and purified by column chromatography (95:5 DCM:MeOH) and then with prep-TLC (95:5 DCM:MeOH), yielding **Re-9** as a deep pink oil (0.012 g, 46.1%). ^{1}H NMR (400 MHz, $CDCl_3$) δ: 1.50-1.54 (m, 1H, H_e), 2.57 (t, 2H, *J* = 5.8 Hz, PEG), 2.84 (dd, *J* = 4.2, 13.8 Hz, 1 H, H_f), 3.12-3.23 (m, 5H, H_a, H_b & H_q), 3.43-3.48 (m, 3H, H_f & PEG), 3.56-3.69 (m, 14H, PEG), 3.81 (t, *J* = 5.8 Hz, 2H, PEG), 3.86 (dd, *J* = 3.4, 12.3 Hz, 1H, H_e), 4.06-4.10 (m, 1H, H_a), 4.19 (d, *J* = 15.5 Hz, 1H, H_g), 4.57-4.70 (m, 5H, H_b, H_d, H_g & H_j), 4.96 (d, *J* = 17.8 Hz, 1H, H_d), 6.95 (br t, 1H, N<u>H</u>), 7.51-7.53 (m, 2H, H_l), 7.77 (br t, 1H, N<u>H</u>), 8.54-8.56 (m, 2H, H_m). ^{13}C{^{1}H} NMR (101 MHz, $CDCl_3$) δ: 21.3 (C_q), 37.2 (PEG), 39.5 (PEG), 39.7 (C_f), 43.3 (C_j), 48.6 (C_a), 60.1 (C_b), 63.3 (C_g), 64.5 (PEG), 67.4 (C_e), 68.6 (PEG), 69.6 (C_d), 70.3 (PEG), 70.4 (PEG), 70.5 (PEG), 70.6 (PEG), 123.6 (4° C), 124.5 (4° C), 128.3 (C_m), 128.4 (C_l), 130.9 (4° C), 143.7 (4° C), 165.7 (C=O), 172.1 (C=O), 188.4 (C=O). HRMS (ESI) *m/z*: $[M+H]^+$ calculated for $C_{29}H_{43}N_8O_8ReS_2$: 883.23, found 883.22.

V_HH bioconjugation

The method of V_HH bioconjugation detailed for DBCO-PEG_4-CA (**7**) was also applied to the conjugation of TCO-PEG_3-CA (**12**). The purified TCO-V_HH product was analysed using SEC-HPLC (HPLC method C): 16.72 min, 89.0% purity. ESI-MS *m/z* (decon.) calculated for TCO-V_HH: 27090.3, found: 27088.0.

^{188}Re-radiolabelling and IEDDA click reaction

The radiolabelling of the N_2S_2-PEG_4-MeTz chelator (**9**) was done over two steps using the optimised conditions from the labelling of N_2S_2-PEG_3-N_3 (**4**). The IEDDA click reaction was done at an apparent molar activity of 5 MBq/nmol, also following the procedure previously described.

CHARACTERISATION DATA

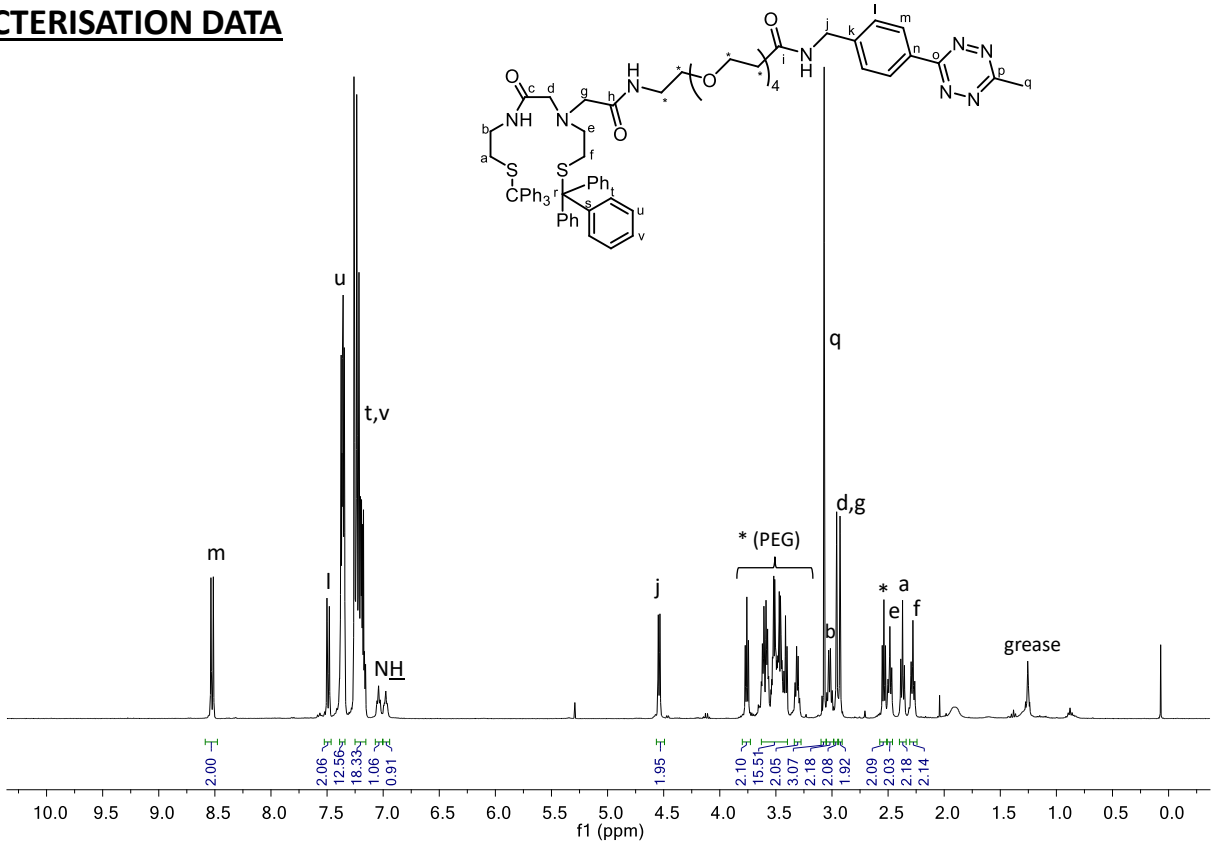

Figure S41. ^{1}H NMR spectrum of compound **9** in $CDCl_3$.

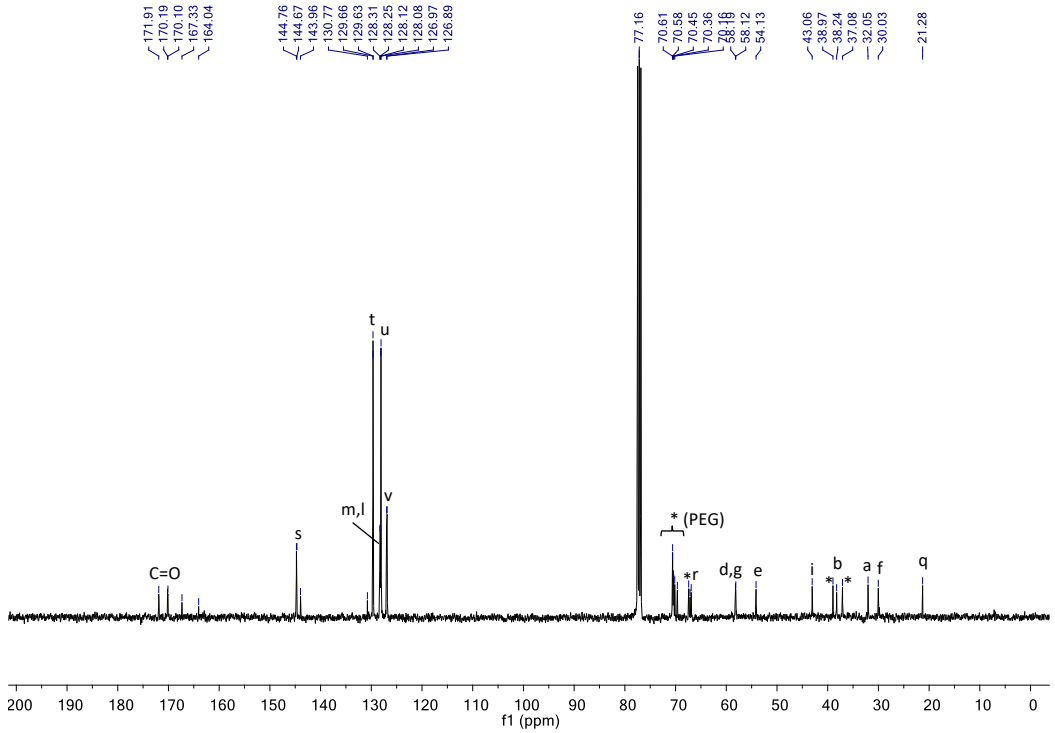

Figure S42. $^{13}C\{^{1}H\}$ NMR spectrum of compound **9** in $CDCl_3$.

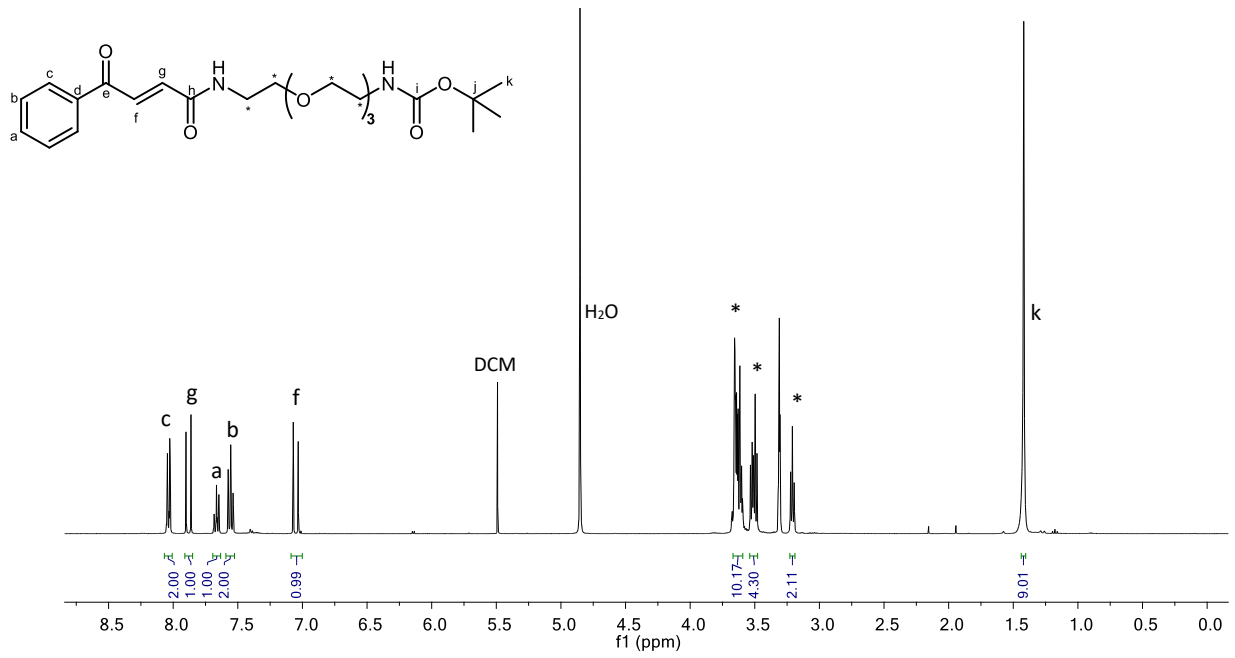

Figure S43. ^{1}H NMR spectrum of compound **10** in CD_3OD.

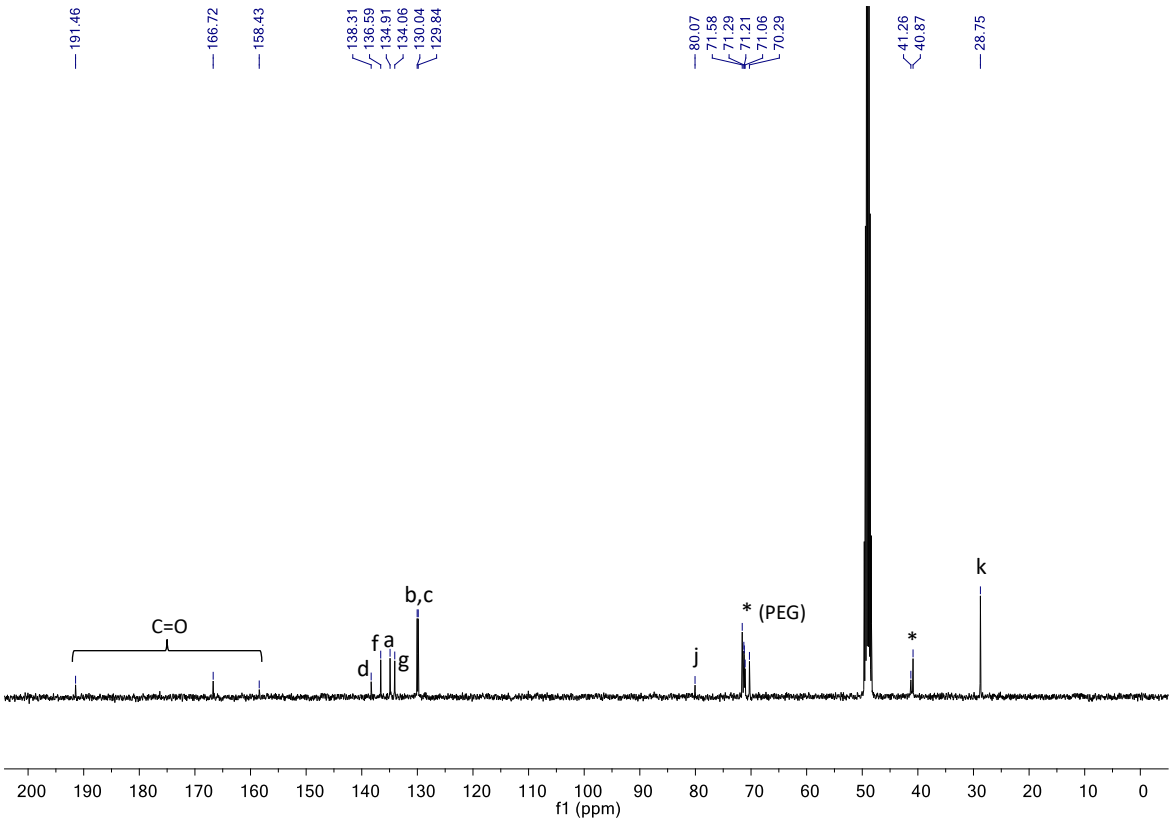

Figure S44. $^{13}C\{^{1}H\}$ NMR spectrum of compound **10** in CD_3OD.

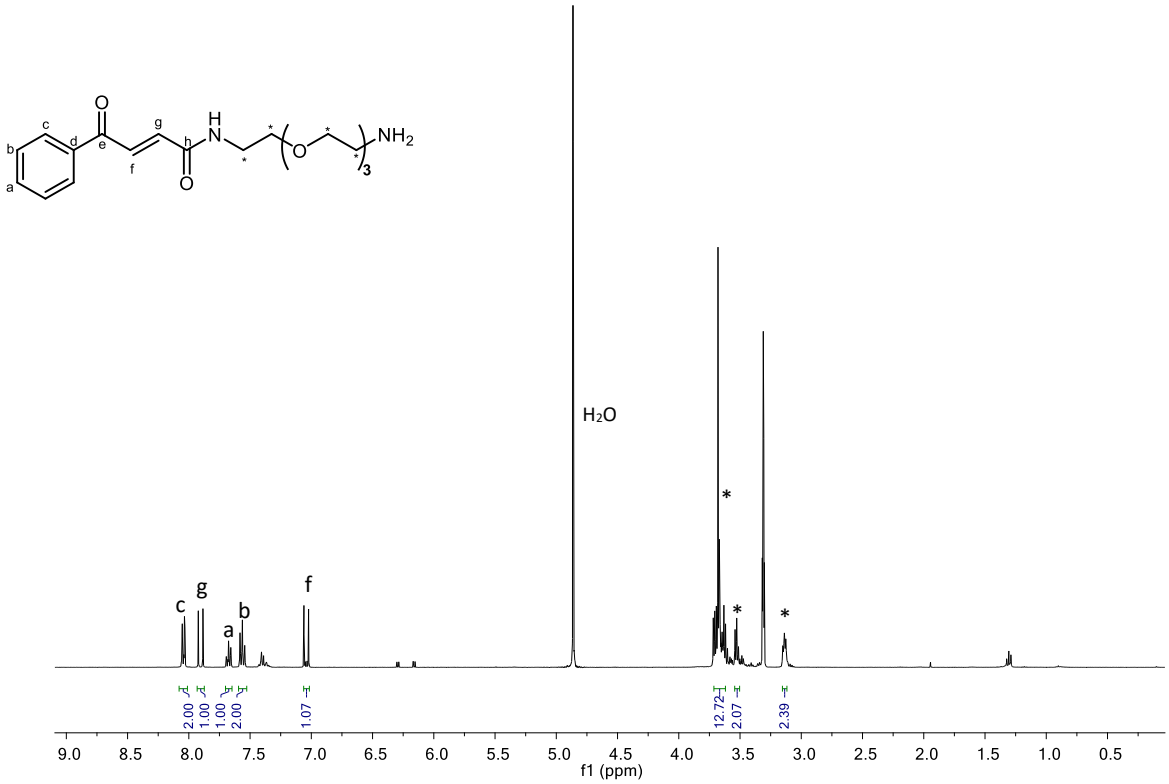

Figure S45. ^{1}H NMR spectrum of compound **11** in CD_3OD.

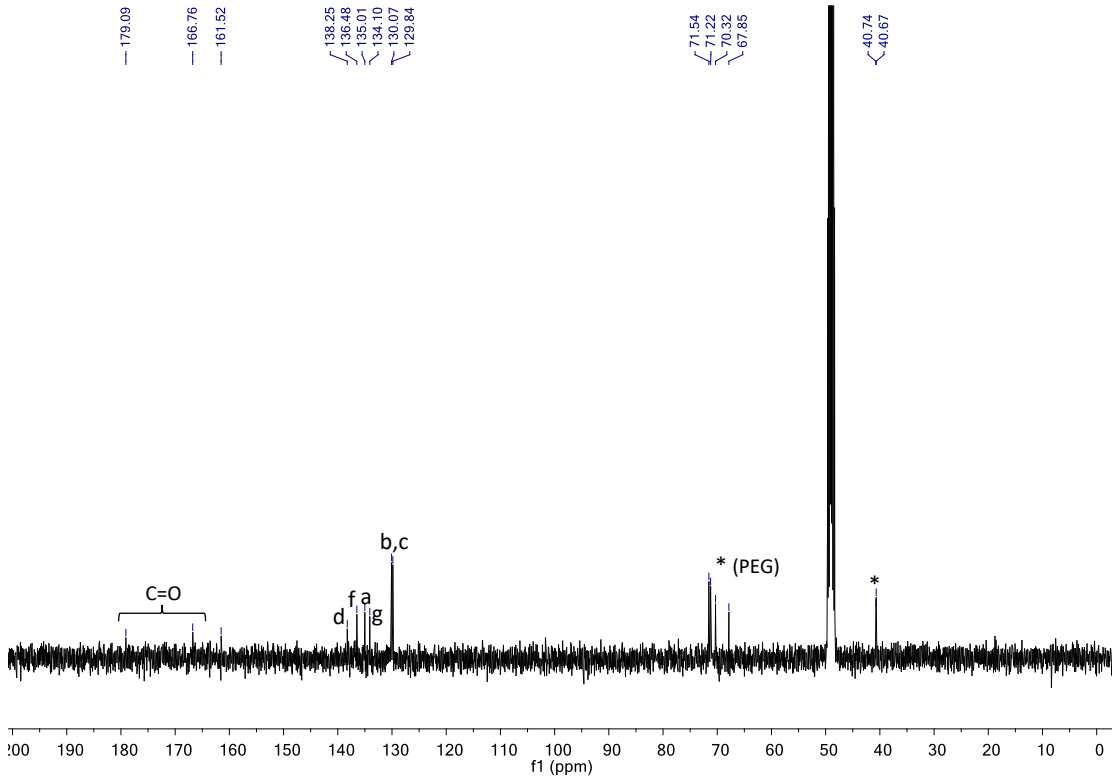

Figure S46. $^{13}C\{^{1}H\}$ NMR spectrum of compound **11** in CD_3OD.

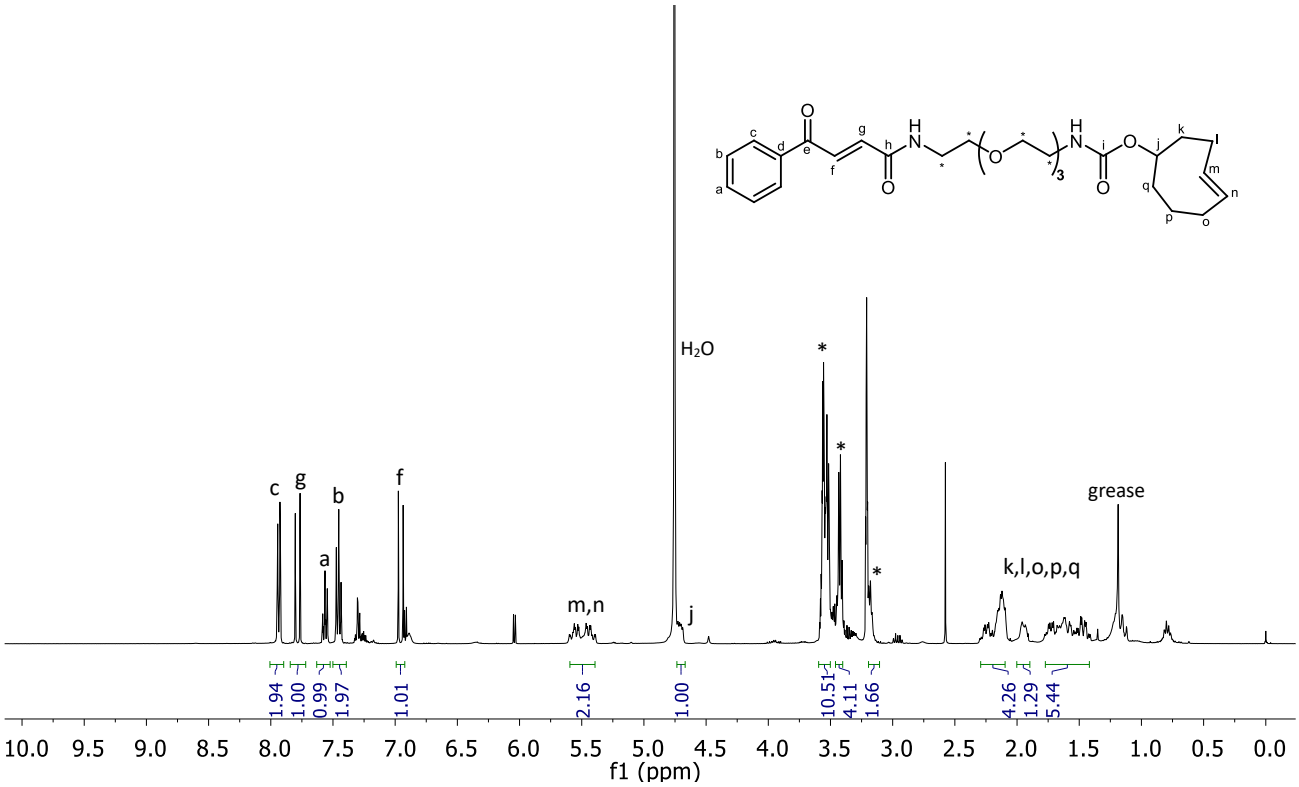

Figure S47. ^{1}H NMR spectrum of compound **12** in CD_3OD.

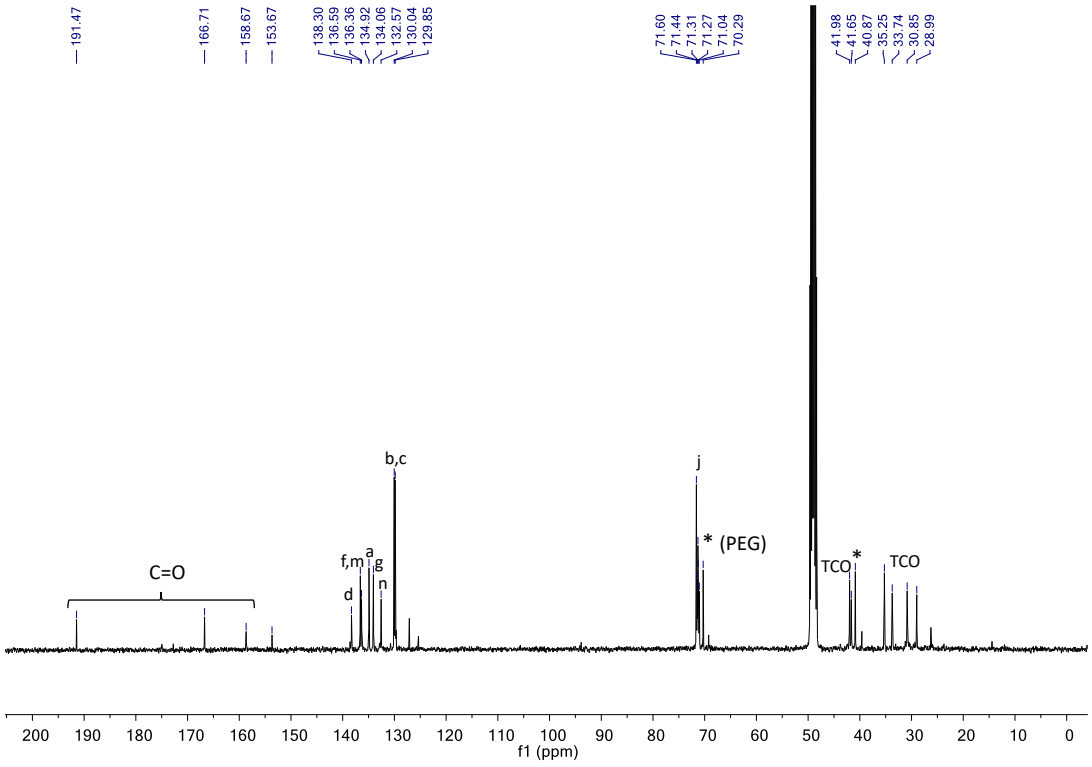

Figure S48. $^{13}C\{^{1}H\}$ NMR spectrum of compound **12** in CD_3OD.

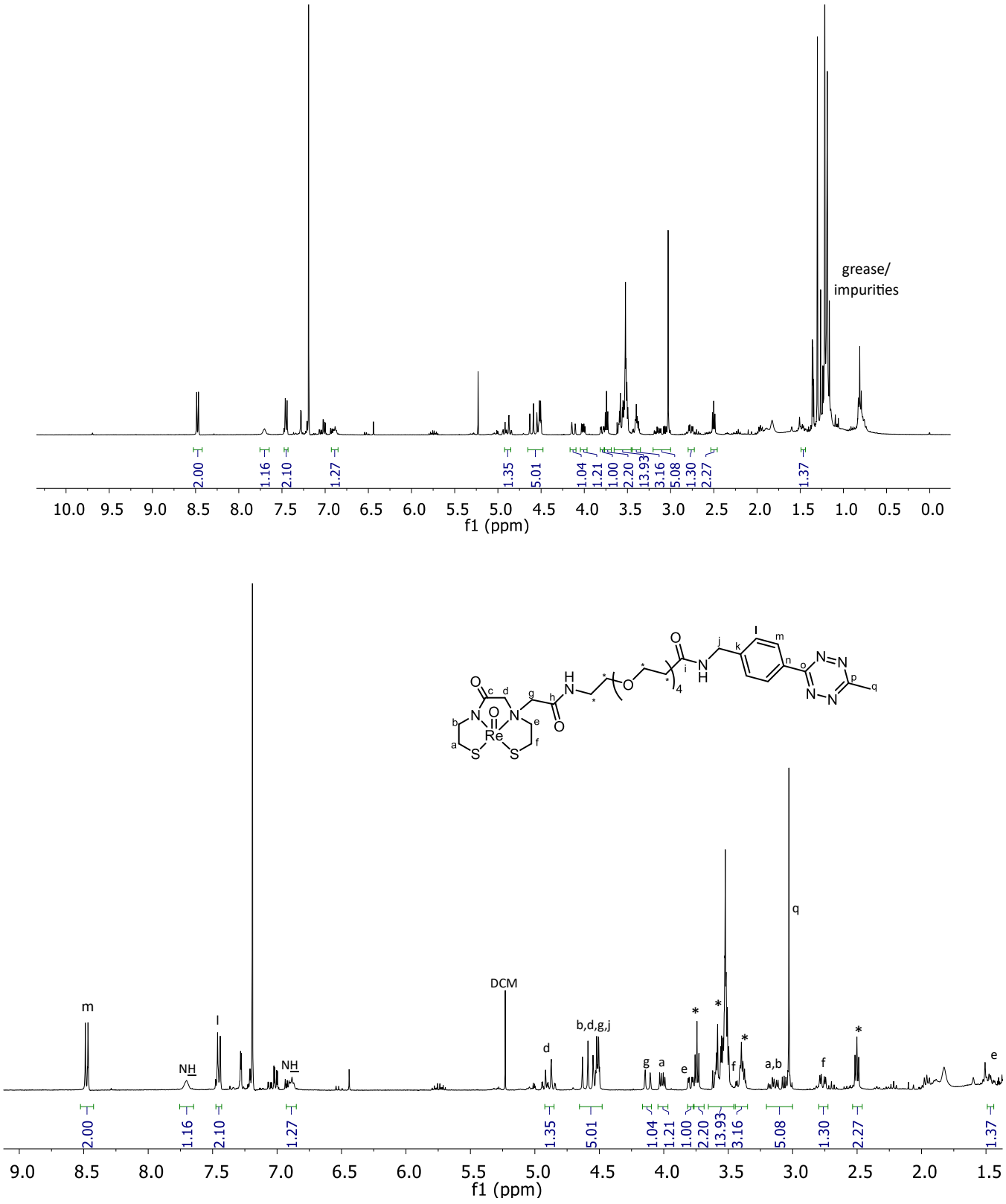

Figure S49. ^{1}H NMR spectrum (full and expanded) of complex **Re-9** in $CDCl_3$.

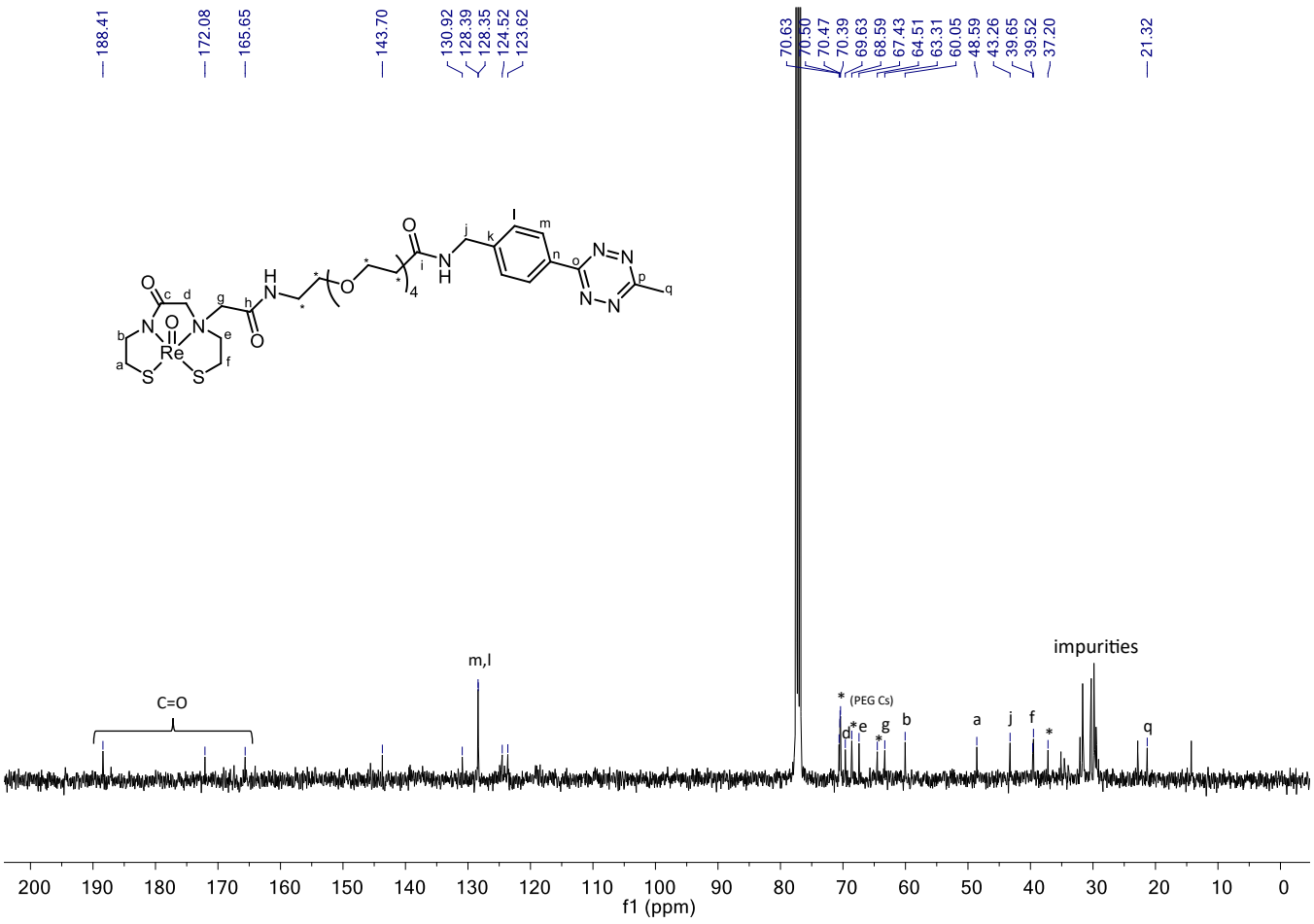

Figure S50. $^{13}C\{^{1}H\}$ NMR spectrum of compound **Re-9** in $CDCl_3$.

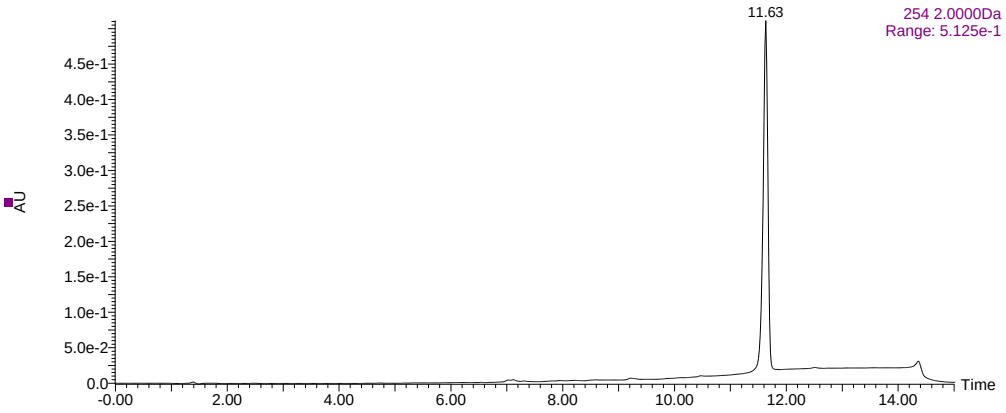

Figure S51. HPLC chromatogram of compound **9** recorded at 254 nm using HPLC method A.

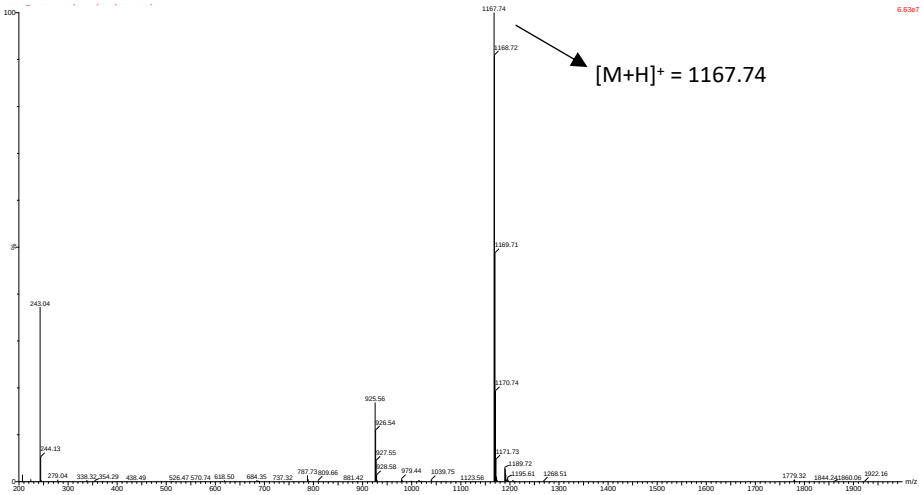

Figure S52. ESI-MS spectrum of compound **9**.

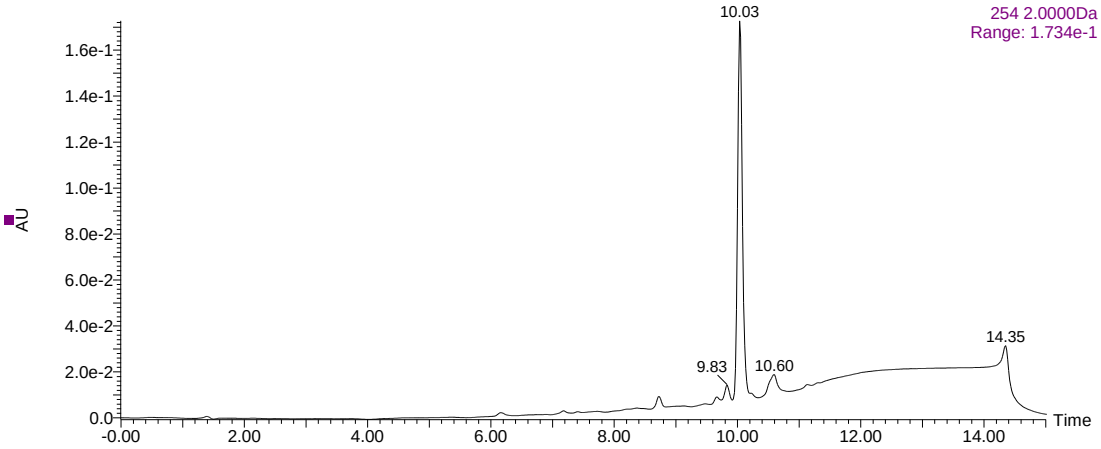

Figure S53. HPLC chromatogram of compound **12** recorded at 254 nm using HPLC method A.

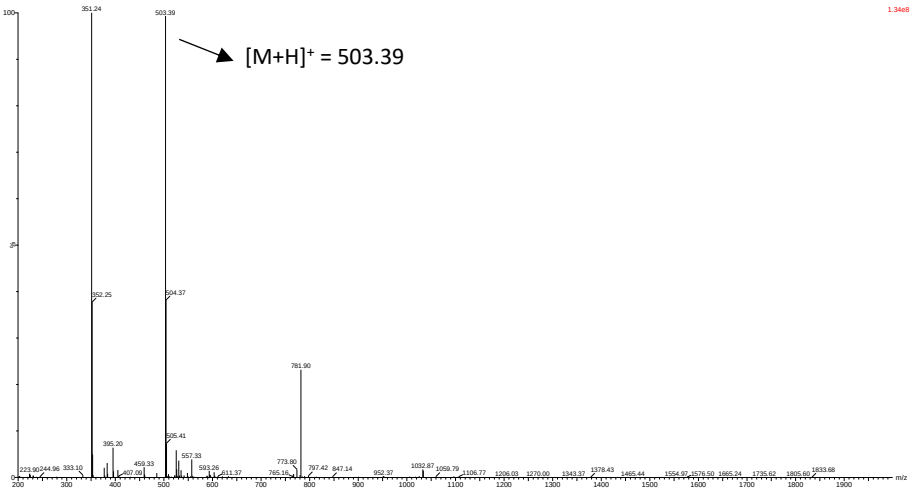

Figure S54. ESI-MS spectrum of compound **12**.

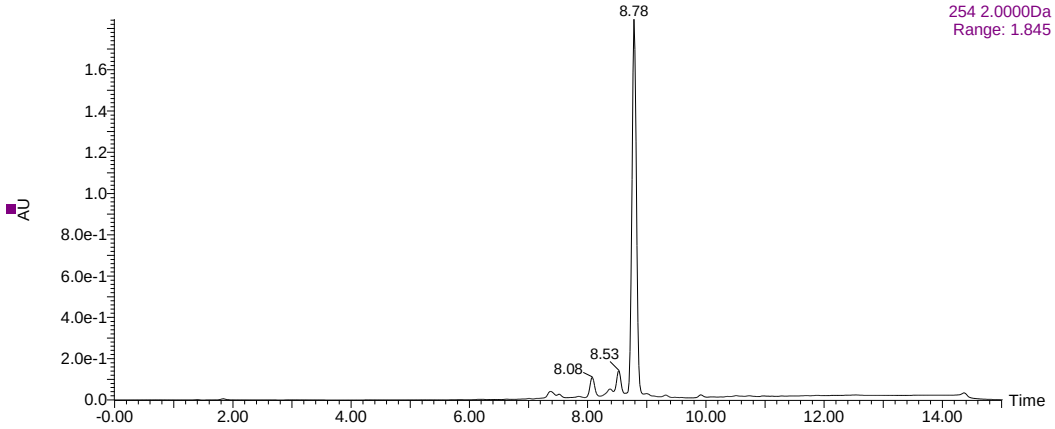

Figure S55. HPLC chromatogram of compound **Re-4** recorded at 254 nm using HPLC method A.

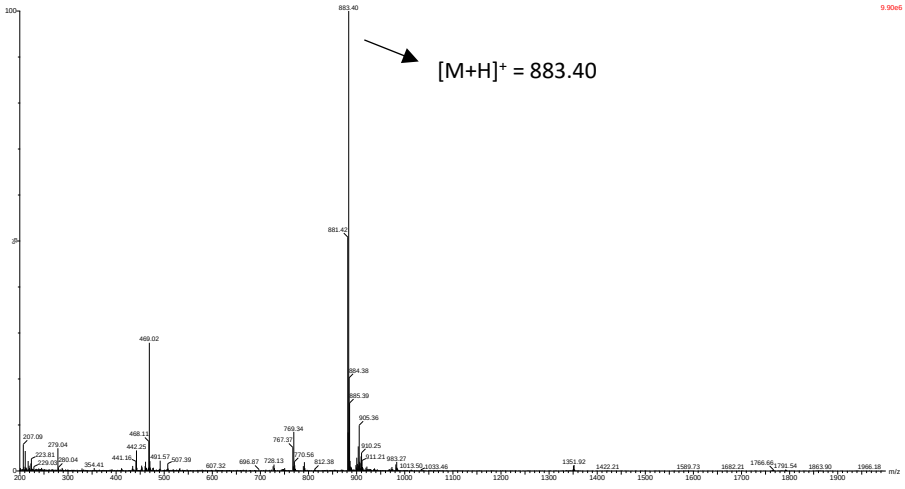

Figure S56. ESI-MS spectrum of compound **Re-4**.

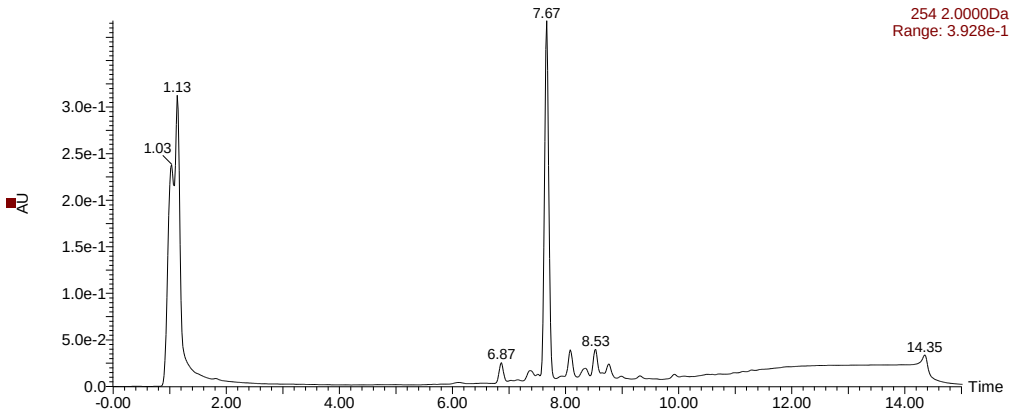

Figure S57. HPLC chromatogram of compound **Re-4** after intentional reduction of the tetrazine with excess $SnCl_2$, recorded at 254 nm using HPLC method A.

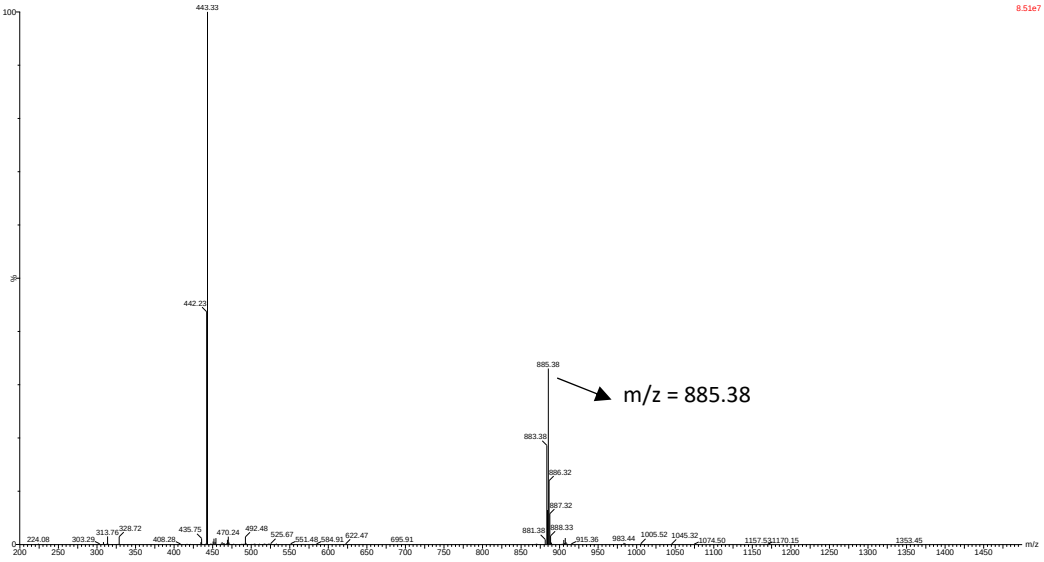

Figure S58. ESI-MS spectrum of compound **Re-4** after intentional reduction of the tetrazine with excess $SnCl_2$. (Mass spectrum of HPLC peak at 7.67 min in Figure S54). The *m/z* of 885.38 indicates the formation of a dihydrotetrazine.

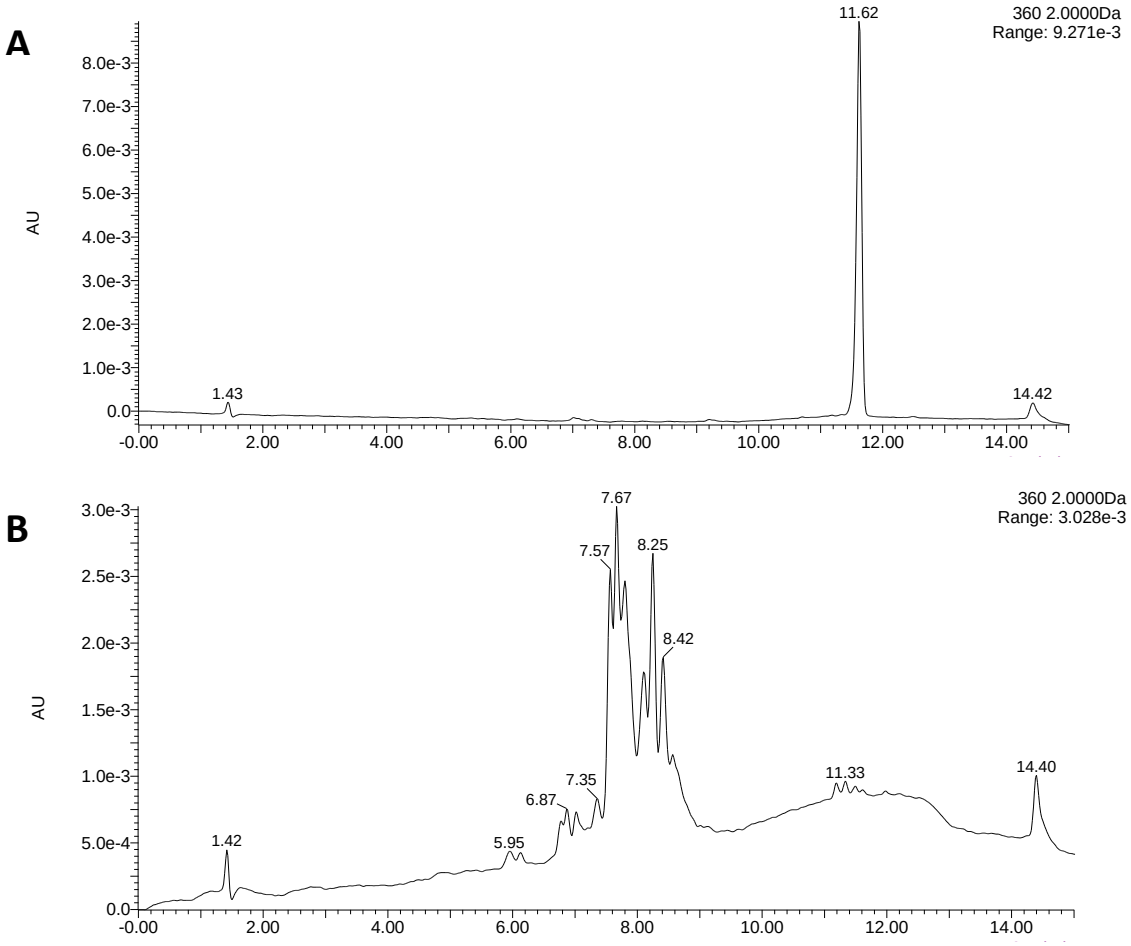

Figure S59. HPLC chromatogram of (**A**) compound **9** recorded at 360 nm and (**B**) compound **9** after reaction with TFA for 15 min at room temperature, using HPLC method A.

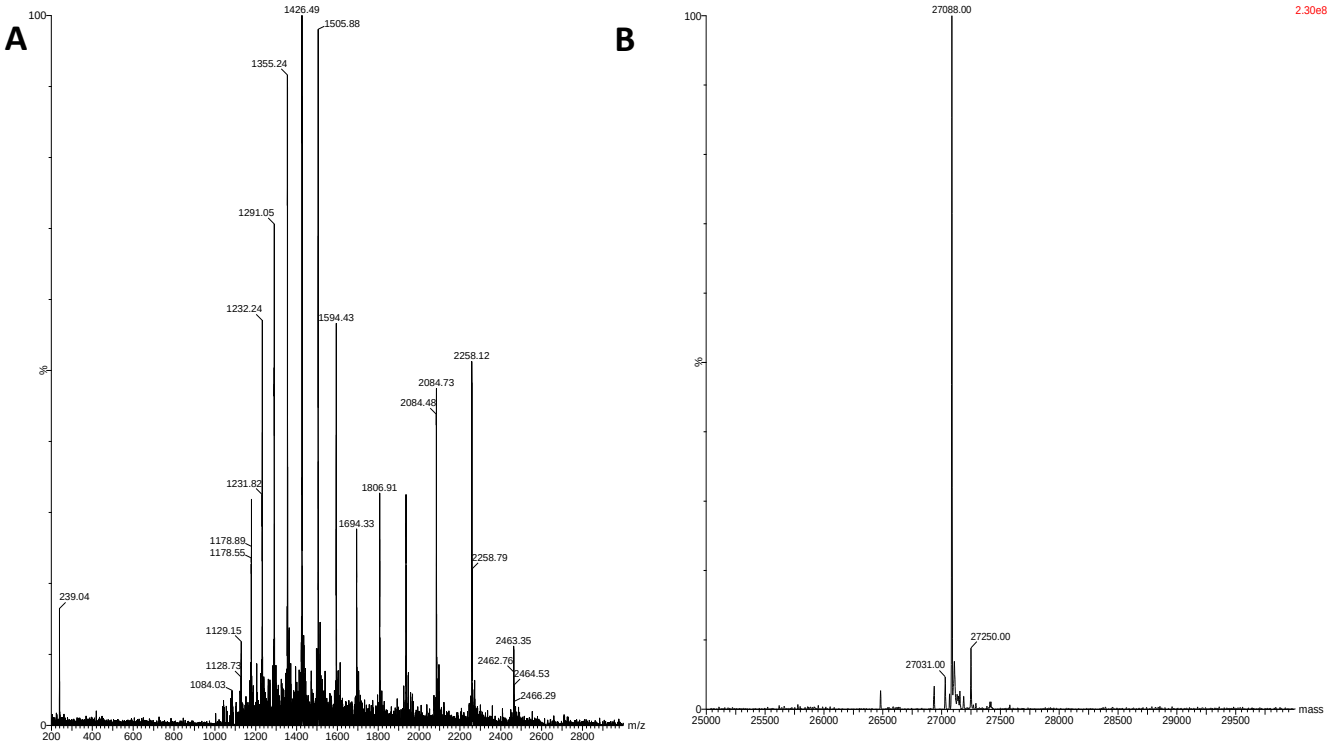

Figure S60. LC-MS analysis of TCO-PEG$_3$-V$_H$H. (**A**) Continuous ion series and (**B**) deconvoluted mass spectrum obtained using the MaxEnt algorithm. Solvent: 1:1 mixture of milli-Q water and acetonitrile (0.1% formic acid).

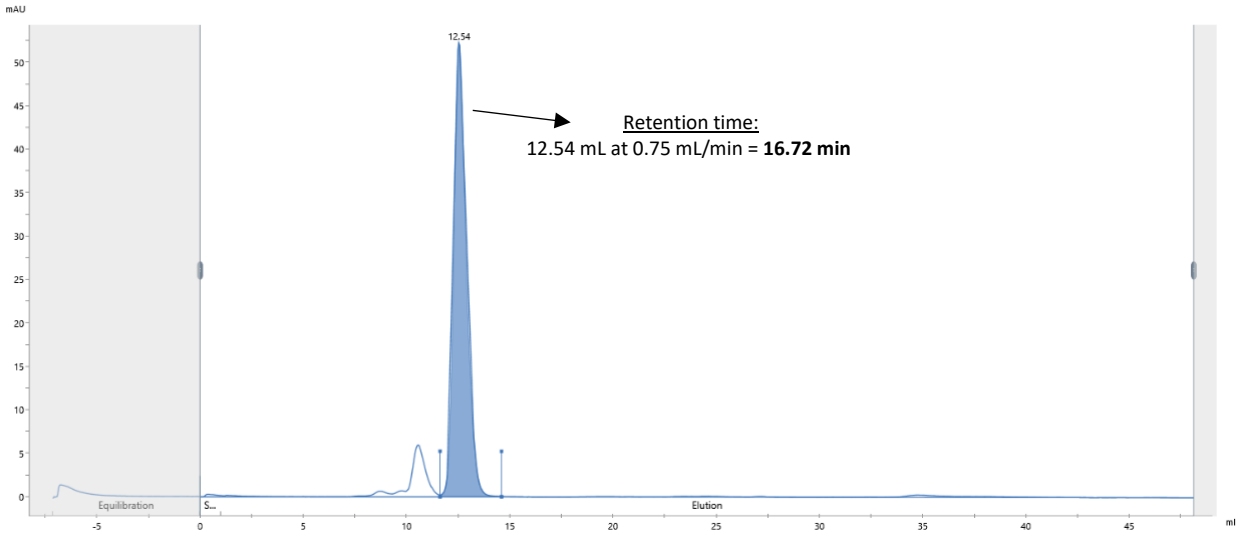

Figure S61. SEC-HPLC chromatogram of TCO-PEG$_3$-V$_H$H showing its purity using HPLC method C on an ÄKTA pure™ chromatography system. The purity of the conjugate (highlighted) is 89.0%

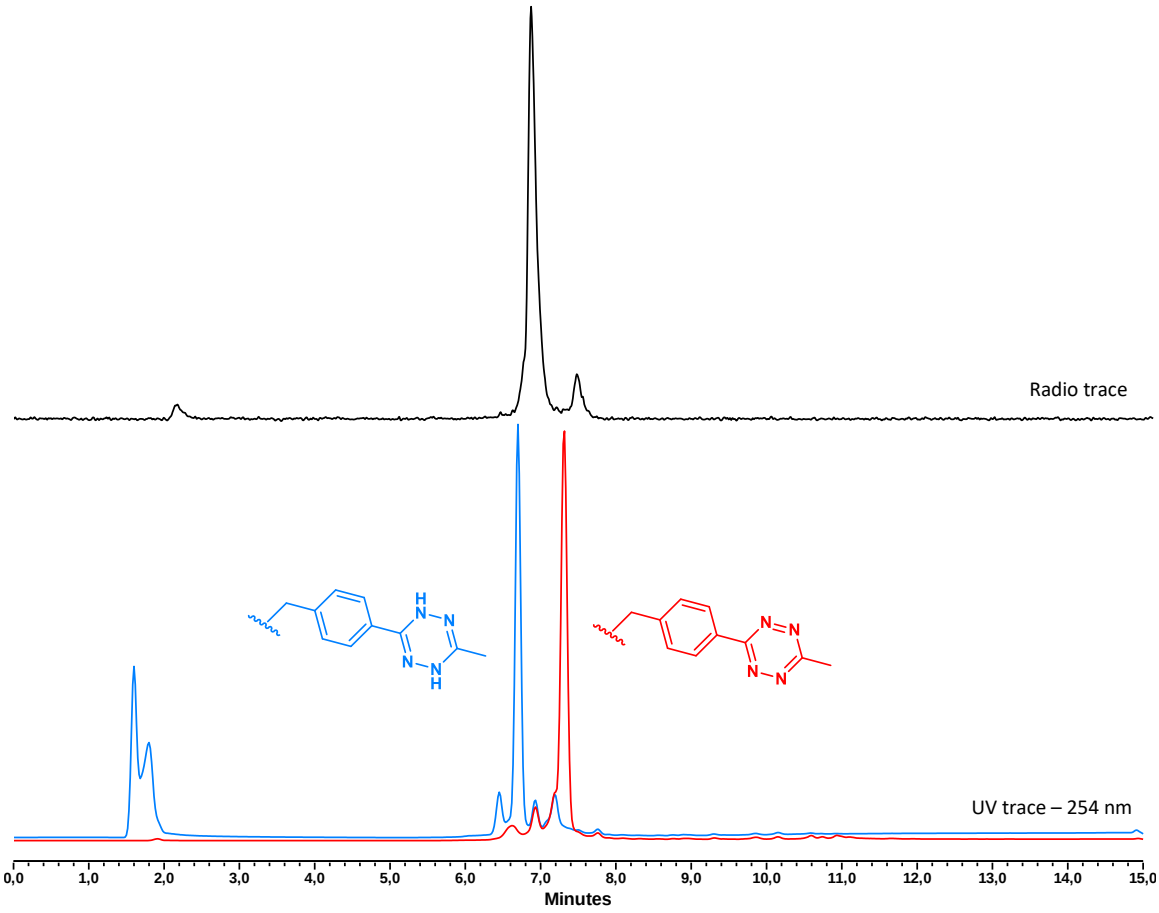

Figure S62. Radio-HPLC chromatogram of the labelling mixture after prep-HPLC purification (black) compared to the UV chromatograms of the ^{nat}Re(V) complexes, **Re-9** (red) and **Re-9** reduced with $SnCl_2$ (blue).

REFERENCES

1 M. Ono, R. Ikeoka, H. Watanabe, H. Kimura, T. Fuchigami, M. Haratake, H. Saji and M. Nakayama, *ACS Chem Neurosci*, 2010, **1**, 598–607.

2 L. Mei, Y. Wang and T. Chu, *Eur J Med Chem*, 2012, **58**, 50–63.

3 A. Kuzmin, A. Poloukhtine, M. A. Wolfert and V. V. Popik, *Bioconjugate Chemistry*, 2010, **21**, 2076–2085.

4 V. F. C. Ferreira, B. L. Oliveira, A. D'Onofrio, C. M. Farinha, L. Gano, A. Paulo, G. J. L. Bernardes and F. Mendes, *Bioconjugate Chemistry*, 2021, **32**, 121–132.

5 D. P. Sanders, K. Fukushima, D. J. Coady, A. Nelson, M. Fujiwara, M. Yasumoto and J. L. Hedrick, *Journal of the American Chemical Society*, 2010, **132**, 14724–14726.

6 R. C. Clark and J. S. Reid, *Acta Crystallographica Section A*, 1995, **51**, 887–897.

7 *Rigaku Oxford Diffraction Ltd*, 2021, preprint, Rigaku Oxford Diffraction Ltd:version 1.171.41.122a.

8 O. V. Dolomanov, L. J. Bourhis, R. J. Gildea, J. A. K. Howard and H. Puschmann, *Journal of Applied Crystallography*, 2009, **42**, 339–341.

9 G. M. Sheldrick, *Acta Crystallographica Section A Foundations and Advances*, 2015, **71**, 3–8.

10 G. M. Sheldrick, *Acta Crystallographica Section C Structural Chemistry*, 2015, **71**, 3–8.

11 A. L. Spek, *Acta Crystallographica Section D Biological Crystallography*, 2009, **65**, 148–155.

12 M. Straub, M. Leresche, C. Pilloud, F. Devynck, N. Stritt and R. Hesselmann, *EJNMMI Radiopharmacy and Chemistry*, 2018, **3**, 5.

13 R. Fridman, G. Benton, I. Aranoutova, H. H. Kleinman and R. Daniel Bonfil, *Nature Protocols*, 2012, **7**, 1138–1144.

14 A. R. Fritzberg, W. P. Whitney, C. C. Kuni and W. Klingensmith, *International Journal of Nuclear Medicine and Biology*, 1982, **9**, 79–82.

15 H. L. Foster, J. David Small and J. G. Fox, *The Mouse in Biomedical Research*, Academic Press: New York, 1983.

16 D. Zeng, B. M. Zeglis, J. S. Lewis and C. J. Anderson, *Journal of Nuclear Medicine*, 2013, **54**, 829–832.

17 T. Reiner and B. M. Zeglis, *J Labelled Comp Radiopharm*, 2014, **57**, 285–290.

18 S. Mushtaq, S.-J. Yun and J. Jeon, *Molecules*, 2019, **24**, 3567.

19 X. Zhong, J. Yan, X. Ding, C. Su, Y. Xu and M. Yang, *Bioconjug Chem*, 2023, **34**, 457–476.

20 M. Handula, K. T. Chen and Y. Seimbille, *Molecules*, 2021, **26**, 4640.

21 E. J. L. Stéen, J. T. Jørgensen, C. Denk, U. M. Battisti, K. Nørregaard, P. E. Edem, K. Bratteby, V. Shalgunov, M. Wilkovitsch, D. Svatunek, C. B. M. Poulie, L. Hvass, M. Simón, T. Wanek, R. Rossin, M. Robillard, J. L. Kristensen, H. Mikula, A. Kjaer and M. M. Herth, *ACS Pharmacol Transl Sci*, 2021, **4**, 824–833.

22 J. A. G. L. Van Buggenum, J. P. Gerlach, S. Eising, L. Schoonen, R. A. P. M. Van Eijl, S. E. J. Tanis, M. Hogeweg, N. C. Hubner, J. C. Van, K. M. Bonger and K. W. Mulder, *Scientific Reports*, 2016, **6**, 22675.

23 L. Bohrmann, C. B. M. Poulie, C. Rodríguez-Rodríguez, S. Karagiozov, K. Saatchi, M. M. Herth and U. O. Häfeli, *PLOS ONE*, 2024, **19**, e0300466.

24 H. Zhang, W. S. Trout, S. Liu, G. A. Andrade, D. A. Hudson, S. L. Scinto, K. T. Dicker, Y. Li, N. Lazouski, J. Rosenthal, C. Thorpe, X. Jia and J. M. Fox, *Journal of the American Chemical Society*, 2016, **138**, 5978–5983.

25 A.-C. Knall and C. Slugovc, *Chemical Society Reviews*, 2013, **42**, 5131.

26 M. L. Blackman, M. Royzen and J. M. Fox, *Journal of the American Chemical Society*, 2008, **130**, 13518–13519.

27 Y. Fang, A. S. Hillman and J. M. Fox, *Topics in Current Chemistry*, 2024, **382**, 15.

28 G. S. Kumar and Q. Lin, *ChemBioChem*, 2022, **23**, e202200175.

29 H. Wu and N. K. Devaraj, *Accounts of Chemical Research*, 2018, **51**, 1249–1259.